



Geographisches Institut  
Rheinische Friedrich-Wilhelms-Universität Bonn

# **Alpine sediment cascades in the Swiss National Park, Graubünden**

MASTERARBEIT  
im Studiengang Geographie Master of Science

vorgelegt von  
**Karoline Meßenzehl**

betreut durch  
**Prof. Dr. Richard Dikau**

**Bonn, Februar 2013**

## DECLARATION OF AUTHORSHIP

### Erklärung

Ich versichere, dass ich die Arbeit selbstständig verfasst habe, dass ich keine anderen Quellen und Hilfsmittel als die angegebenen benutzt und die Stellen der Arbeit, die anderen Werken dem Wortlaut oder dem Sinn nach entnommen sind, in jedem Fall als Entlehnung kenntlich gemacht habe. Das Gleiche gilt auch für beigegebene Zeichnungen, Kartenskizzen und Abbildungen.

Bonn, den

## DANKSAGUNG

An dieser Stelle möchte ich mich sehr herzlich bei allen Personen bedanken, die direkt und indirekt zum Gelingen der vorliegenden Masterarbeit beigetragen haben.

Mein erster Dank gilt der Leitung des Schweizerischen Nationalparks, insbesondere Ruedi Haller, für die Möglichkeit, dass ich die Geländearbeit im Nationalpark durchführen konnte. Vielen Dank außerdem für die Bereitstellung aller GIS-Daten.

Ein ganz besonderer Dank gilt Herrn Prof. Dikau für die vielen fachlichen Gespräche und konstruktiven Diskussionen, den großen Freiraum in der Gestaltung dieser Arbeit und die vielseitigen Denkanstöße, nicht nur während der Masterarbeitsphase, sondern auch im Verlauf des gesamten Studiums in Bonn. Bedanken möchte ich mich insbesondere für die intensive Unterstützung, Hilfsbereitschaft und das stetig offene Ohr während des letzten Jahres.

Die Anfertigung dieser Arbeit wäre außerdem nicht möglich gewesen ohne Dr. Thomas Hoffmann. Vielen Dank für die exzellente thematische und methodische Betreuung, die unermüdliche Geduld und für den immer zur rechten Zeit kommenden Motivationsschub. Außerdem habe ich Thomas Hoffmann für die großartige Exkursion durch die Rocky Mountains im Sommer 2011 zu danken, welche wohl damals in mir die Begeisterung für alpine Sedimentkaskaden geweckt hatte!

Ein großes Dankeschön geht an Tobias Müller, Anna Schoch und Tomas Baumann für die tatkräftige Unterstützung und fröhliche Stimmung während der Geländearbeit. Ohne Plumps und Pepple wäre die Zeit nur halb so schön gewesen!! Darüber hinaus möchte ich Tobias Müller vielmals für das kritische Lesen dieser Arbeit danken.

Des Weiteren soll ein großer Dank ausnahmslos der gesamten AG Dikau gelten. Die sehr warmherzige Atmosphäre hat in einem großen Maß dazu beigetragen, dass ich mich bis zuletzt jeden Morgen gerne an meine Arbeit im GIS-Raum gesetzt habe. Besonders erwähnen möchte ich hier Robert Mertens und Adrian Strauch.

Abschließend möchte ich mich herzlich bei meiner Mutter und meinem Vater bedanken. Ohne ihre liebevolle und uneingeschränkte Unterstützung hätte ich mein gesamtes Studium und zuletzt meine Masterarbeit nicht beenden können. Ein großer Dank gilt auch meinen wunderbaren Freundinnen Christina Fichtner, Anna Konopczak und Julia Tüshaus, die vor allem in schwierigeren Zeiten während der Masterarbeit für mich da waren.

Abschließend geht mein größter Dank an Oliver Schüler. Während meines gesamten Studiums und der finalen Masterarbeitsphase hat er mit voller Kraft und großer Liebe mich fortwährend motiviert, für meine innere Ausgeglichenheit gesorgt und mir stets einen so wichtigen Rückhalt gegeben. Vielen Dank!!!

## ABSTRACT

Referring to the concept by CHORLEY & KENNEDY (1971), the transfer of sediments from alpine hillslopes to the stream network occurs in a cascading way across various intermediate sediment storage landforms. The operation of alpine sediment cascades is significantly influenced by “buffers” that may interrupt the sediment fluxes and prevent sediment from reaching the fluvial system for various periods of time. The disconnectivity and decoupling within alpine basins contribute directly to the sediment delivery problem (WALLING 1983). Due to the relevance for sediment budgets and for the management of recent and future environmental and anthropogenic changes, there is still a need to increase the understanding of sediment cascades in alpine systems. The main aim of this master thesis is to gain further insights regarding the operation of sediment cascades and their role within the sediment flux systems of meso-scale alpine basins with respect to both spatial and temporal dynamics.

Two small ( $< 10 \text{ km}^2$ ), formerly glaciated alpine valleys of contrasting morphometry – Val dal Botsch and Val Müschauns – are studied in the Swiss National Park (Graubünden, Switzerland). The two basins represent excellent study sites as they offer a diversity of geomorphic transfer and storage processes undisturbed by human influences. By combining classical geomorphological mapping on a scale of 1:5000 and interpretation of air photos and hillshades, detailed geomorphic maps are created for each basin. The geomorphic mapping provides the base for a comprehensive inventory of sediment storage landforms. In order to characterise the various storage types, different geomorphometric attributes are studied using ArcGIS. Based on the concept by SPEIGHT (1974), toposequences from ridge crest to valley bottom are mapped topologically to delineate the sediment trajectories along hillslopes. In order to relate the different toposequences to alpine sediment cascades with (de)coupled sediment fluxes, the functional relationships between neighbouring sediment storages are analysed. For that reason, a new conceptual framework is developed that examines the material throughput, the event frequencies as well as the long-term displacement of the separating boundary between neighbouring storages. In order to evaluate the sediment flux systems, the connectivity to the fluvial system is assessed both qualitatively, based on a conceptual approach, and quantitatively using a modified GIS algorithm by BORSELLI et al. (2008). Finally, the sediment connectivity is combined with the recent degree of activity in order to estimate the sediment delivery potential of individual storages.

The investigations reveal a unique set of storage landforms in each study site. While around 25 % of Val dal Botsch’s surface is covered by moraine deposits reworked by cryogenic creep, more than half (59 %) of the basin of Val Müschauns represents bedrock. However, both valleys are similar concerning their dominance of gravitational storage and transfer processes, which might

be interpreted as typical paraglacial signal of meso-scale basins. The morphometric characterisation of individual storage types displays an evident spatial regularity that is controlled by hillslope morphometry, which in turn affects ecological and climatic factors. Based on the toposequence study, the sediment storages can be organised in up to 33 different topological sequences in each valley. The analysis of the functional relationships indicates that 90 % of the storage boundaries in Val dal Botsch are coupled resulting in sediment cascades of five coupled consecutive storages on average. In contrast, only 74 % of the storage boundaries of Val Müschauns are coupled. As a consequence, almost all toposequences are buffered in-between leading to only three coupled storages along a cascade on average. These discrepancies can be explained by the specific storage pattern, the valley morphometry and the influence of debris flows.

Furthermore, the results reflect a noticeable temporal dynamic of sediment cascades. In both valleys, more than 28 % of the storage boundaries is dominated by a continuous sediment throughput. A key driver is the coupling between the steep rock faces and talus slopes via continuous low-magnitude rockfall events. The results give also reason to assume that the gradual shift of storage boundaries over time will affect the long-term coupling and connectivity of sediment cascades notably. Around 66 % of the storages boundaries behaves regressively, mainly due to the detachment of rock particles and the incision of debris flows.

Finally, the qualitative connectivity assessment indicates that around 15 % of the surface of Val dal Botsch is currently decoupled from the fluvial system. In Val Müschauns, the amount of decoupled surface is nearly as twice as much as 28 % of the surface might have presently no connection to the stream network. Despite of a number of promising findings of the numeric connectivity study, most of the results highly differ from the qualitative analysis inferring the need for a profound knowledge of the geomorphic system to validate the numeric investigations.

Finally, this study demonstrates that the two alpine valleys Val dal Botsch and Val Müschauns play a distinctive role within the sediment flux system of the Swiss National Park. Thus, depending on the valley morphometry and the specific glacial history, alpine sediment cascades are characterised by typical spatial and temporal dynamics. Furthermore, the methodological framework of this study underlines the potential of a combination of classical geomorphic mapping, providing an essential systemic knowledge, and geomorphometric analyses in ArcGIS to increase the understanding of alpine sediment cascades.

## ZUSAMMENFASSUNG

In alpinen Systemen erfolgen die Prozesse des Sedimenttransportes kaskadenartig entlang einer Abfolge von verschiedenen Sedimentspeichern. CHORLEY & KENNEDY (1971) veranschaulichen diese Systemvorstellung durch das Bild der Sedimentkaskade. Sogenannte „Buffers“ können zur Zeitverzögerung bis hin zur vollständigen Unterbrechung des kaskadenförmigen Sedimentflusses führen. Der Grad der Kopplung und Konnektivität hat damit direkten Einfluss auf das „sediment delivery problem“ (WALLING 1983) in alpinen Einzugsgebieten.

Aufgrund der Relevanz für Untersuchungen zum Sedimenthaushalt und zur Sensitivität gegenüber klimatischen und anthropogenen Veränderungen ist ein tiefgehendes Verständnis von Sedimentkaskaden in hochdynamischen alpinen Systemen von großer Notwendigkeit. Um zu weiteren Kenntnissen beizutragen, hat die vorliegende Masterarbeit zum Ziel die raum-zeitliche Dynamik alpiner Sedimentkaskaden und ihre Rolle im Sedimentfluss-System alpiner mesoskaliger Einzugsgebiete näher zu analysieren. Als Untersuchungsgebiete dienen zwei ehemals vergletschert und unterschiedlich morphometrische Täler ( $< 10 \text{ km}^2$ ) – Val dal Botsch und Val Müschauns – im Schweizerischen Nationalpark (Graubünden, Ostschweiz).

Mit Hilfe einer klassischen geomorphologischen Kartierung im Maßstab 1:5000 und der Interpretation von Luftbildern und Schummerungskarten werden zwei geomorphologische Karten entworfen. Die detaillierten Karten stellen die weitere Grundlage für eine umfangreiche Lokalisierung und morphometrische Charakterisierung aller Sedimentspeicher mit ArcGIS dar. Anschließend werden Sedimenttrajektorien identifiziert und deren interner Kopplungsgrad qualitativ bewertet. Basierend auf dem Toposequenzkonzept von SPEIGHT (1974) werden topologische Sequenzen von Sedimentspeichern von der Wasserscheide bis zum Talboden ermittelt. Zur Untersuchung der funktionalen Beziehungen zwischen benachbarten Speichern dient ein neu entwickelter konzeptioneller Ansatz, der den zeitlich variablen Materialaustausch und die Lageveränderung der Speichergrenzen näher analysiert. Abschließend wird die Konnektivität zum fluvialen System sowohl qualitativ als auch quantitativ untersucht. Dafür wird eine qualitative Konnektivitätsanalyse einer modifizierten Version des GIS-Algorithmus von BORSELLI et al. (2008) gegenübergestellt. Die Verschneidung der Konnektivität mit dem Grad der Aktivität ermöglicht schließlich das Sedimentaustragspotential individueller Sedimentspeicher zu bewerten.

Die Untersuchungen zeigen in beiden Tälern eine individuelle Zusammensetzung von Sedimentspeichertypen. Während in Val dal Botsch ca. 25 % der Oberfläche von Moränenmaterial bedeckt ist, wird in Val Müschauns der große Anteil an Festgestein (59 %) deutlich. Beide Täler werden jedoch gleichermaßen von gravitativen Speicherungs- und Transportprozessen dominiert, was möglicherweise als typisches paraglaziales Signal mesoskaliger, alpiner Täler interpretiert werden kann. Des Weiteren zeigen die morphometrischen Untersuchungen eine spezifische

räumliche Organisation der einzelnen Speichertypen auf, welche aus dem Wechselspiel zwischen Hangmorphometrie und klimatisch-ökologischen Faktoren resultiert. In beiden Tälern existieren bis zu 33 verschiedene topologische Abfolgen von Speichertypen am Hang. Die Analyse der funktionalen Nachbarschaftsbeziehungen zeigt dabei auf, dass in Val dal Botsch über mehr als 90 % der Speichergrenzen aktuell ein Materialaustausch stattfindet. Im Durchschnitt wird das Sediment über fünf miteinander gekoppelte Speicher vom Hang zum Gerinne transportiert. In Val Müschauns sind hingegen nur 74 % der Speichergrenzen gekoppelt. Aufgrund der häufigen Unterbrechung durch Felsvorsprünge findet ein durchgehender Sedimentfluss nur entlang von drei benachbarten Sedimentspeichern statt. Insgesamt lassen sich diese Diskrepanzen zwischen den beiden Tälern durch ein komplexes Zusammenspiel von Speichernachbarschaften, Talmorphometrie sowie dem Einfluss von Murgängen erklären.

Die Ergebnisse spiegeln ferner eine zeitliche Dynamik von Sedimentkaskaden wider. Infolge der direkten Kopplung zwischen Felswänden und Schutthalden durch Sturzprozesse kleiner Magnituden weisen mehr als 28 % der Speichergrenzen in jedem Tal einen kontinuierlichen Sedimentaustausch auf. Rund 66 % der Grenzen verhalten sich zudem regressive, insbesondere aufgrund von Steinschlagprozessen und der Hangeinschneidung durch Murgänge. Es ist anzunehmen, dass die zeitliche Dislokation der Speichergrenze signifikant die Intensität der Kopplung und Konnektivität auf langer Zeitskala beeinflussen kann.

Die qualitative Konnektivitätsanalyse verdeutlicht schließlich, dass derzeit 28 % der Oberfläche in Val Müschauns und 15 % in Val dal Botsch vom fluvialen System entkoppelt sind und damit nicht zum Sedimenteintrag ins Gerinne beitragen. Die quantitative Modellierung zeigt diesbezüglich deutliche Diskrepanzen zu den qualitativen Befunden, was die Notwendigkeit systemischer, wissensbasierter Untersuchungen zur Validierung von numerischen Analysen hervorhebt.

Diese Masterarbeit zeigt folglich auf, dass die beiden alpinen Täler Val dal Botsch und Val Müschauns eine unterschiedliche Rolle im Sedimentfluss-System des Schweizerischen Nationalparks einnehmen. Abhängig von der Talmorphometrie und der individuellen glazialen Geschichte weisen alpine Sedimentkaskaden verschiedene räumliche und zeitliche Dynamiken auf. Der methodologische Rahmen dieser Arbeit verdeutlicht zudem, dass die Kombination aus einer klassischen geomorphologischen Feldkartierung und morphometrischen Analysen in ArcGIS ein großes Potential für ein besseres Verständnis alpiner Sedimentkaskaden birgt.

## CONTENTS

|   |             |
|---|-------------|
| <b>Declaration of authorship.....</b>                                 | <b>II</b>   |
| <b>Danksagung .....</b>   | <b>III</b>  |
| <b>Abstract.....</b>  | <b>IV</b>   |
| <b>Zusammenfassung.....</b>   | <b>VI</b>   |
| <b>List of figures and tables .....</b>                               | <b>X</b>    |
| <b>List of abbreviations .....</b>                                    | <b>XIII</b> |
| <b>Index of appendices.....</b>                                       | <b>XIV</b>  |
| <b>Index of supplemented maps.....</b>                                | <b>XV</b>   |
| <b>1 INTRODUCTION.....</b>  | <b>1</b>    |
| 1.1 Problem statement .....   | 1           |
| 1.2 Main questions and objectives of the study.....                   | 2           |
| <b>2 STATE OF THE ART .....</b>                                       | <b>3</b>    |
| 2.1 Spatio-temporal variability of alpine systems .....               | 3           |
| 2.2 Alpine geosystems as cascading systems.....                       | 4           |
| 2.2.1 The concept of alpine sediment cascades.....                    | 4           |
| 2.2.2 System connectivity and landform coupling.....                  | 6           |
| 2.3 Sediment storage landforms and associated processes.....          | 8           |
| 2.3.1 Talus slopes.....   | 8           |
| 2.3.2 Protalus rampart .....  | 10          |
| 2.3.3 Debris flow cone and channel.....                               | 11          |
| 2.3.4 Rock glacier .....  | 14          |
| 2.3.5 Moraine deposit.....  | 15          |
| 2.3.6 Alluvium .....  | 16          |
| 2.4 Toposequences as tool for studying alpine sediment cascades ..... | 16          |
| 2.5 Sediment fluxes and activity in mountain environments .....       | 17          |
| <b>3 HYPOTHESES AND RESEARCH SYNOPSIS .....</b>                       | <b>20</b>   |
| <b>4 STUDY AREA.....</b>  | <b>22</b>   |
| 4.1 Geographical overview.....  | 22          |
| 4.2 Geological and tectonic setting .....                             | 23          |
| 4.3 Lateglacial history and present glacial setting .....             | 24          |
| 4.4 Geomorphology.....  | 25          |
| 4.5 Climate, vegetation and anthropogenic influences.....             | 26          |

|  |           |
|--|-----------|
| <b>5 DATA AND METHODS .....</b>  | <b>27</b> |
| 5.1 Data .....   | 27        |
| 5.2 Geomorphological mapping .....   | 28        |
| 5.2.1 Pre-mapping .....  | 28        |
| 5.2.2 Mapping catalogue .....  | 28        |
| 5.2.3 Mapping campaign and field work .....  | 29        |
| 5.2.4 Data processing: digitalisation and cartographic representation.....   | 29        |
| 5.3 Inventory and geomorphometric characterisation of landforms .....  | 31        |
| 5.4 Assessment of toposequences and neighbourhood relationships .....  | 32        |
| 5.5 Analysis of connectivity between hillslopes and the fluvial system.....  | 34        |
| 5.5.1 Qualitative estimation of connectivity .....   | 34        |
| 5.5.2 Modelling of connectivity index .....  | 35        |
| 5.6 Calculation of storage activity and sediment supply potential.....   | 37        |
| <b>6 RESULTS.....</b>  | <b>39</b> |
| 6.1 Geomorphological setting of the study areas ( <i>M-1, M-2</i> ) .....  | 39        |
| 6.2 Spatial distribution and characteristics of storage landforms ( <i>M-3, M-4</i> ).....   | 42        |
| 6.3 Major toposequence types ( <i>M-5, M-6</i> ) .....   | 46        |
| 6.4 Functional relationships between neighbouring landforms.....   | 48        |
| 6.5 Strength of connectivity between storage landforms and stream.....   | 51        |
| 6.5.1 Connectivity degree based on conceptual approach ( <i>M-7, M-8</i> ) .....   | 51        |
| 6.5.2 Quantitative connectivity index based on numeric approach ( <i>M-9, M-10</i> ) .....   | 54        |
| 6.6 Activity of sediment storages ( <i>M-11, M-12</i> ) .....  | 56        |
| 6.7 Potential for sediment supply to the fluvial system ( <i>M-13, M-14</i> ) .....  | 58        |
| <b>7 DISCUSSION .....</b>  | <b>60</b> |
| 7.1 Potential error sources of the study and limitations of basic assumptions.....   | 60        |
| 7.2 Spatial organisation of sediment storages in meso-scale alpine systems.....  | 63        |
| 7.3 Evidence of paraglacial activity in the deglaciated alpine basins?.....  | 66        |
| 7.4 Understanding sediment trajectories and the role of functional storage relationships with respect to time and space .....      | 68        |
| 7.5 The role of alpine sediment cascades within the sediment flux system.....  | 71        |
| 7.6 Can conventional geomorphological mapping be replaced by numeric methods to explain the complexity of alpine geosystems? ..... | 77        |
| <b>8 CONCLUSION AND OUTLOOK .....</b>  | <b>79</b> |
| <b>9 References .....</b>  | <b>81</b> |
| <b>10 Appendix</b>   |           |
| <b>11 Supplemented maps</b>  |           |

## LIST OF FIGURES AND TABLES

|  |    |
|--|----|
| <b>Fig. 2.1:</b> Conceptual model of the lateral sediment cascade illustrating the different processes and storage types in each subsystem. Own illustration (image: Val Müschauns) referring to SCHROTT et al. 2003. ....                                       | 5  |
| <b>Fig. 2.2:</b> Talus slopes in the upper Val Müschauns, SNP. Single solifluction lobes indicating active cryogenic processes as well as small debris flow tracks with the talus debris are visible. ....   | 9  |
| <b>Fig. 2.3:</b> Protalus rampart along the upper slopes of Val dal Botsch.....  | 11 |
| <b>Fig. 2.4:</b> Hillslope-type debris flows in the lower Val dal Botsch (a) and torrent-bed type debris flows (b) along the southern slopes of Val Müschauns (b). ....  | 12 |
| <b>Fig. 2.5:</b> Schematic diagram of a debris flow surge. Source: HUNGR 2005: 18. ....  | 13 |
| <b>Fig. 2.6:</b> Single-phase continuum models. Source: TAKAHASHI 2007: 39 ....  | 13 |
| <b>Fig. 2.7:</b> Schematic illustration of logarithmic relationship between drainage area (km <sup>2</sup> ) and local slope (m/m) showing the hypothetical topographic signatures for hillslope and valley processes. For a detailed description see text. .... | 14 |
| <b>Fig. 2.8 (top):</b> Moraine deposits in the upper Val dal Botsch, reworked by rill erosion and cryogenic creep resulting in the formation of garlands (Girlandenrasen).   |    |
| <b>Fig. 2.9 (right):</b> Alluvial deposits with large inputs of gravitational hillslope processes in Val Müschauns. ....   | 15 |
| <b>Fig. 2.10:</b> The nine-unit slope model by DALRYMPLE et al. (1968) (modified). For description see text. ....  | 16 |
| <b>Fig. 2.11:</b> The paraglacial sedimentation during the paraglacial period. Source: BALLANTYNE 2002a: 372. ....   | 19 |
| <b>Fig. 2.12:</b> The paraglacial sedimentation cycle modified by CHURCH & SLAYMAKER (1989). Source: SLAYMAKER 2009: 76. ....  | 19 |
| <b>Fig. 3.1:</b> Flow chart of the structure and the major research steps of the master thesis. All created maps are labelled by a M- (M-1, M-2) and supplemented at the end of this thesis. ....  | 21 |
| <b>Fig. 4.1:</b> Swiss National Park (small map) and position of the two study sites Val dal Botsch (red border) and Val Müschauns (orange border) as well as major locations (large map). Image source: Landsat © 2012. Swisstopo. ....                         | 22 |
| <b>Fig. 4.2 (right):</b> Val Müschauns, a northern tributary of the Val Trupchun. Image source: Google Earth 2011. ....  | 23 |
| <b>Fig. 4.3 (left):</b> Val dal Botsch in the northeast of the SNP. Image source: Google Earth 2011. ....  | 23 |

|   |    |
|---|----|
| <b>Fig. 4.4:</b> Geomorphic setting and vegetation characteristics of the study areas. Talus slopes bordered by moraine deposits within the upper valley of Val dal Botsch (a). Debris flow deposits near the outlet of Val dal Botsch (b). Typical vegetation zones within the study areas (c). Interfingering of active and vegetated hillslope debris flows in the middle basin of Val Müschauns (d). Upper U-shaped trough of Val Müschauns (e). Typical plants of the alpine zone in Val Müschauns (f).....  | 25 |
| <b>Fig. 5.1:</b> Calculation of the normed distance (ND) to the watershed (ws).....   | 31 |
| <b>Fig. 5.2:</b> Semi qualitative assessment of connectivity between storage landforms and stream, regarding temporal dynamics and vegetation cover.....  | 34 |
| <b>Fig. 5.3:</b> Graphic illustration of the numeric GIS-modelling approach. For explanation see text. Source: by BORSELLI et al. 2008 (modified).....  | 35 |
| <b>Fig. 5.4:</b> Evaluation of the sediment supply potential. Own graphic, referring to THELER et al. (2010).....   | 38 |
| <b>Fig. 6.1:</b> Morphometric characteristics of storage landforms in Val dal Botsch: a) Slope gradients, b) altitudinal distribution and c) normed distance to watershed (0= watershed, 1=stream). The boxplots depict the minimum, maximum, median as well as the upper and lower quartile of the data for each landform. The thickness of the boxplots in Val dal Botsch represents the sample size (number of objects/number of raster cells). In Val Müschauns, the specific thickness of boxplots is not illustrated, since the sample size of some landforms was tool small..... | 44 |
| <b>Fig. 6.2:</b> Topological sketches of major toposequence types in Val dal Botsch. Relative frequency and major position within the catchment is also displayed. Red lines specify decoupled boundaries, as will be explained in chapter 6.4. The storage type talus slope comprises talus slopes as well as talus slope/debris flows.....  | 46 |
| <b>Fig. 6.3:</b> Topological sketches of major toposequence types in Val Müschauns. For description see fig. 6.2.....   | 48 |
| <b>Fig. 6.4:</b> Comparison of overall qualitative (qual.) and quantitative (quant.) connectivity degree in Val dal Botsch (VdB) and in Val Müschauns (Mue).....  | 52 |
| <b>Fig. 6.5:</b> Variation in modelled connectivity degree with increasing proximity to the stream (a), altitude (b) and slope angle (a). Val dal Botsch (white boxes), Val Müschauns (grey boxes), see also appendix G-21.....   | 55 |
| <b>Fig. 6.6:</b> Variation in activity depending on altitude (a), slope position (b) and slope gradients (c). Val dal Botsch (white boxes) and Val Müschauns (grey boxes).....  | 57 |
| <b>Fig. 6.7:</b> Sediment supply potential of the land surface of Val dal Botsch and of Val Müschauns. Comparison between the qualitative and the quantitative assessment.....  | 58 |

|  |    |
|--|----|
| <b>Fig. 6.8:</b> Altitudinal variations of sediment supply potential in Val dal Botsch (a) and Val Müschauns (b). White boxplots (semi-qual.), grey (quant.). Variations on slope profile are illustrated in appendix I-27.....  | 59 |
| <b>Fig. 7.1:</b> Qualitative model of the hillslope sediment cascade in the Swiss National Park, based on the analysed in Val dal Botsch and Val Müschauns. ....   | 65 |
| <b>Fig. 7.2:</b> Longitudinal variability of sediment cascades in the Swiss National Park due to spatial variations in storage pattern and neighbourhoods, connectivity, activity and sediment supply.....   | 68 |
| <b>Fig. 7.3:</b> Upper basin of Val dal Botsch. In total, 15 % of the valley is decoupled by moraine deposits, e.g. the talus slopes shown at the right side of the photo.....   | 73 |
| <b>Fig. 7.4:</b> Decoupled talus slopes in Val Müschauns. Nearly the entire upper valley is decoupled buffered by moraine deposits and bedrock outcrops. ....  | 73 |
| <b>Fig. 7.5:</b> Illustration of the sediment fluxes systems of Val dal Botsch and Val Müschauns. The size of boxes correlates to the relative size of storage landform. The relative storage surface is given as percentage n brackets. The median sediment supply potential is displayed for the qualitative (left hand side box colour) and quantitative analysis (right hand side box colour). ....                                    | 75 |
| <br>   |    |
| <b>Table 5.1:</b> Primary and secondary landform attributes according to DIKAU (1989) and their geomorphic relevance (DIKAU & SCHMIDT 1999).....   | 31 |
| <b>Table 5.2:</b> Newly created conceptual framework to study the functional relationships between neighbouring landforms. ....  | 33 |
| <b>Table 6.1:</b> Functional relationships of neighbouring storages in Val dal Botsch. The neighbourhood-types are classified regarding the displacement of the separating storage boundary (columns) and the dynamics of the sediment throughput (rows). “Continuous-episodic” and “continuous-periodic” also operate vis-à-vis as “episodic-continuous” and “periodic-continuous”. The term “channel” defines debris flow channels. .... | 49 |
| <b>Table 6.2:</b> Functional relationship of neighbouring storage in Val Müschauns. For description see table 6.1. ....  | 50 |
| <b>Table 6.3:</b> Connectivity degree of the sediment storage types in Val dal Botsch. Results of the qualitative study approach and numeric modelling. “0” signifies decoupling. See also appendix G-18. ....   | 53 |
| <b>Table 6.4:</b> Connectivity degree of sediment storage types in Val Müschauns. See also appendix G-19. ....   | 54 |

## LIST OF ABBREVIATIONS

|   |   |
|---|---|
| <b>A</b> = contributing area/source point A                             | <b>p<sub>dn</sub></b> = probability that sediment arrives at downslope sink |
| <b>Al</b> = Alluvium  | <b>p<sub>up</sub></b> = probability that sediment arrives at upslope source |
| <b>Al/Col</b> = Alluvium/Colluvium                                      | <b>R<sup>2</sup></b> = correlation coefficient                              |
| <b>a.s.l.</b> = above sea level   | <b>Ramp</b> = Protalus rampart  |
| <b>ArcGIS</b> = Geographic Information System of the concern ESRI       | <b>RI</b> = Roughness Index of surface                                      |
| <b>Bedr</b> = Bedrock   | <b>Rockgl</b> = Rock glacier  |
| <b>C(-factor)</b> = crop/vegetation and management factor of the USLE   | <b>RUSLE</b> = <i>Revised Universal Soil Loss Equation</i>                  |
| <b>CI</b> = Connectivity Index  | <b>S</b> = local slope  |
| <b>Chan</b> = Channel   | <b>s</b> = second(s)  |
| <b>Col</b> = Colluvium  | <b>S(-factor)</b> = slope factor  |
| <b>Compl</b> = Talus slope/debris flows (Complex)                       | <b>SDR</b> = dimensionless sediment delivery ratio                          |
| <b>D<sub>dn</sub></b> = downslope component of connectivity             | <b>semi-qual.</b> = semi-qualitative  |
| <b>Debrisfl</b> = Hillslope debris flows                                | <b>SNP</b> = Swiss National Park  |
| <b>DEM</b> = digital elevation model                                    | <b>SPI</b> = Stream Power Index   |
| <b>du/dz</b> = rate of strain at a velocity <i>u</i> at height <i>z</i> | <b>SSY</b> = Specific Sediment Yield  |
| <b>D<sub>up</sub></b> = upslope component of connectivity               | <b>Std. dev./STD</b> = standard deviation                                   |
| <b>fig.</b> = figure  | <b>SY</b> = Sediment Yield  |
| <b>GIS</b> = Geographic Information System                              | <b>t</b> = tons   |
| <b>GMK 25/100</b> = Geomorphologische Karte 1:25000/1:100000            | <b>tab.</b> = table   |
| <b>I</b> = input of sediment  | <b>tan</b> = tangent  |
| <b>ID number</b> = identification number                                | <b>TK 25</b> = Topographische Karte 1:25000                                 |
| <b>J</b> = Joule  | <b>unsp</b> = unspecified   |
| <b>km</b> = kilometres  | <b>USLE</b> = Universal Soil Loss Equation                                  |
| <b>km<sup>2</sup></b> = square kilometre                                | <b>VdB</b> = Val dal Botsch   |
| <b>km<sup>3</sup></b> = cubic metre                                     | <b>W(-factor)</b> = weighting factor  |
| <b>log</b> = logarithm  | <b>ws</b> = watershed   |
| <b>m</b> = metre  | <b>x<sub>i</sub></b> = value of specific cell within a DEM                  |
| <b>M-</b> = supplemented map-   | <b>x<sub>m</sub></b> = mean value of 25 cells within a DEM                  |
| <b>m<sup>2</sup></b> = square metre                                     | <b>Δ S</b> = change of storage  |
| <b>m<sup>3</sup></b> = cubic metre                                      | <b>Tal</b> = talus slope  |
| <b>mm</b> = millimetre  | <b>τ<sub>y</sub></b> = shear stress   |
| <b>Mor</b> = Moraine  | <b>%</b> = per cent   |
| <b>Mue</b> = Müschauns  | <b>°</b> = degree   |
| <b>ndist/ND</b> = normed distance                                       | <b>°C</b> = degree Celsius  |
| <b>O</b> = output of sediment   | <b>∞</b> = infinite   |

## **INDEX OF APPENDICES**

**A** Sediment storages in alpine environments

**B** Tectonic-geological setting of the study areas

**C** Methods for analysing alpine sediment cascades

**D** Morphometric characterisation of process domains

**E** Spatial distribution and morphometric characteristics of storage landforms

**F** Spatial distribution and morphometric characteristics of storage landforms

**G** Degree of hillslope-channel connectivity in the study areas

**H** Activity of land surface and storage landforms

**I** Potential for sediment supply of the alpine valleys

## **INDEX OF SUPPLEMENTED MAPS**

- M-1** Geomorphological map of Val dal Botsch
- M-2** Geomorphological map of Val Müschauns
- M-3** Sediment storage landforms of Val dal Botsch
- M-4** Sediment storage landforms of Val Müschauns
- M-5** Toposequences of Val dal Botsch
- M-6** Toposequences of Val Müschauns
- M-7** Hillslope-channel-connectivity in Val dal Botsch (conceptual approach)
- M-8** Hillslope-channel-connectivity in Val Müschauns (conceptual approach)
- M-9** Hillslope-channel-connectivity in Val dal Botsch (numeric modelling)
- M-10** Hillslope-channel-connectivity in Val Müschauns (numeric modelling)
- M-11** Sediment storage activity in Val dal Botsch
- M-12** Sediment storage activity in Val Müschauns
- M-13** Potential for supplying sediment to the fluvial system in Val dal Botsch
- M-14** Potential for supplying sediment to the fluvial system in Val Müschauns

# 1 INTRODUCTION

*Alles, was die Natur selbst anordnet, ist zu irgendeiner Absicht gut. Die ganze Natur überhaupt ist eigentlich nichts anderes, als ein Zusammenhang von Erscheinungen nach Regeln; und es gibt überall keine Regellosigkeit.*  
Immanuel Kant, 1724-1804

## 1.1 Problem statement

Alpine environments represent one of the major morphological systems and one of the most inspiring natural features on the Earth's surface. The complex interaction between climate, tectonics and surface processes, all of which operate over various spatial and temporal scales, defines mountains as highly variable and sensitive systems (BARSCH & CAINE 1984, OWENS & SLAYMAKER 2004). As a consequence, alpine geosystems portray a complexly organised and highly dynamic pattern of neighbouring and overlapping geomorphological landforms (BRUNSDEN 1996, DIKAU 1996, 2006). Those landforms store variable amounts of sediment, which have the potential to be mobilised and transported by various geomorphic processes. Alpine environments therefore have to be understood as cascading systems, where sediment is transferred along specific spatial sequences of sediment storage landforms by different mainly gravity-driven processes (CHORLEY & KENNEDY 1971, CAINE 1974). The sediment connectivity and the internal storage coupling play a crucial role for the length of the variable periods of storing and dispersing sediment within a catchment (CAINE 1986, HARVEY 2001, 2002). Particularly, the connectivity of a landform with a stream channel contributes directly to the sediment delivery problem (WALLING 1983) and influences the mode, efficiency and scale of sediment fluxes in mountain basins (BRIERLEY et al. 2006, FRYIRS et al. 2007). Dynamic system changes, which can be induced by climate, tectonics or human influences, cause varying process activities over time. Specifically, the deglaciation of alpine basins may influence the storage of sediment and the efficiency of sediment supply (CHURCH & RYDER 1972; BALLANTYNE 2002a,b). Up to now, there is still a need to gain further insights regarding alpine sediment cascades and their role within the sediment flux system, especially with respect to temporal and spatial dynamics. Today, the lower parts of alpine valleys are occupied by vulnerable human infrastructure. This directly conflicts to the extreme sensitivity of mountain systems to fluctuations in climate. The predicted global warming (IPCC 2001) will perturb alpine geosystems, which in turn may react with increasing geomorphic activity. In particular, the loss of glacier ice masses or the degradation of permafrost due to the temperature rise will expose and destabilise rock faces and debris accumulations (HEARBERLI & BENISTON 1998, GRUBER & HEABERLI 2007, STOTT & MOUNT 2007). The creation of new sediment sources will considerably affect the sediment transport and connectivity within alpine systems (OTTO & SCHROTT 2010). Consequently, the volume of transported sediment will increase and pose significant hazards to human settlements and economic infrastructure in alpine areas (EVANS & CLAGUE 1994). In order to identify areas in alpine catchments, which are sensitive to future climate and geomorphic changes, a comprehensive analysis of sediment storages, routing pathways and internal

relationships will be the future task for the research of geomorphology. Thereby, a profound understanding of alpine sediment cascades will provide important knowledge for sediment budget studies and for future land-use and risk management activities in those highly dynamic systems.

## 1.2 Main questions and objectives of the study

The main intention of this master thesis is to better understand alpine cascading geosystems. In this study, the alpine sediment cascade is defined to be restricted to the lateral sediment transfer along hillslopes from valley ridge to the channel stream and the storage of material in-between. Hence, the channel network and the valley outlet (the fluvial system) are considered as final sink of the hillslope sediment fluxes. Following SLAYMAKER (1991), the meso- ( $10^2 - 10^4 \text{ km}^2$ ) and macro-scales ( $10^4 - 10^8 \text{ km}^2$ ) might be the only spatial scales at which the unique signals of alpine cascading geosystems can likely be expected. In this thesis, two meso-scale, deglaciated valleys in the Swiss National Park (SNP) – Val dal Botsch and Val Müschauns – are studied, which offer a high diversity of geomorphic processes and sediment storage types. The catchment morphometry differs greatly: While Val dal Botsch is a reasonably V-shaped valley, Val Müschauns considerably broadens to a U-shaped valley within its upper trough. Due to its status as national park, the SNP is an excellent place to examine almost natural geomorphic transfer and storage processes, undisturbed by human influences. The focus of this study is on the *recent/current* geomorphic situation of storage landforms and geomorphic processes. The alpine sediment cascade will be examined on three different spatial scales: On the level of the individual sediment *storage landform*, along the *hillslope* profile and on the *catchment* scale. Several questions are of particular interest:

- *In which manner is sediment stored in meso-scale basins?*
- *In which manner is sediment routed along hillslopes in meso-scale basins?*
- *What functional relationship exists between neighbouring storage landforms?*
- *How much does the connectivity between hillslopes and the fluvial system vary spatially in meso-scale basins and what are the major controlling factors on this variability?*
- *What can be inferred from the connectivity and activity regarding the sediment flux system?*

To answer these questions, a thorough analysis of sediment storage landforms, trajectories and internal linkages is needed. This task results in following main objectives:

- A) Identification and characterisation of sediment storage landforms.*
- B) Assessment of trajectories of sediment routing through the alpine sediment cascade.*
- C) Comprehension of the functional relationships between neighbouring storage landforms.*
- D) Assessment, both qualitatively and quantitatively, as well as interpretation of the strength of connectivity between the hillslope system and the stream channel.*
- E) Evaluation of the role of alpine sediment cascades within the alpine sediment flux system.*

A flow chart of the thesis structure and all working steps is presented in figure 3.1.

## 2 STATE OF THE ART

In the following chapter, significant studies, theoretical and methodological concepts and terminologies will be presented to reveal major research gaps and to deduce the hypotheses.

### 2.1 Spatio-temporal variability of alpine systems

Up to now, there is no precise definition for alpine environments. German mountain geomorphologists, such as TROLL (1966), differentiate between high mountains, mountains and uplands/highlands. With a more geomorphic focus, BARSCH & CAINE (1984) introduce four key characteristics: elevation, steep gradients, rocky terrain and the presence of snow or ice. Since not all of those features are explicitly present in high elevations (OWENS & SLAYMAKER 2004), further criteria specify mountain systems: indicative climatic-vegetative zones, high potential energy for sediment movement, clear evidence of late-Pleistocene glaciation and active tectonic rates, sometimes exceeding those of erosion (TROLL 1973, BARSCH & CAINE 1984).

All these definitions indicate that alpine geosystems are characterised by a high variability of geomorphic processes, landforms and environmental conditions, all of which strongly influence each other (OTTO 2006): Whereas the high relief and the steep slopes are responsible for low temperatures and high precipitation, the mountain climate, in turn, controls the morphodynamic activity and may result in infrequent processes of intense magnitude. Consequently, alpine geosystems are situated in a metastable state and are characterised by an inherent fragility and high sensitivity to external disturbances (BARSCH & CAINE 1984).

Mountain geomorphology is faced with the problem of linking an observable process with an existing landform, because alpine landscapes represent a “mosaic of landforms” of different sizes and evolution stages (TWIDALE 1985). BÜDEL (1981, in DIKAU 1996) defines a (alpine) landscape as a composite of various “relief generations”, in terms of nested, hierarchically organised landforms as result of consecutively or/and parallel acting processes of different intensity and duration. CHORLEY et al. (1984) describe this nested hierarchy as palimpsest, where smaller landforms occur on top of larger ones and older forms are partially removed by younger landforms. Thereby, older landforms create the boundary conditions for current processes (see OTTO & DIKAU 2004: 324). From this perspective, alpine environments have to be understood as multiphase and polygenetic systems, which contain a more or less strongly developed “memory” of past processes of varying temporal and spatial scales (DIKAU 1996, 2006).

BRUNSDEN (1996) translates this spatio-temporal scale-dependency of landforms into a graphical form (see appendix A-1). According to this, alpine environments are characterised by a pronounced temporal and spatial landform hierarchy, expressed in landform size as well as duration of formation/erosion. For instance, the several Pleistocene glaciation cycles gave rise to the typical shape of alpine valleys within long time scales of several thousand years. After

deglaciation, landforms such as talus slopes were accumulated along the steep hillslopes within a timespan of only a few hundred or thousand years. Those landforms act as sediment sources and provide the boundary conditions for current, short-living processes such as debris flows or solifluction. Those rapid events subsequently erase older, relict landforms, in turn creating superimposed forms within a very short time of a few years up to seconds (see OTTO 2006: 9).

Alpine geosystems respond to external disturbances in a complex way. This is due to the spatially and temporally variable system configuration and various internal thresholds (variable sensitivity) within these system components, as shown by SCHUMM (1979) and BRUNSDEN (2001). PHILIPPS (1992, 2003) goes one step further and assumes a complex, nonlinear dynamic within (alpine) geosystems due to nine sources of nonlinearity (see summary in PHILIPPS 2003: 9f.). Hence, the outputs of a complex nonlinear geosystem (= landforms) are not proportional to the inputs (= processes). Although PHILIPPS's concept seems to complicate the interpretation of source-sink-linkages remarkably, it may provide a good explanation of chaotic phenomena. Moreover, it replaces the previous idea of a "geomorphology of equilibrium" (see DIKAU 2006: 173).

Instead of reaching an equilibrium state, alpine environments evolve along trajectories. It seems that current system responses are still controlled by their specific history, indicating a path dependence of geosystems (DIKAU 2006). Past events have changed the internal thresholds in such a way, that the future reactions of the geosystem will be remarkably determined by its inherent history for several thousands of years. A specific case of path dependence is the paraglacial cycle, as studied by VERLEYSDONK et al. (2011), in the terms that glacially conditioned sediment are still key driver for the relief development and sediment flux after glacier retreat.

## **2.2 Alpine geosystems as cascading systems**

### **2.2.1 The concept of alpine sediment cascades**

In alpine environments, the transfer of sediment and the resultant formation of specific sediment storage landforms occur in a cascading way according to the "concept of sediment cascades" developed by CHORLEY (1962) and popularised by CHORLEY & KENNEDY (1971). A cascading system is composed of a chain of different subsystems, which are dynamically coupled or connected by a cascade of mass and/or energy proceeding along a gravitational gradient. The output of mass – and specifically of sediment – from a higher subsystem creates the input into a subsequent lower subsystem. The intermediate storage of sediment might result in notable time lags or, moreover, in a total interruption of the transport path (CHORLEY & KENNEDY 1971). OTTO et al. (2009) point out that in alpine basins, sediments mostly reside much longer in storage than in transport.

Concerning the terminology of the storage term, it is suitable to differ between "sediment stores", which are more transient, short-lived and quickly modifiable landforms (e.g. channel bars,

levees), and “sediment sinks”, representing more permanent zones of storage, where sediments spend considerable periods of time (e.g. talus slopes, floodplains) (HOOKE 2003, FRYIRS 2012).

The intensity of immediate storage of sediment and the degree of sediment transfer is basically controlled by regulators (e.g. vegetation cover), which, in turn, depend on internal (e.g. angle of slope) and external thresholds (e.g. rainfall or frost activity) (GÖTZ et al. 2010). Moreover, the catchment morphometry and specifically, the available accommodation space (wide alluvial valleys vs. partly-confined valleys), plays a crucial role in whether sediment is more likely to be stored for varying periods or conveyed by cascading trajectories (FRYIRS 2012).

Significant feedback effects may influence the cascading system, as the transfer of sediment may contemporarily modify the system configuration such as the role of regulators and the availability of material. For instance, debris flow events may erode the vegetation cover or/and change the material fills within hillslope channels (HAAS et al. 2004).

Referring to SCHROTT et al. (2002), an alpine sediment cascade can be roughly divided into three subsystems, each with a specific suite of storage landforms (fig. 2.1): Subsystem I represents the rock walls and cirques, subsystem II comprises the hillslopes and subsystem III consists of the valley floor and the stream channel. Providing an ultimately gravity-controlled sediment transfer, the subsystems and their specific storages are connected by distinct geomorphic processes acting either discontinuously through time as large fluxes or slowly, more continuously over longer time-scales (REID & DUNNE 1996).

The major initial source of sediment is the exposed bedrock of the cliff face providing weathered material. Debris production is mainly dominated by mechanical (e.g. frost action) and chemical (e.g. biotic influence) weathering processes, as well as locally active bedrock erosion (e.g. through movement of rainwater and sediment) (CAINE 1974). The subsequent transfer of the freshly

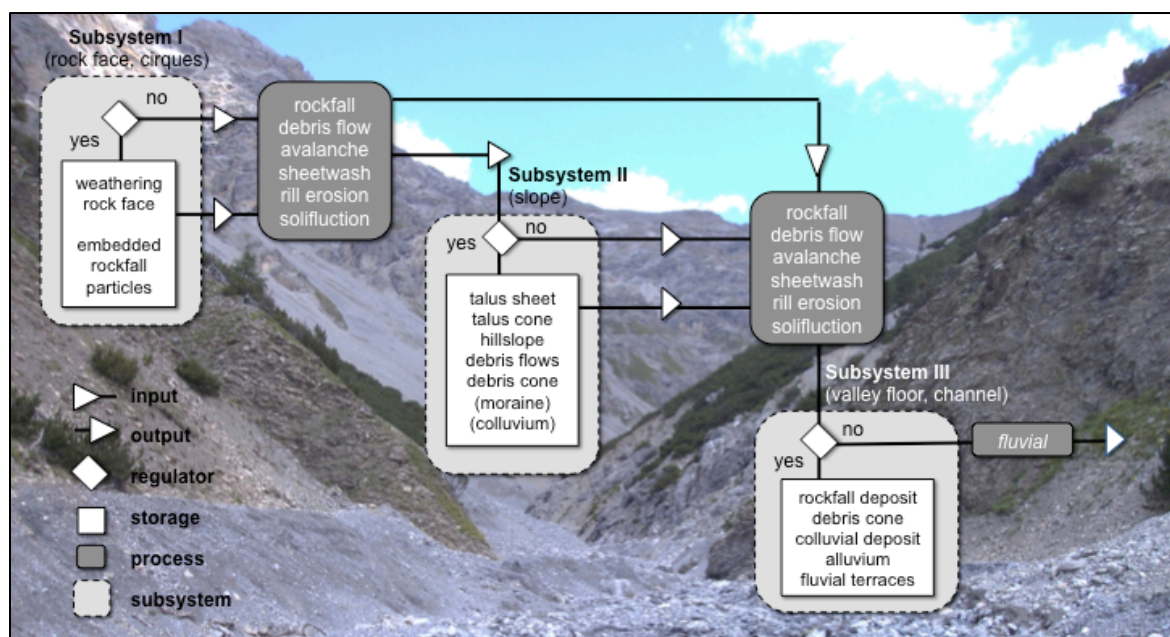


**Fig. 2.1:** Conceptual model of the lateral sediment cascade illustrating the different processes and storage types in each subsystem. Own illustration (photo: Val Mütschans) referring to SCHROTT et al. 2003.

detached material from the steep rock face commonly occurs in the form of primary and secondary rockfall processes (KRAUTBLATTER & DIKAU 2007), varying from small-scale debris falls to catastrophic failure of several million cubic metres (WHALLEY 1984). The accumulated sediments along the hillslopes might build up talus slopes, in the form of sheets and cones. Contemporarily, large amounts of rock particles can still rest in immediate storages within small irregularities inside the cliffs until they will be removed as a secondary rockfalls.

Subsequently, talus slopes display the starting point for ensuing gravitational processes that become activated with decreasing slope gradient. Debris flows are one of the major events incising the accumulated talus deposits afterwards. They remobilise and transport the material further downslope resulting in the deposition of debris cones at the footslopes. Besides debris flows, sheetwash and linear rill erosion with gully erosion, solifluction and snow avalanches represent further mechanisms of sediment reworking and onward transportation.

In alpine basins with a stream channel along the valley floor, the deposited sediment storages may be directly coupled with the fluvial system via distinct transport pathways or through changing system conditions like flooding events. Therefore, the output of sediment from the hillslope subsystems built up the input into the stream channel. Finally, flood events and inundations may result in the deposition of alluvial and fluvial deposits within the valley floor, representing one of the ultimate storage types within the lateral alpine sediment cascade.

### 2.2.2 System connectivity and landform coupling

Significant uncertainties remain over the relationship between storage landforms, both among each other and the fluvial system, and the role that this relationship plays in controlling the mode and efficiency of the cascading sediment transfer (HARVEY 2001, 2002, BEEL et al. 2011). In this context, the concept of connectivity and coupling provides the central framework. However, until today, there is no uniform scientifically evaluated basis. The use of the terms connectivity and coupling seems to be relatively ambiguous, as stated by WAINWRIGHT et al. (2011), and moreover without specific terminological distinction.

In this study, the use of the term “connectivity” is based on the definition of FRYIRS (2012: 3) describing connectivity as “water mediated transfer of sediment between two different compartments of the catchment sediment cascade”. Connectivity focuses on the *potential* that sediment is routed along the hillslopes down to the stream network and finally, to the basin outlet. Instead, the term “coupling” is used in this study to describe the *functional relationship* between two (or more) neighbouring sediment storages. Hence, the combined effect of lateral coupling along a hillslope leads finally to connectivity (HECKMANN & SCHWANGHART 2012: 1). In this study, the functional relationship between storages is assumed to manifest in the sediment throughput across the separating storage boundary as well as the long-term displacement of the landform boundary.

Since the first studies in the 1980s by CAINE & SWANSON (1989), literature and theoretical concepts that focus on the linkages between the subsystems of a catchment have increased, particularly in geomorphology research. For instance, in the context of landscape sensitivity, BRUNSDEN & THORNES (1979) and BRUNSDEN (1993) differentiate between coupled, not coupled and decoupled. CROOKE et al. (2005) differ between direct connectivity, which is given through channels or gullies, and diffuse connectivity, where sediment is transferred by overland flow or surface runoff. In most of the geomorphic studies, connectivity between two system compartments develop either through physical contact or through the transfer of material. On the basis of these two factors, JAIN & TANDON (2010) proposed four connectivity types, thereby considering the temporal variability of sediment transfer. Although mainly oriented to river-channel systems, HOOKE (2003) provided valuable ideas for sediment connectivity and describes connectivity as “partial/episodic”, where sediment transfer occurs only during episodic extreme events, and a “potential”, where a connection will be attained by a change of the current system configuration.

This selection of common conceptual frameworks already shows that connectivity and coupling operate at different spatial and temporal scales. For instance, BRIERLEY et al. 2006, FRYIRS et al. (2007) and FRYIRS (2012) consider in their significant concept a longitudinal, lateral and vertical operation of sediment cascades. Accordingly, sediment transfer can be affected by three types of (dis)connecting landforms at different spatio-temporal scales: Buffers, barriers and blankets. With regard to the lateral sediment cascades along hillslopes, on which this study focuses, buffers may play a key role. Buffering landforms such as vegetated, less inclined moraine valley fills, bedrock outcrops or fluvial terraces may disrupt the lateral linkages within a catchment and impede sediment delivery from slopes to the fluvial system. Buffers may lead to residence times in order of hundreds to thousands of years (FRYIRS 2012). Furthermore, the strength of connectivity highly varies, depending on catchment position. As time of residence increases and sediment delivery decreases from headwaters to lowlands, the longitudinal and lateral connectivity weakens downstream. In contrast, channel-floodplain connection intensifies in lowland areas (FRYIRS 2012).

Concerning the temporal variability of connectivity, key drivers are tectonics, climatic or land use changes. For instance, uplift in headwater regions will increase channel gradients and therefore the overall connectivity. Extreme events induced by climate change may result in enhanced erosion of sediment storages and therefore in an increase of hillslope-channel-coupling (JAIN & TANDON 2010). In addition, several studies (e.g. HOOKE 2003, JAIN & TANDON 2010) indicate that the temporal dynamic of geomorphic processes might also play a crucial role for the connectivity of geosystems. Thus, referring to WOLMAN & MILLER (1960), the strength of connectivity depends on both, magnitude and frequency characteristics of sediment transfer processes.

Finally, it becomes clear that the degree of a basin's connectivity controls the volume of sediment fluxes that will be delivered by specific geomorphic transport processes into the fluvial system

(BEEL et al. 2011). Consequently, although not explicitly mentioned, the concept of sediment connectivity is an essential part of the sediment budget approach (BRACKEN & CROKE 2007). It explains the discrepancy between the catchment erosion and the sediment yield at the outlet of a valley (FRYIRS 2012). Moreover, the internal linkages influence the sensitivity of a geosystem towards environmental and anthropogenic changes (BRUNSDEN 2001). The strength of connectivity determines the probability whether a local on-site effect will propagate downslope causing off-site effects (see BORSELLI et al. 2008: 269). While well-coupled basins are sensitive to upstream disturbance and freely transfer any perturbation, a weak connectivity diminishes those upstream impacts for lowlands basins (BEEL et al. 2011).

Sediment connectivity is conventionally analysed based on qualitative interpretation of geomorphological field studies (e.g. SCHLUNEGGER et al. 2005, BEEL et al. 2011) or by using geophysical surveys (e.g. SCHROTT et al. 2003). In contrast, connectivity assessments by means of numeric modelling approaches are scarce, particularly for alpine regions. In the last years, promising numeric studies derived from BORSELLI et al. (2008), HECKMANN et al. (2009), HECKMANN & SCHWANGHART (2012) and CAVALLI et al. (2012). Above all, BORSELLI et al. (2008) developed an automatic procedure to calculate a connectivity index in the context of soil erosion in lowlands, based on a DEM and on the C-factor of USLE. SOUGNEZ et al. (2011) modify this connectivity approach by replacing the C-factor by a relative erosion index that predicts interrill and rill erosion. Likewise, CAVALLI et al. (2012) successively applied a modification of BORSELLI's algorithm in two alpine basins, which are quite similar to the study areas in the Swiss National Park. However, the question arises if such numeric approaches sufficiently explain connectivity between landforms or if qualitative methods are more accurate?

### **2.3 Sediment storage landforms and associated processes**

Alpine environments are characterised by a variety of geomorphic processes that mobilise, transport and deposit variable amounts of sediments along cascading pathways. Each process is related to a specific depositional landform. In the following chapter, the major storage landforms and – if recently active – their associated processes will be presented, with a special focus on debris flows.

#### **2.3.1 Talus slopes**

Rockfall talus slopes (American term) or scree slopes (English term) are steep valley-side accumulations of rock debris that has fallen down more or less continuously from a rockwall dominated by physical weathering and gravitational processes. Hence, they mainly represent one of the first steps of the alpine sediment cascade. According to RAPP (1960b), smaller rockfall events ( $10^1$ - $10^2$  m<sup>3</sup>) are mainly responsible for talus formation: Triggered by pressure release, freeze-thaw activity or weathering on the cliff face, primary processes transfer the freshly detached material from the rock face to the foot of the slope. On rockwalls with irregularities such as benches or

gullies, rock particles can still rest for some time in intermediary storages until they are transported by secondary processes like snow avalanches or surficial water flow (LUCKMAN 2007).

In plan view, three types of rockfall talus slopes can be ideally distinguished (appendix A-2): Relatively featureless rock faces with uniform sediment supply tend to produce straight “talus sheets” (CHURCH et al. 1979). In contrast, on more complex or dissected cliffs rockfalls become concentrated and channelled into gullies or basins leading to the development of “talus cones”. The third type are “coalescing talus cones”. They are formed when single talus cones intersect laterally. However, all three types are most often transitional (LUCKMAN 2007).

In profile view, active and unmodified talus slopes are typified by a segmented profile with an upper rectilinear unit of an overall gradient of 33-35° and a concave basal zone of around 5-30° (FRANCOU & MANTÉ 1990). Due to factors such as lithology, cliff height and modifying geomorphic processes, variations of talus morphology are possible. Depending on lithological characteristics of the source rock face (e.g. joints and bedding, rock type), the talus material is generally composed of angular, irregular rock fragments with a wide range of particle sizes. Once detached from the cliff, rock particles may bounce or roll or/and disintegrate into smaller clasts until they accumulate along the slope. Ideally, there is a downslope increase in particle size with the finest particles near the top and the largest boulders below the talus foot. This “fall sorting” can be attributed to the greater kinetic energy of larger boulders and the frictional resistance (roughness) of the sliding surface (RAPP 1960b). Over time, due to a combination of complex processes of cryogenic action (fig. 2.2), running water, snow avalanche, rockfall impact etc. individual particles on the talus surface may creep downslope, often with an average rate of 1-10 cm/year (LUCKMAN 2007).

Rockfalls of different scales are not only a major component of the sediment transfer, they are also primary drivers of the long-term evolution of hillslope topography (BEYLICH & KNEISEL 2009). The continuous sediment throughput between rock faces and talus slope is related to a gradual rockwall retreat, as studied for example by ANDRÉ (1997), SASS & WOLLNY (2001) or SASS et al. (submitted).



**Fig. 2.2:** Talus slopes in the upper Val Müschauns, SNP. Single solifluction lobes indicating active cryogenic processes as well as small debris flow tracks with the talus debris are visible.

The retreat rate is highly variable in space and time. It can be either discontinuous, but of large magnitude or more continuous through small-scale rockfalls. The focus of this thesis is on low-magnitude, continuous rockfalls representing stable drivers of cliff retreat over longer time scales.

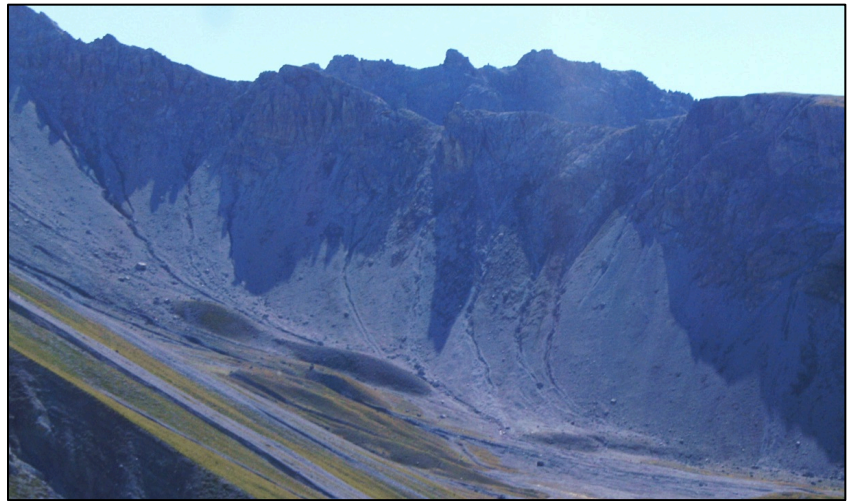
It is traditionally believed that talus deposition is a periglacial phenomenon as result of intensive freeze-thaw cycles in the postglacial period. Yet, many talus slopes are vegetated, possibly indicating that they are essentially relict/fossil features where rockfall activity is currently not existent (see e.g. ANDRÉ 1997). The limited efficiency of periglacial processes therefore appears too less to account for the great volume of some talus deposits. As a consequence, in the last two decades, a paradigm shift occurred as talus slopes are viewed not longer to be wholly periglacial, but more and more as paraglacial landforms whose evolution is already completed (see WILSON 2009: 134). In fact, some studies (e.g. CURRY & MORRIS 2004, HALES & ROERING 2005, HINCHLIFFE & BALLANTYNE 1999, 2009) attribute talus evolution to rapid and extensive sediment accumulation that started immediately after ice retreat, when stress releases and exposure of the rockwalls result in a high susceptibility to cliff failure and mass wasting (“paraglacial concept” see BALLANTYNE 2002a,b, 2008). It is supposed that after several millennia, rockfall supply progressively diminishes due to equilibration of the rockwall to postglacial conditions. Vegetation begins to cover the relict talus slopes and other geomorphic processes (e.g. debris flows) result in a redistribution of sediment and modification of talus form. However, the assumed paraglacial origin of talus slopes must be reviewed critically, as demanded by MCCOLL (2012). Instead, it may be more suitable to consider an interfingering and coexistence of periglacial and paraglacial processes (ITURRIZAGA 2011).

### **2.3.2 Protalus rampart**

A protalus rampart is a ridge or ramp of debris that forms along the downslope margin of a perennial or semi-permanent snowfield (fig. 2.3, appendix A-2). It is typically located near the base of a steep rock face (with a talus) in periglacial environments. Since not all ramparts lie at the foot of a talus, the term “protalus” may be confusing. In contrast, “pronival rampart” seems to be a more preferable term, as proposed by SHAKESBY et al. (1995). Early studies have assumed that ramparts develop entirely through the accumulation of coarse rockfall debris rolling, bouncing and sliding downslope on a snow patch. This supposed simplicity turned ramparts to less interesting and seldomly mentioned landforms in literature. Until the early 1980s, they have been described by many misleading terms such as “talus of snow” or “terminal moraines”. Since most of the studies wrongly identified ramparts as fossil, it is no surprise that there was a circular reasoning linking rational but hypothetical processes to assumed fossil ramparts (SHAKESBY 1997, GOUDIE 2004).

Few studies of active features indicate that a great number of processes may contribute to rampart formation such as rockfall, but also debris flows, avalanches or solifluction. Moreover, bulldozing and large stresses exerted by creeping of the snowfield represent possible involved mechanisms.

**Fig. 2.3:** Protalus rampart along the upper slopes of Val dal Botsch.



Moreover, ramparts are more diverse in material than had been supposed. Single ridges can vary from 1-2 m up to substantial heights of 30 m in thickness (SHAKESBY et al. 1995, 1997). The mainly curved or sinuous ridges have relatively steep slopes with short proximal (adjacent to the snowbed) and long distal slopes (GOUDIE 2004). As a diagnostic criterion, the distance between rampart crest and cliff foot is less than 30-70 m, marked by a shallow backing depression. BALLANTYNE & BENN (1994) assumed that with growing snow thickness, shear stresses generate ice and rampart begins to migrate, increasing the distance to the slope foot.

Finally, two opposing views on rampart formation persist up to now: According to some scientists (e.g. HAEBERLI 1985), a rampart is interpreted as embryonic rock glaciers within a linear developmental continuum of rock glaciers due to permafrost creep. The other view envisages ramparts and rock glaciers as independently products of modified talus occurring in a non-developmental morphological continuum (e.g. SHAKESBY et al. 1995, 1997)

### 2.3.3 Debris flow cone and channel

Debris flows are one of the major mechanisms of sediment transport in mountain systems (BENDA & DUNNE 1987). The deposited cone can be both an important connecting and disconnecting feature in the sediment cascade. Various terminologies and classifications of mass movements belonging to the flow category exist (see INNES 1983). However, referring to COROMINAS et al. (1996: 161): “A debris flow consists of a mixture of fine material (sand, silt and clay) and coarse material (gravel and boulders) with a variable [relatively small] quantity of water, that forms a muddy slurry, which moves downslope, usually in surges induced by gravity and the sudden collapse of bank material”. A more mechanistic distinction is made by IVERSON (1997), positioning the debris flow process between gravitational and fluvial processes as mechanism of interacting solid and fluid forces.

Debris flows are episodic events occurring within a very short time but often moving large quantities of sediments. The initiation of a debris flow essentially depends on three factors: Abundant sources of unconsolidated debris, abundant water saturation/large hydrological drainage area and a steep slope or channel gradient (RICKENMANN 2001). On sediment-mantled hillslopes,

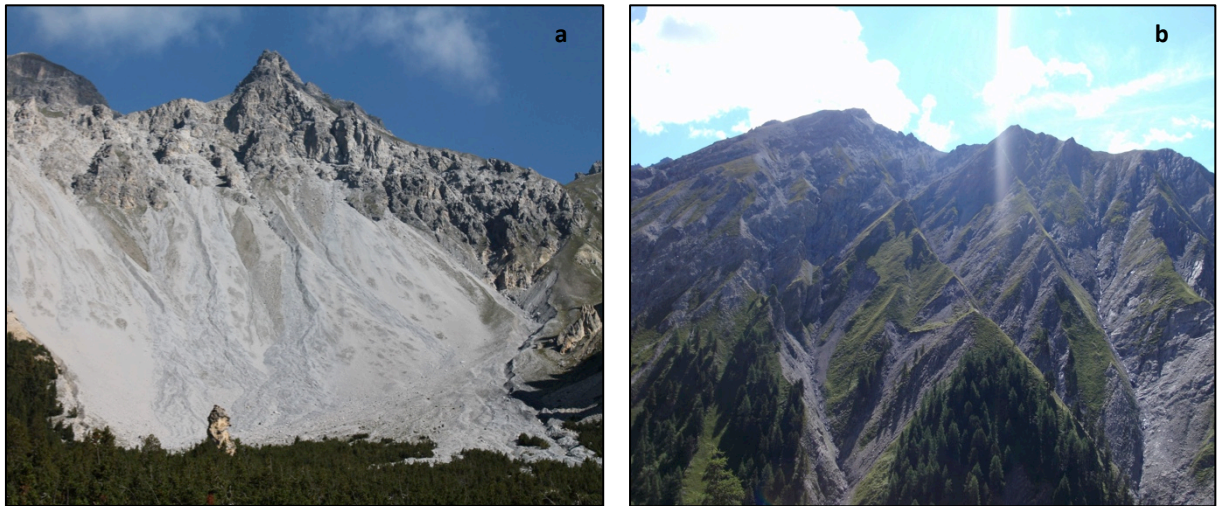


**Fig. 2.4:** Hillslope-type debris flows in the lower Val dal Botsch (a) and torrent-bed type debris flows (b) along the southern slopes of Val Müschauns (b).

debris flows usually develop along slopes steeper than  $30^\circ$ , particularly with sparse vegetation. Accordingly, talus slopes propose excellent initiation zones. Within moraine material, which is more cohesive than nonconsolidated hillslope material, the minimum event triggering gradient ranges between  $27^\circ$  and  $38^\circ$  (RICKENMANN 1995). In this study, depending on the specific initiation site, two different types of debris flows are distinguished: “Slope or hillslope debris flows” (fig. 2.4a, GLADE 2005), which are initiated within the less consolidated talus material, and “torrent bed-type debris flows” as rapid, channelized material flows within hillslope or bedrock channels (fig. 2.4b, SLAYMAKER 1988) – see also appendix A-2.

The most common trigger of debris flows is prolonged or heavy rainfall, often accompanied by snowmelt and permafrost degradation. Undrained loading on talus slopes through e.g. rockfalls, vibration by thunder as well as channelled water in gullies may represent further triggers (INNEN 1983). When regolith becomes saturated, pore pressure increases and shear strength decreases resulting in a failure (COSTA 1984). Various studies (e.g. CAINE 1980, WIEZOREK & GLADE 2005, GUZZETTI et al. 2008) tried to define a threshold relationship between rainfall intensity and duration controlling the initiation of debris flows. Rainfall events of similar magnitude do not necessarily always initiate a debris flow event (GLADE 2005); one major controlling factor is the sediment availability within the initiation area (SELBY 1993). In turn, each event may change the sediment availability and therefore, may constantly modify its own system configuration.

Once triggered, debris flows follow pre-existing drainage ways or move on unobstructed talus slopes in almost any direction by forming their own channels. They can grow dramatically in size and speed, reaching densities of up to  $1.6 - 2.4 \text{ t/m}^3$  and viscosities of more than  $10 \text{ m/s}$  (RICKENMANN 2001). Individual debris flows might develop volumes from less than  $0.1 \text{ m}^3$  to over  $10^9 \text{ m}^3$  resulting in high potential energy of more than  $10^{16} \text{ J}$  (IVERSON 1997) and long travelling distances, sometimes up to several kilometres (TAKAHASHI 1981). As a consequence, debris flows are one of the most dangerous mass movements in alpine regions (RICKENMANN 2001).

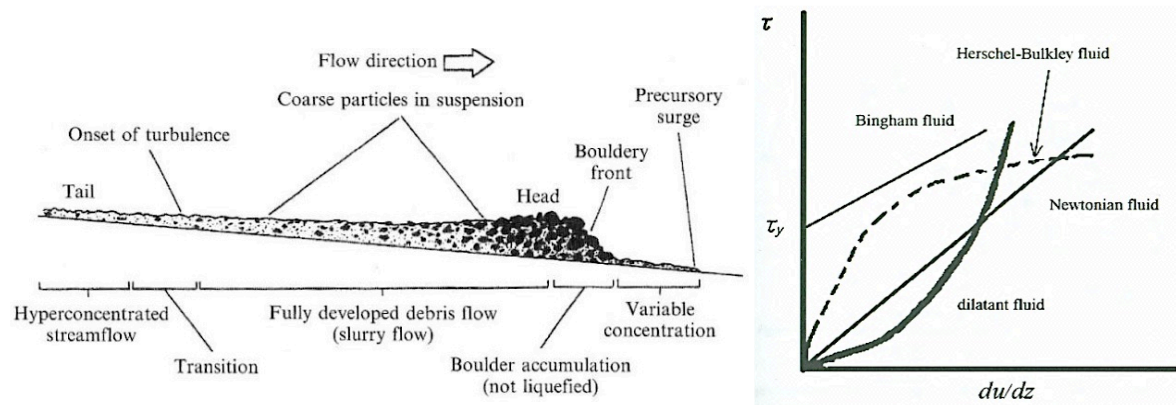


**Fig. 2.5:** Schematic diagram of a debris flow surge. Source: HUNGR 2005: 18.

**Fig. 2.6:** Single-phase continuum models. Source: TAKAHASHI 2007: 39

Debris flows typically move in series of distinct surges, separated by watery intersurge flow (COSTA 1984). As shown in figure 2.5, the front of the debris flow surge is mainly composed of coarse material and boulders. In contrast, the main body is a finer mass of liquefied debris. A more dilute, turbulent flow of sediment-charged water, built up the debris flow tail (RICKENMANN 2001). Along the lateral boundaries of the U-shaped track, ridges of coarse material, so-called “levees”, develop, due to the slower velocity of the mass at the margins.

Even today, the knowledge on the physics of the debris flow and the rheology of the moving solid-fluid mixture is still limited. Currently, this solid-fluid-interaction is best explained by “single-phase continuum models” considering a debris flow as a simple homogeneous fluid. The mechanical characteristics of the fluid are determined by the relationship between the shear stress ( $\tau_y$ ) and the rate of strain ( $du/dz$ ) (TAKAHASHI 2007, fig. 2.6). Due to the high viscosity generated by the solid phase, debris flows obviously behave differently to laminar flow of pure water, representing Newtonian fluids. Simple Non-Newtonian models, such as the widely used Bingham fluid, are possibly more suitable. Here, the single-phase material only deforms when a certain threshold  $\tau_y$  is reached. After this threshold, the Bingham fluid behaves like a Newtonian fluid. For further reading, particularly with regard to model limitations, see IVERSON (1997) and TAKAHASHI (2007).

Once reaching a relatively low gradient (ca.  $5\text{-}10^\circ$ ) or an area of decreased confinements (e.g. alluvial plains), debris flows immediately stop accumulating a debris cone near the footslope. Usually, the main part of the surge collapses and the front slows down, steepening to form a lobate deposit or spread out in width (HUNGR 2005). The surface of debris cones is characterised by a low gradient of ca.  $12\text{-}25^\circ$  (even up to  $30^\circ$ ). The material is unsorted and unstratified with a typical floating texture, where large clasts are randomly embedded in a fine-grained matrix. An inverse grading with large boulders on the top – the boulders seems to swim – reflects buoyant forces and dispersive pressures between individual particles during deposition (INNES 1983). However, during fieldwork in Swiss National Park, only few evidence of an inverse grading could be found, turning the “swimming theory” in a doubtful hypothesis.

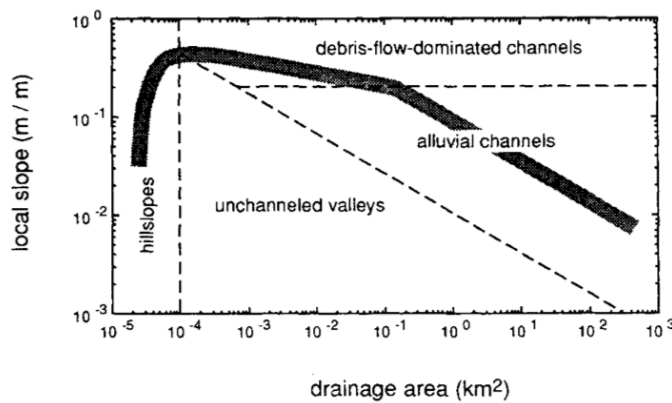


**Fig. 2.7:** Schematic illustration of logarithmic relationship between drainage area (km<sup>2</sup>) and local slope (m/m) showing the hypothetical topographic signatures for hillslope and valley processes. For a detailed description see text. Source: MONTGOMERY & FOUFOULA-GEORGIU 1993.

As studied by DIETRICH & DUNNE (1978) and STOCK & DIETRICH (2003), debris flows play a striking role in relief evolution of mountain valleys. Over long time scales, the sum of multiple debris flow events generates a geomorphologically relevant imprint on topography, as they limit the maximal local slope gradient and progressively reduce the elevation of a mountain range. The influence of debris flows on relief evolution can be described by the relationship between the local slope ( $S$ ) and the contributing area ( $A$ ) within on a double-logarithmic slope-area-plot.

With view to figure 2.7, very steep slopes near the watershed with very small drainage areas ( $< 10^{-4}$  km<sup>2</sup>), dominated by diffusive hillslope processes, show a pronounced positive slope-area-relation. In contrast, basins with drainage areas larger than 0.1-1 km<sup>2</sup> are characterised by an obvious linear negative relationship between  $S$  and  $A$ . Here, fluvial processes are the dominant geomorphic mechanisms (MONTGOMERY & FOUFOULA-GEORGIU 1993). Interestingly, drainage areas with steep gradients and drainage areas between 10<sup>-4</sup> km<sup>2</sup> and 0.10 km<sup>2</sup> often show a non-linear, slightly curved slope-area-plot, indicating processes that are different from fluvial or hillslope origin. STOCK & DIETRICH (2003) interpret this curvature as “topographic fingerprint” for debris flow bedrock incision. The scaling break at drainage areas of 0.03-0.10 km<sup>2</sup> defines the transition from debris flow to fluvial incision. Below this location, the local slope is too small to activate debris flows.

### 2.3.4 Rock glacier

Rock glaciers are typical features of periglacial environments, formed by the creeping mixture of sediment and ice (appendix A-2). According to WASHBURN (1979), they are distinct tongue-line bodies of angular boulders resembling a small, dark glacier. They are characterised by a lobate surface and a steep front at the angle of repose. Active rock glaciers creep downslope with velocities of ca. 1 m/a, sometimes up to 5 m/a. Rock glaciers, where no movement takes place and no ice is present, are relict or, if vegetation cover is present, fossil. If they are still frozen, but movement rates are very low, rock glaciers are classified as inactive (BARSCH 1996). In general, rock glaciers can reach lengths of around 1 km (up to 3 km), and widths of hundred metres. Up to now, different theories exist describing the origin of rock glacier. They range from debris-covered glaciers to a slow creeping of frozen material by permafrost (see e.g. BARSCH 1996, GOUDIE 2004).

Rock glaciers can represent important storage and transport processes within alpine sediment cascades. BARSCH (1977) and GÄRTNER-ROER & NYENHUIS (2010) analysed rock glaciers in the Swiss Alps and calculated a total transported sediment volume of  $500\text{-}800 \times 10^6 \text{ m}^3$  representing around 20 % of all mass-wasting processes and a denudation rate of 2.5 mm per year.

### 2.3.5 Moraine deposit

Moraines are glacial landforms created by the deposition or deformation of sediment by glacier ice. Moraine material, so-called “till”, can vary in size depending on its source area. Moraine deposits can be classified genetically according to their formative process and geographically according to their position within the glacial system. Generally, it is distinguished between supraglacial, ice-marginal and subglacial moraine types (BENN & EVENS 2010). In this study, moraine deposits include all types of glacial depositional material.

Supraglacial moraine sediments are ephemeral features above the ice surface. The melting of glaciers results in the destruction and redeposition of supraglacial till. Ice marginal moraines develop around the edges of glaciers and can be either lateral or frontal. They may reach heights of tens or hundreds of meters and may stretch for hundreds of kilometres (GOUDIE 2004). The maximum extent of a glacier advance represents a terminal frontal/end moraine. Ground moraines can be formed both subglacially and by descending supraglacial material during deglaciation. The latter process is often related to so-called “hummocky terrain” (MUNRO-STASIUK & SJOGREN 2006). Moraine deposits play a significant role within the alpine sediment cascade as important sediment storage and source. Diverse geomorphic processes such as solifluction, rill erosion and debris flows may lead to the modification and remobilisation of the glacial sediment (fig. 2.8). Furthermore, vegetated, less inclined moraine valley fills represent a kind of buffering element in the sense of BRIERLEY et al. (2006), as the sediment transfer is immediately stopped or extremely decelerated occurring as cryogenic creep at low velocities rates of less than 1 m/year (MATSUOKA 2001).



**Fig. 2.8 (top):** Moraine deposits in the upper Val dal Botsch, reworked by rill erosion and cryogenic creep resulting in the formation of garlands (Girlandenrasen).

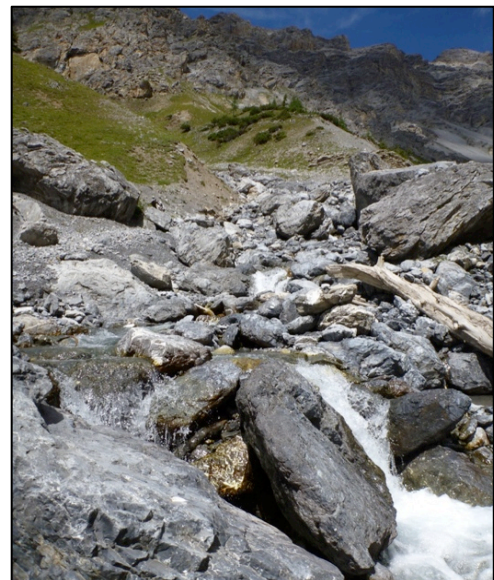


**Fig. 2.9 (right):** Alluvial deposits with large inputs of gravitational hillslope processes in Val Müschauns.

### 2.3.6 Alluvium

Alluvial deposits are sediments transported and accumulated by flowing water in river valleys. The material originally derived from the breakdown and weathering of sediments within other storage landforms. It is then transported downslope by different geomorphic processes along the sediment cascade and deposited in flat areas within the valley bottom (GOUDIE 2004). The alluvium represents one of the final sediment storages within the alpine sediment cascade, (dis)connecting the slope-subsystem with/from the channel-subsystem (OTTO 2006). Depending on catchment topography, channel size and slope and, accordingly, fluvial mechanism, the morphology of alluvium in alpine basins can range from steps, pools, and riffles, plane beds and fans (MONTGOMERY & BUFFINGTON 1997). Typical alluvial sediments are stratified, built up of gravels, sand, silt and clay. Due to the input of sediment from adjacent hillslopes, the alluvium is often a direct result of the interplay of fluvial and slope processes (fig. 2.9).

## 2.4 Toposequences as tool for studying alpine sediment cascades

The last chapters emphasise that landforms are not randomly distributed along a hillslope. Instead, they are spatially arranged from ridge crest to valley bottom in a certain regularity. A systematic classification and morphometric characterisation of landforms can help to understand the nature of alpine cascading systems (MCMILLAN & SHARY 2009). For that, the science of geomorphometry represents a modern and analytical-cartographic approach for the quantitative analysis of alpine systems based on geometrical and topological characteristics. Nonetheless, it is important to stress that a successful application of geomorphometry highly depends on theoretical and conceptual preliminary considerations (SCHMIDT & DIKAU 1999).

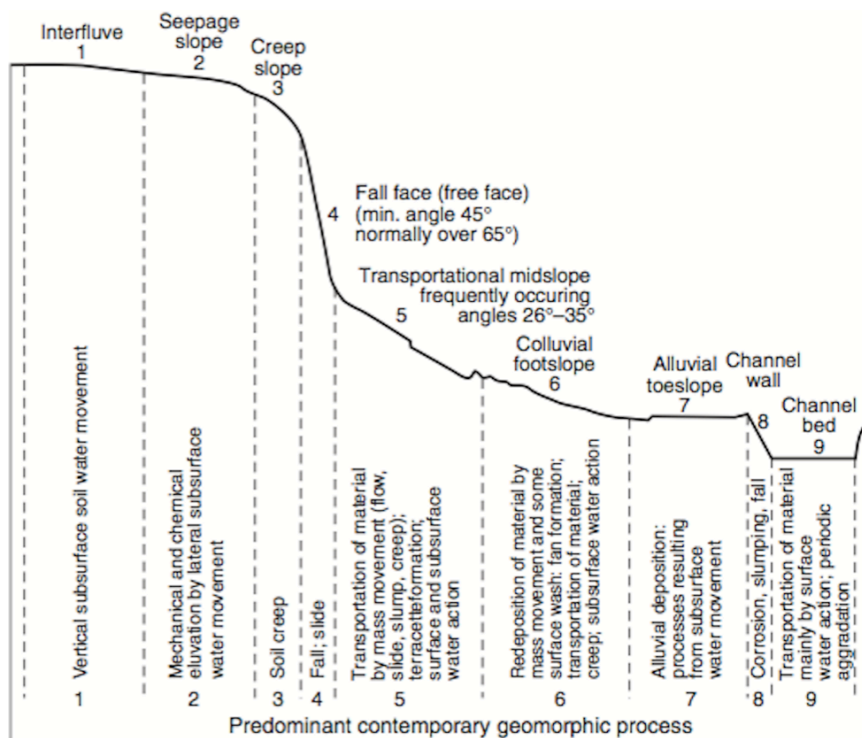


**Fig. 2.10:** The nine-unit slope model by DALRYMPLE et al. (1968) (modified). For description see text.

Source: GOUDIE 2004: 520.

Even though rarely applied in geomorphology, the concept of toposequences provides an excellent framework to subdivide the complex continuum of nested landforms into smaller, successive units. This considerably helps to understand the functional neighbourhood relationship between adjacent sediment storages. Referring to the principle of the catena in soil science (MILNE 1935), a toposequence is defined as “a topographic succession of landforms that is passed by an imaginary particle, which moves downslope driven by gravity” (see RASEMANN 2004: 34, after SPEIGHT 1974). In contrast to a catena, the focus of a toposequence lies not on soil properties. Instead, it allows a segmentation of hillslopes into relative homogeneous areas with typical storage landforms, geomorphic and climatic-ecological processes and morphometric attributes.

Several models of toposequences have been developed. Probably the most widely used hillslope classification was presented by RUHE & WALKER (1986). By using downslope variations in gradient, slope length and width, they divide a hillslope into five components and relate them to specific soil properties (see also VENTURA & IRVIN 2000). This approach was extended by PENNOCK et al. (1987). In a significant work, SPEIGHT (1974, 1990) defines a toposequence as large-scale landform pattern (300 m in radius), which is composed of a chain of small-scale landform elements (20 m in radius). By using parameters such as slope, altitude, morphological type, dimensions, mode of geomorphic activity and geomorphic process, he distinguishes between around 40 types of large-scale landform patterns (e.g. floodplain, hills) and more than 70 types of landform elements (e.g. cliff, footslope). One of the key concepts of toposequence derives from DALRYMPLE et al. (1968) and CONACHER & DALRYMPLE (1977). In their nine-unit slope model (fig. 2.10), they combine landforms with contemporary geomorphic processes of water and material transfer.

Up to now, there is no automatic method to extract toposequences from a digital elevation model. RASEMANN (2004) derives specific types of toposequences for the Turtmann Valley using representative quantitative geomorphometric parameters along hillslope transects extracted from a DEM. The study demonstrated that an automatic delineation of toposequence types might often be very problematic due to small-scale variation of the high-alpine relief. OTTO (2006) identifies seven toposequence types of the Turtmann Valley by a manual and qualitative mapping based on a storage landform database. Finally, it needs to be stressed that the toposequence approach does not consider real sediment pathways, where (de)coupling of landforms may cause intermediate storage or transfer of sediment. Obviously, the concept is also relatively static and does not include the significant role of time. Thus, a toposequence constitutes a coupled, uninterrupted sediment cascade only when material is incessantly routed from one landform to the lower one (OTTO 2006).

## **2.5 Sediment fluxes and activity in mountain environments**

There is an on-going debate on how and at which rate sediments are conveyed through an alpine basin to the outlet. The sediment budget approach may help to understand the cascading nature of

highly dynamic alpine systems. According to REID & DUNNE (1996: 3) “a sediment budget is an accounting of the source and disposition of sediment as it travels from its point of origin to its eventual exit from a drainage basin”. The concept provides a framework to determine the three major components of a sediment flux through a system: sediment sources, transfer processes and intermediate storages, including their internal linkages (DIETRICH et al. 1982, MARSTON & PEARSON 2004). The sediment budget can be mathematically described by a basic relationship between the input  $I$  and the output  $O$  of sediment and change of storage over time  $\Delta S$  (SLAYMAKER 2003):

$$I = O + \Delta S \quad (2.1)$$

This relationship directly highlights the key role of sediment storage landforms. As major drivers between source and sink, sediment storage landforms determine the balance of the sediment flux crucially. Consequently, the sediment budget approach considers the concept of connectivity, even though not explicitly mentioned (FRYIRS et al. 2007). The intermediate decoupling of neighbouring storages might result in significant time lags between input and output of sediment. In this context, HINDERER (2012) emphasises that the arrangement of multiple sinks along a routing pathway from erosional areas to the ultimate sink highly complicates sediment budgeting in alpine basins.

A good index of catchment erosion and sediment delivery is given by the sediment yield  $SY$ , defining the total outflow of sediment from a drainage basin, measured at a certain cross-section in a specific time period (HOFFMANN 2006). Many sediment budget studies – except for those in glaciated basins (see e.g. CHURCH & SLAYMAKER 1989) – indicate a gradual decrease in  $SY$  with growing catchment size (see e.g. MILLIMAN & MEADE 1983, MILLIMAN & SYVITSKI 1992). This is due to the fact that with growing basin area, slope and channel gradients decrease, which in turn reduce the transport capacity of rivers and favour the opportunity for accumulation. The  $SY$  can be related to a specific catchment area, expressed as specific sediment yield  $SSY$ . Due to the intermediate storage of sediment, only a fraction of the eroded sediment amount will be transported to the catchment outlet. WALLING (1983) defines this buffering capacity of basins as “sediment delivery problem”. To explain this effect, the dimensionless sediment delivery ratio  $SDR$  is widely used. Depending on specific geomorphic factors including e.g. relief, slope, vegetation cover, land use or material texture, the  $SDR$  ranges from 100 % to less than 1 % (WALLING 1983). The concept of connectivity by BRIERLEY et al. (2006) and FRYIRS et al. (2007) revolutionised the sediment delivery problem significantly. Lesser magnitude of the  $SDR$  reflects a small degree of connectivity as well as a greater influence of (temporary) storage of sediment within a basin (GÖTZ et al. 2010).

The sediment budget approach became popular in the 1970s, mainly related to fluvial systems. The first alpine sediment budgets were conducted by JÄCKLI (1957) in the upper Rhine watershed and by RAPP (1960a) in an alpine valley of Karkevagge. CAINE (1974) already demonstrated that the alpine sediment transfer represents a cascading system with different controlling factors, activity stages and reaction times, variable in space and time. Based on this work, BARSCH & CAINE (1984)

developed a conceptual model, which allows the differentiation of high-alpine systems. In a path-breaking sediment budget, JORDEN & SLAYMAKER (1991) quantified sources, storages and yield of clastic sediment in the Lillooet River watershed and indicated that only half of the estimated sediment production appears to explain the long-term sediment yield in the basin. Instead, the unexplained sediment supply may be composed of large landslides or more recently of human impact, but also of paraglacial sediments, as supposed by CHURCH & RYDER (1976).

Over the last few decades, there has been an increasing trend to explain changes in activity of sediment transfer and storage after deglaciation in alpine regions within the framework of paraglacial geomorphology (RYDER 1971, CHURCH & RYDER 1972). According to the most recent definition by BALLANTYNE (2002b: 1938), the term “paraglacial” considers all “non-glacial Earth-surface processes, sediment accumulations, landforms, land systems and landscape that are directly conditioned by glaciation and deglaciation”. It is assumed that sediment fluxes progressively relax from the disturbance and develop towards a new stable state (BRUNSDEN & THORNES 1997). According to CHURCH & RYDER (1972), the paraglacial sediment movement can be generally described by a declining curve (fig. 2.11), where the paraglacial sediment fluxes shift from a maximum yield soon after the start of deglaciation towards an asymptotical decline. CHURCH & SLAYMAKER (1989) demonstrate in their significant paper the scale-dependency of paraglacial impulses (fig. 2.12), as small subsystems may have already adjusted with their non-glacial environment whereas larger subsystems ( $> 3 \times 10^4 \text{ km}^2$ ) are still responding to glaciation. Contradicting conventionally accepted models (e.g. WALLING 1983, MILLIMAN & SYVITSKI 1992), CHURCH & SLAYMAKER (1989) explain the rise of sediment yield as a delayed peak of the remobilisation of paraglacial sediment storages.

However, MCCOLL (2012) emphasises that the term paraglacial has to be used very carefully and with a certain amount of personal judgement. It is not to be understood as a “panacea” for all geomorphic processes occurring after deglaciation. He points out, instead of a simple cause-effect relation, many triggering factors – some of glacial origin, other related to climate, weathering or tectonics – may affect the spatial and temporal pattern of sediment fluxes after deglaciation.

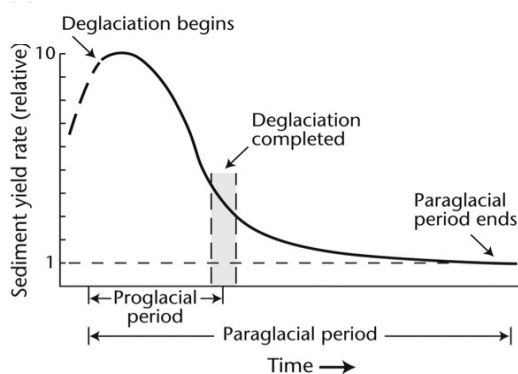


**Fig. 2.11:** The paraglacial sedimentation during the paraglacial period. Source: BALLANTYNE 2002a: 372.

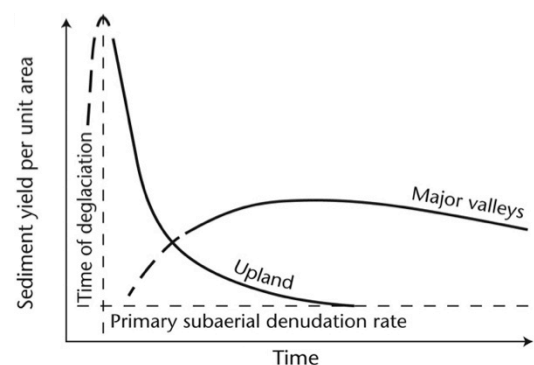


**Fig. 2.12:** The paraglacial sedimentation cycle modified by CHURCH & SLAYMAKER (1989). Source: SLAYMAKER 2009: 76.

Until now, only a limited number of quantitative sediment budgets exist for alpine basins, since long-term field studies become increasingly difficult to conduct and error-prone with increasing spatial scales (BEYLICH 2011). Alpine sediment budgets are largely descriptive models or based on integral data (e.g. DIETRICH & DUNNE 1997, OTTO & DIKAU 2004, GÖTZ et al. 2010). Nevertheless, in recent years, efforts in geophysical and modelling techniques offer a encouraging potential, particularly for the volumetrically quantification of sediment storages. As a consequence, the focus of sediment budgets recently shifted towards the role of sediment storages in long-term sediment fluxes and landscape evolution (e.g. HOFFMANN & SCHROTT 2002, SCHROTT & ADAMS 2002, GÖTZ & SCHROTT 2007, SCHROTT et al. 2002, 2003, 2006, OTTO 2006, OTTO et al. 2009).

### 3 HYPOTHESES AND RESEARCH SYNOPSIS

The review of the recent state of research clearly highlights that there are still some knowledge gaps concerning the complex nature of alpine sediment cascades and their role within sediment fluxes of alpine basins. Firstly, even though it is widely proven that debris flows are a major driver for sediment fluxes in mountain environments, thereby modifying the mountain relief over time, their role in alpine sediment cascades needs further knowledge. Particularly, the influence of debris flows on short- and long-term storage coupling and hillslope-channel-connectivity is of key interest. Therefore, the first, mostly process-oriented hypothesis claims:

***Hypothesis 1:*** *In alpine cascading systems, the coupling behaviour along sediment trajectories and the connectivity to the fluvial system is considerably controlled by debris flows.*

Furthermore, the role of sediment cascades within the sediment fluxes of alpine basins is still related to some uncertainties, particularly regarding the connectivity between hillslopes and the fluvial system. A number of studies reveal that sediments prevail longer in storage than in transport and that decoupling of storage landforms reduces the sediment supply to the channel network. With focus on the Swiss National Park, the second, substantially systemic hypothesis is:

***Hypothesis 2:*** *Only a fraction of the sediment transferred within the catchments will make its way to the basin outlet of the alpine valleys and will contribute to the sediment flux system.*

Within this context, connectivity will be qualitatively examined by a specifically developed conceptual approach and tested against a GIS-modelling algorithm. The conceptual framework is based on the assumption that the functional relationships between neighbouring storage landforms determines the sediment connectivity to the stream. Based on the toposequence concept, these functional relationships between storages were qualitatively analysed based on the sediment throughput, its temporal dynamics and the displacement of the separating storage boundary.

The quantitative connectivity assessment is performed using the modified GIS-modelling approach by BORSELLI et al. (2008), originally applied for soil erosion in lowlands. Currently, there is an increasing trend to explain the complexity of alpine sediment cascades by using numeric modelling approaches instead of qualitative, often more time-consuming field examinations. In this context, the third, highly method-oriented hypothesis states:

**Hypothesis 3:** *The numeric modelling approaches existing today still insufficiently explain the connectivity between alpine sediment storages and the stream channel.*

A flow chart of the thesis structure and of the research synopsis is presented in figure 3.1. In general, the geomorphological map is the key knowledge base for all subsequent methodical procedures.

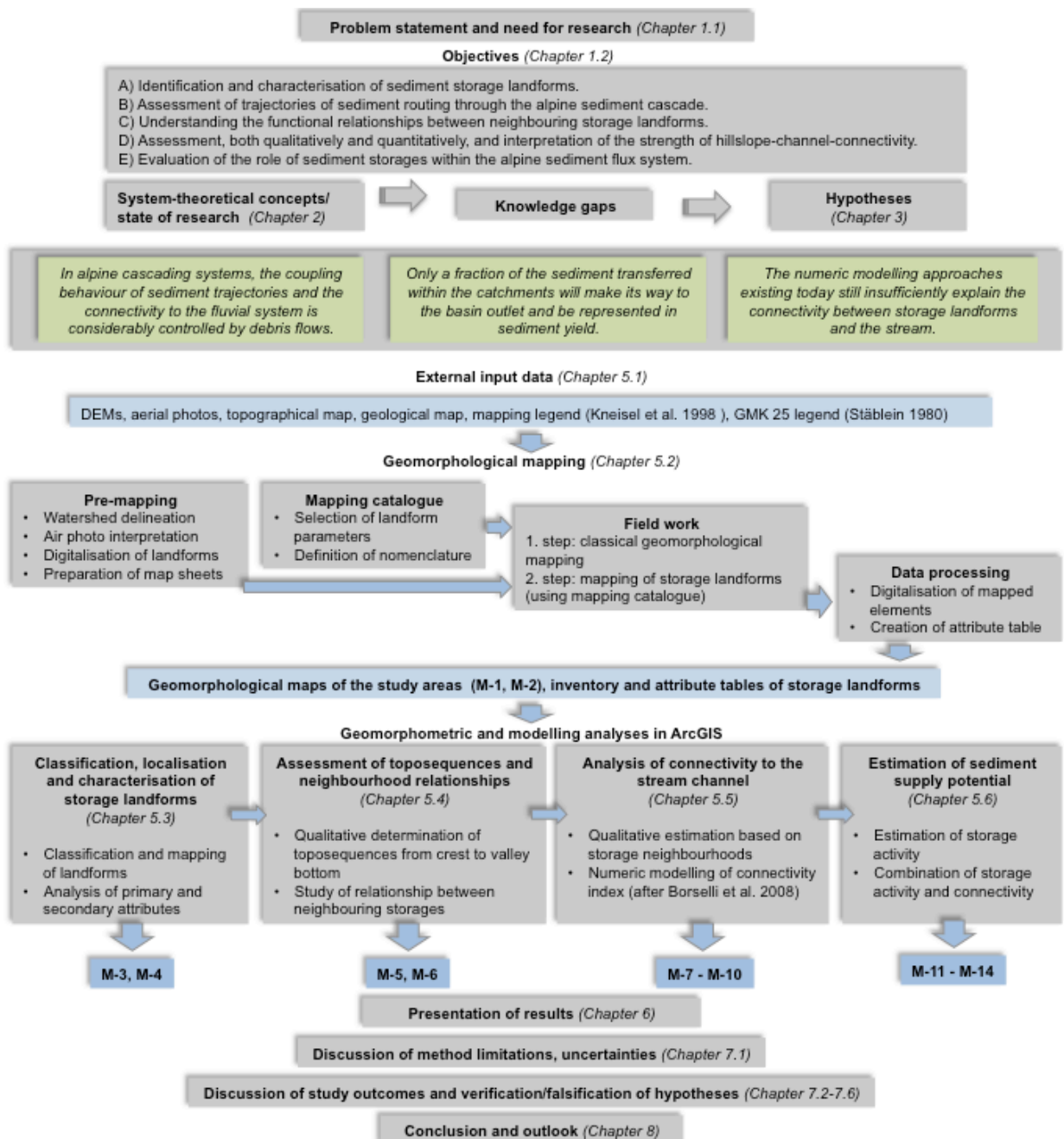


**Fig. 3.1:** Flow chart of the structure and the major research steps of the master thesis. All created maps are labelled by a M- (M-1, M-2) and supplemented at the end of this thesis.

## 4 STUDY AREA

### 4.1 Geographical overview

For this study, two contrasting alpine, deglaciaded catchments are examined, both lying in the Swiss National Park (SNP) within Switzerland's easternmost canton Graubünden, along the border to Italy (fig. 4.1). The alpine valley Val dal Botsch is located within the north-eastern margin of the SNP between Zernez and Buffalora. The other valley Val Müschauns is situated in the southwest of the SNP, in the east of the community S-Chanf. Both basins drain into the Inn river.

Established in 1914, the SNP was the first national park in the Alps and in central Europe. With an area of about 172 km<sup>2</sup>, it is the largest protected region of Switzerland today (MÜLLER & KOLLMAIR 2004). The park is a strictly sheltered wilderness area, where hunting, agriculture, forestry and housing are prohibited in order to allow an unhindered development of natural geomorphic processes as well as of flora and fauna (ECK 1994). The only road that runs through the park is the "Pass dal Fuorn" (german: "Ofenpass") connecting Zernez and Buffalora (fig. 4.1).

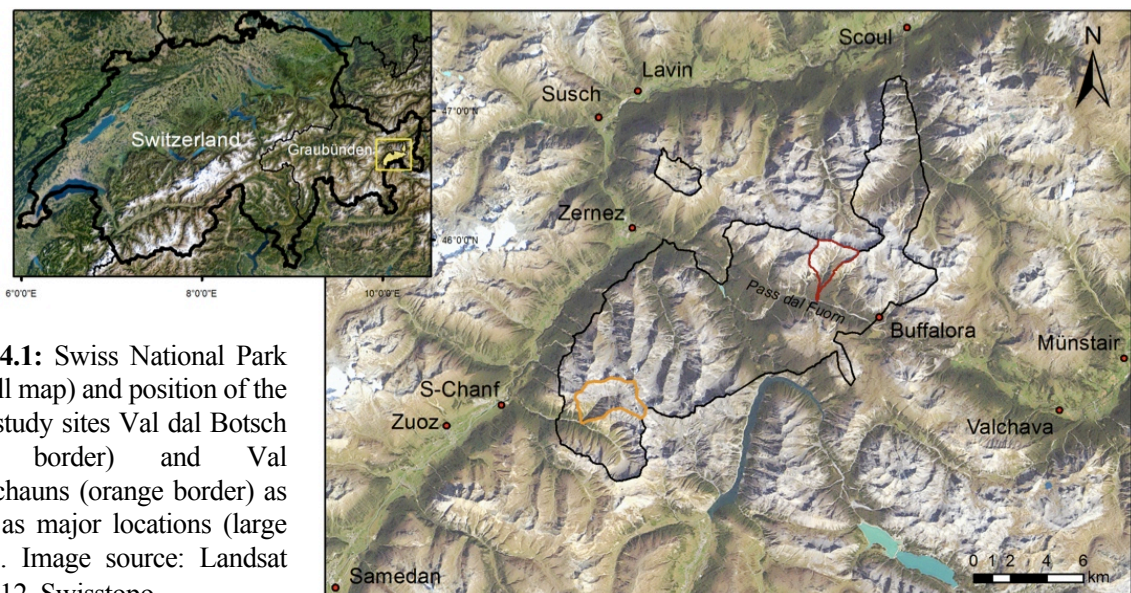


**Fig. 4.1:** Swiss National Park (small map) and position of the two study sites Val dal Botsch (red border) and Val Müschauns (orange border) as well as major locations (large map). Image source: Landsat © 2012. Swisstopo.

The **Val dal Botsch** (fig. 4.2) is a north-south oriented, V-shaped alpine valley with a length of around 3 km and a width increasing from ca. 200 m (lower valley) up to 1.5 km (upper valley). The catchment comprises an area of around 3.47 km<sup>2</sup> and drains into the Ova dal Fuorn, one of the major streams of the SNP parallel running to the Pass dal Fuorn. The altitudes range between 1800 m a.s.l. and ca. 3000 m a.s.l., with the Piz dal Botsch (2852 m) being one of the highest peaks. According to the Rhaeto-Romanic name "Val dal Botsch", meaning "valley of beef", the catchment was once used agriculturally until the establishment of the national park in 1914.

Lying in the south of the SNP, the **Val Müschauns** is the larger one of the two tributary valleys of the Val Trupchun (fig. 4.3). While the slopes of the lower and middle basin are rather steep, the upper basin resamples a typical glacial trough with a pronounced U-like shape. The ca. 6.18 km<sup>2</sup>

large basin is drained by the Ova dal Müschauns that flows into the Ova da Trupchun, one of the park's major streams. Controlled by the geological setting, the valley is dominated by a change in orientation in its middle part: while the upper valley (ca. 1.87 km long, 1.67 km wide) is basically oriented from east to west, the lower basin (ca. 1.7 km long, 1.9 km wide) has a northeast-to-southwest orientation. The catchment is characterised by altitude differences ranging between 1800 m a.s.l. up to ca. 3200 m a.s.l. The Piz Quattervals (3165 m) is one of the highest peaks along the valley's ridge – and contemporary the highest in the entire SNP area. Melt waters of some local glaciers feed the lake Lai da Müschauns situated in a cirque at 2741 m a.s.l.



**Fig. 4.3 (left):** Val dal Botsch in the northeast of the SNP. Image source: Google Earth 2011.

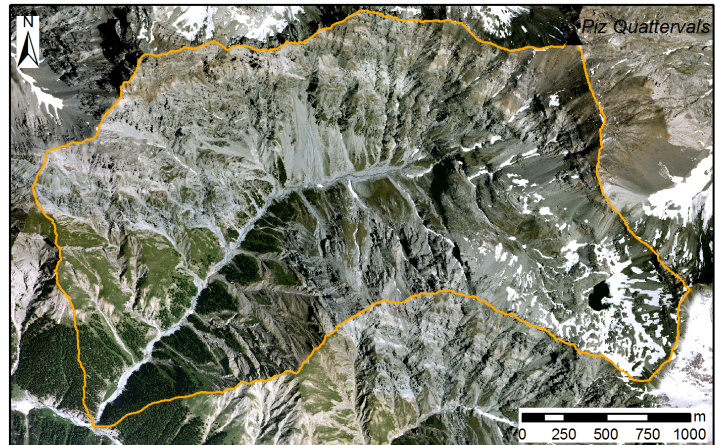


**Fig. 4.2 (right):** Val Müschauns, a northern tributary of the Val Trupchun. Image source: Google Earth 2011.

## 4.2 Geological and tectonic setting

Since the boundary between Western and Eastern Alps passes through Graubünden, the SNP and therefore the two study sites tectonically belong to the Eastern Alps, more precisely to the Upper Austroalpine nappe (see appendix B). As large tectonic super-unit, the eastern Alps have been obducted over the Penninic nappe ca. 40 Ma ago and today, cover an area of 400 (W-E) x 100 (N-S) km extending into the eastern regions of Graubünden (LABHART 1992). The SNP is entirely situated in so-called “Engadine Dolomite”, a relatively brittle type of rock with a potential for rapid erosion. The ca. 1-2 km thick complex of several Triassic dolomite nappes is primarily composed, from south to north, of the Ortler and the S-charl nappe. The latter can be subdivided into the Quattervals and upper Terza nappe. This grey and sometimes reddish to yellowish layering reflects a complicated folding process with unusual westward and even southward obduction movements (LABHART 1992).

The Val dal Botsch tectonically belongs to the Lower and Upper S-charl nappe. The catchment is mostly dominated by banked dolomite rocks (Murteret Dolomite). Occasionally, small outcrops of the yellowish Raibler-Formation, a layering of dolomite rocks, sandstone, slate and breccia, are

visible along the western hillslopes. Grey-banked dolomite rocks of the Vallatascha-Dolomite are present in the valley's central part. The majority of the basin is largely covered by thick sheets of debris, derived from quaternary gravitational processes, and moreover, by quaternary moraine deposits resampling a hummocky terrain. There is no uniform strike and dip direction (20-70°), reflecting the complicated obduction and folding processes.

The geologic setting of the Val Müschauns is significantly controlled by the east-west oriented thrust-fold, the so-called "Trupchun-Braulio-line", where the older Quaternary nappe was obducted above the younger sediments of the Ortler nappe. The lower valley is dominated by folded sediments of the Ortler nappe, mainly grey stratified limestone with layers of marl and breccia (Allgäu-Formation) and small, yellowish outcrops of the Raibler-Formation. In contrast, grey-banked dolomites (Müschauns Dolomite) of the Quaternary nappe build up the upper catchment. The northern valley ridge below the Piz Quaternary exposes a layering of dolomites, limestone and shale (Pra-Grata-Formation) as well as a black limestone with shale-intrusions (Quaternary Formation). The general striking direction is east-west and north-west with an average dipping of 40° and 50°. However, similar to Val dal Botsch, quaternary debris extensively covers the valley.

### **4.3 Lateglacial history and present glacial setting**

During the Pleistocene, the area of the SNP was entirely ice covered except for some higher mountain peaks. The maximum altitude of the ice surface is estimated to be at 2200 m to 2800 m (ROESCH 1937). The glacial erosion and oversteeping of the alpine valleys occurred mainly during the second-last glacial period, the Riss glaciation (ca. 150000 years ago). In contrast, the recent landscape of the SNP and its typical glacial erosion and accumulation features are attributed to the overprinting by the last glacial period, the Würm glaciation, ca. 110,000-12,000 years ago (TRÜMPFY et al. 1997). During this time, the Inn glacier was dammed between Zernez and Susch and entered far into the major side valleys, such as Val Trupchun or within the Pass dal Fuorn. In addition, local glacier systems developed within the cirques of the tributary valleys. The ice eroded and oversteepened the slopes thereby accumulating numerous granite boulders (ROESCH 1937). Above the ice-free height (2200-2800 m a.s.l.), sharp mountain ridges remained behind. Within the two study sites, particularly in Val dal Botsch, deposits of moraine material are well preserved but often modified by current geomorphic processes such as solifluction, debris flows and overland flow. Erratic blocks are rare, but can be found near the outlets of the valleys.

Today, with a recent ice coverage of 1 % of the entire area, the glaciation of the SNP is extremely sparse. One of the major local glaciers can be found along the northern flank of the Piz Quaternary (3165 m a.s.l.) – along the opposite site of the Val Müschauns. The ground is expected to be permanently frozen during the year above a height of ca. 2200 m a.s.l. along northern slopes, and above 2800 m a.s.l., along southern slopes. Typical cryogenic features are visible in both studied

catchments. Seasonal and diurnal freeze-thaw action result in the development of patterned grounds, solifluction lobes as well as vegetation stripes and terraces (in garlands) within moraine deposits. Only in summer, the uppermost 1 to 2 m of the permafrost layer may thaw (at daytime).

#### 4.4 Geomorphology

Since the SNP has been almost unaffected by human influence for about hundred years, the region shows a manifold and almost undisturbed geomorphological features. The existence of various Triassic nappes with varying resistance to erosion in combination with the glacial history resulted in a rugged, high-alpine landscape. The study sites are glacially shaped, high-alpine valleys that are deglaciated today. While Val dal Botsch is largely characterised by a prominent V-shape – only the uppermost cirque is trough-like – the middle and upper basin of Müschauns gradually broadens to a typical U-shaped glacial trough.

Both studied catchments show a variety of high alpine geomorphic processes and landforms. Until now, geomorphological studies are rare in the SNP and hence, no geomorphological maps exist. Thus, the geomorphic setting of the two valleys will be described in detail in chapter 6 as one of the major outcomes of this study. Nevertheless, a first impression should be given (fig. 4.4a,b,d,e): Extensive talus slopes are one of the most dominant phenomenon in the entire SNP and within the studied alpine valleys. At the Munt Buffalora close to Val dal Botsch, HARTMANN-BRENNER (1973) studied the genesis of talus slopes and the local overprinting by debris flows. Based on geophysical and photogrammetric studies, the volume is estimated to be ca. 624000 m<sup>3</sup> inferring a mean rockwall retreat rate of ca. 1.2 mm/year since deglaciation. Moreover, debris flows are very active



**Fig. 4.4:** Geomorphic setting and vegetation characteristics of the study areas. Talus slopes bordered by moraine deposits within the upper valley of Val dal Botsch (a). Debris flow deposits near the outlet of Val dal Botsch (b). Typical vegetation zones within the study areas (c). Interfingering of active and vegetated hillslope debris flows in the middle basin of Val Müschauns (d). Upper U-shaped trough of Val Müschauns (e). Typical plants of the alpine zone in Val Müschauns (f).

and ubiquitous features within the studied valleys. Due to the high protection status and the intensity of scientific studies, the SNP offers excellent opportunities to study the characteristics and hazard potential of debris flows, as done for example by STOLZ & HUGGLE (2008). Based on grain-size analysis and empiric parameters, the authors calculated event magnitudes of up to 50,000 m<sup>3</sup> and flow velocities ranging between 5-12 m/s. Yet, the damage level is comparatively low due to the very sparse infrastructure in the SNP.

#### 4.5 Climate, vegetation and anthropogenic influences

The climatic situation of Val dal Botsch and Val Müschauns is typical for the Upper Engadine region. As major influencing factor, the Alps act as a climatic divide between a more continental north and a Mediterranean south. Due to the inner alpine position, the Upper Engadine and therefore the study sites are dominated by continental climate conditions and are considerably shielded from precipitation from the north and south. As a consequence, the region is remarkably dry with a mean annual precipitation of 680-800 mm/year (METEOSCHWEIZ 2009). The SNP is one of Switzerland's most wildfires-susceptible regions (STÄHLI et al. 2006). Transferring the values of the three climate stations in close distance to the SNP, the mean annual temperature (1961-1990) ranges from -5 °C (Scuol, 1303 m a.s.l.) to -10.3 °C (Buffalora, 1968 m a.s.l.) and to -9.2 °C (Samedan, 1708 m a.s.l.) during the coldest month of January. The maximum mean temperature occurs in July with about 9.90 to 14.02 °C (METEOSCHWEIZ 2012).

Despite of the dry inner alpine location, the carbonate rocks leads to a remarkable biodiversity in the SNP. The 172 km<sup>2</sup> area is dominated by around 1/3 forest, 1/3 alpine and subalpine grasslands, while the remaining area represents vegetation-free rock faces. The growing season starts in early June and ends in late September (DOLDER & DOLDER 1979). The alpine valleys show a typical vertical vegetation zoning, controlled by elevation (fig. 4.4c): Up to a height of ca. 2200 m a.s.l., the hillslopes are covered by relatively dense forest such as pine (*Pinus*), larch (*Larix*) and spruce forest (*Picea*), representing the subalpine zone. The upper margin of the subalpine zone is the timberline, the elevation where trees fail to grow. Above this altitude, grasses and low-growing shrubs (e.g. alpine rose, erica) dominate the alpine zone up to an elevation of ca. 2600 m, often in insular form (fig. 4.4f). Extensive rock faces, covered by coarse debris or ice, built up the nivale zone. Here, vegetation is reduced to scattered pioneer plants and lichens (TGETGEL 1981, ECK 1994).

Today, anthropogenic influence is almost negligible within the SNP. Nevertheless, the area has been agriculturally used a century ago. In that time, extensive clear-cutting caused significant changes in forest cover and extinction of wild ungulates in some areas. In Val dal Botsch, the absence of forest cover along some slopes is still a visible remnant of the former deforestation and cattle farming. After the park's foundation in 1914, grazing activity, logging and hunting was stopped, resulting in the gradual re-invasion of the red deer (THIEL-EGENTER et al. 2007).

## 5 DATA AND METHODS

Next, all basic data and the methodological approaches will be presented. The specific working steps are structured in orientation to the major objectives of this thesis – see flow chart of figure 3.1.

### 5.1 Data

One of the major data sets of this study are two **digital elevation models** (DEM from 2012 by Swisstopo) with a resolution of 2 m (Val dal Botsch) and a 0.5 m (Val Müschauns). To guarantee comparability between both study areas, both DEMs should have the same resolution. Therefore, the 0.5m-DEM (Münschauns) has been converted to a cell size of 2 m by using the bilinear interpolation method in ArcGIS. An advantage of this method is that irregularities in the raster become smoothed. For all following analyses, various morphometric and hydrological parameters have been extracted from the DEMs by using ArcGIS including e.g. shaded relief, slope, aspect, curvature, flow direction, flow accumulation, Euclidian distance and stream power index.

**Aerial photos** (from GoogleEarth) available from the year 2011 serve as further data basis, particularly for the geomorphological mapping. The high-resolution images (17 to 19 metres) of the study areas provide first, almost excellent information about the geomorphic system even prior to the in-situ mapping campaign in the field. Contrary to orthophotos, air photos are not orthorectified. Hence, they have no uniform scale and do not represent an accurate Earth surface with true distances. To remove these distortions, the aerial images were geometrically corrected and transformed into orthophotos by using the rectification and georeferencing tool in ArcGIS.

Additionally, the **topographical map** 1:25,000 (TK 25 by Swisstopo) as well as the **geological map** 1:50,000 (Geologische Spezialkarte Nr. 122, by Schweizerische Geologische Kommission) are used for additional information. Despite of the relatively small scale, both maps support the geomorphological mapping during fieldwork considerably.

Finally, for the creation of the geomorphological maps, the mapping legend for high mountain areas (**GMK Hochgebirge**) by KNEISEL et al. (1998) is used. Widely based on the signatures of the GMK 25, the GMK 100 and on the GMK of Königssee, the legend focuses on the presentation of landforms and processes. It enables a detailed and multi-scale illustration of the complex geomorphological system. In addition, the mapping of process domains is based to the **GMK 25 legend** (STÄBLEIN 1980). To avoid overloading and to meet the specific requirements of this study, only a selection of KNEISEL's symbols is applied and additionally extended and/or modified, if necessary. Since the main focus is on the individual storage landforms (form, process, material), information concerning valley form, scarps, steps and curvature are not included.

However, this relatively limited amount of basic input data underlines the importance of the geomorphological field mapping, as it will represent one of the major data and knowledge basis for the subsequent geomorphometric and GIS-analyses of this study.

## **5.2 Geomorphological mapping**

In this study, the geomorphological mapping serves as a major data and knowledge basis for a detailed study of the geomorphic system of the two alpine valleys Val dal Botsch and Val Müschauns. As a very complex tool, a geomorphological map systemises a landscape and provides an excellent inventory of key elements of the geomorphic system such as landforms, (sub-)surface material and structures, current geomorphic processes as well as potential past processes at micro- and meso-scale (OTTO & DIKAU 2004: 327, OTTO 2006: 41). For the creation of the maps, a combination of traditional geomorphological field mapping and pre-mapping analyses in ArcGIS is chosen. Since the study is focused on the current geomorphic setting, the mapping is based on the observed recent geomorphic processes and the actual distribution of storage landforms.

### **5.2.1 Pre-mapping**

As first step, the watershed/catchment area and drainage network of each study site have been automatically delineated using the hydrological tools of ArcGIS. Then, prior to the field campaign, pre-mapping analyses were performed based on the interpretation of aerial photographs and the overlay of hillshade and slope angle maps. The shaded relief and the slope gradients facilitate the interpretation and mapping of geomorphic processes and landforms, even under dense forest cover. The high-resolution aerial photos allow mapping and estimation of vegetation cover and types. Subsequently, polygons of landforms were digitalised by using ArcGIS and assigned to a specific ID number. For the field mapping, map sheets containing the pre-mapped landform boundaries and ID numbers were prepared for each study site (see appendix C-5, C-6). A relatively large scale of 1:5000 was chosen. This scale appears to be the best to guarantee a precise illustration of the variety of geomorphic transfer and storage processes in alpine systems. In total, two versions of the map sheets were created (DIN A3). While one shows the aerial photo, the other is based on the hillshade.

### **5.2.2 Mapping catalogue**

For the mapping campaign, a specific mapping catalogue was determined previously in order to obtain a maximum of detailed information of each sediment storage landform in addition to the classical geomorphological map. The mapping catalogue is supplemented in appendix C-7.

The documentation of material predominantly concentrates on the grain size class, homogeneity or heterogeneity and the rounding degree. With regard to vegetated landforms, information on subsurface material was recorded if possible, e.g. in the case of exposures.

Concerning the geomorphic process, subareas with a homogeneous spectrum of active geomorphic processes, so-called process domains, were documented. Major process domains within the study areas are e.g. gravitational, fluvial, cryogenic, slope erosion, glacial. A combination of two or even more process domains is possible. Referring to BRARDINONI & HASSAN (2006: 1) “process domains

are defined as regions within which one or a collection of Earth surface processes prevails for the detachment and transport of mass". Therefore, the delineation of process domains within this study includes the processes, which are active on the surface today, and not former depositional processes. For instance, the process domain of moraine deposits, which are currently reworked by solifluction, is defined as "cryogenic" and not "glacial", as one might expect due to the Pleistocene origin.

To understand process-form linkages, it was distinguished between the formative process types, which might have originally created the landform, and the modifying processes. Additionally, superimposed microforms (e.g. levees, rills) were documented.

Finally, a special focus was laid on the state of process activity of storage landforms. Referring to OTTO & DIKAU (2004), vegetation may serve as indicator for the activity degree. Hence, the recent vegetation cover, the specific vegetation type and visible signs of damage by actual geomorphic processes were recorded for each landform. Lastly, this detailed characterisation of each landform subsequently resulted in the identification of the specific type of storage landform. The nomenclature of the sediment storage type is mainly based on the classification scheme by BALLANTYNE & HARRIS (1994), as illustrated in appendix A-2.

### **5.2.3 Mapping campaign and field work**

The fieldwork for the mapping campaign in the Swiss National Park was performed in August 2012. If possible, each part of the two study sites and the pre-mapped sediment storages were mapped in close proximity. However, due to the steep relief and the difficult accessibility of some hillslopes, some parts of the study sites were analysed from larger distances with binoculars. For that, various suitable and accessible locations were chosen, which provided a wide view over the catchment (e.g. valley crest, initiation sites of debris flows).

The mapping procedure was divided into two working steps. First, the mapping was focused on the geomorphic system of the basins. Hence, individual geomorphic processes, singular landforms, morphometric features and the basin hydrology were mapped. Based on the prepared mapping sheets, a geomorphological map was compiled on the scale of 1:5000 by using the mapping legend and symbols by KNEISEL et al. (1998).

Second, each sediment storage was analysed in more detail. For that, the mapping catalogue was used and all parameters were recorded as far as possible. In the case of vegetated landforms, material only was documented when exposures were visible. If necessary, the pre-mapped boundaries of the storage landforms were corrected and new landforms were added in the map.

### **5.2.4 Data processing: digitalisation and cartographic representation**

Immediately after the fieldwork, a geomorphological map of each study site was created using ArcGIS. All mapped elements of the mapping sheets were transferred in an ArcGIS project and

digitalised. The boundaries of some storage landforms were corrected or new polygons were added. Likewise, the parameters of the mapping catalogue were transferred into attribute tables.

The final maps include six thematic components, referring to OTTO & DIKAU (2004): Geomorphic processes, singular landforms, geomorphography, hydrology, material as well as process domains and vegetation. For the cartographic representation, the special ArcView symbol set was used, which has been generated for the creation of the geomorphologic map of the Turtmann valley (OTTO & DIKAU 2004). The symbols are based on the legend signatures by KNEISEL et al. (1998).

In addition, some new symbols were designed. For instance, it is distinguished between slope-type debris flows (white arrow) and torrent bed-type debris flows (dark arrow). Concerning the process of solifluction, three different symbols were defined; one for bounded solifluction (with the existence of garlands), one for unbounded solifluction (without pronounced vegetation stripes) and one for single solifluction lobes (within talus slopes). Likewise, a new symbol was designed for talus slope/debris, which represent a combination of both talus slope and hillslope debris flows that is equally accumulated by rockfalls and debris flows. Furthermore, since it was often not possible to differentiate between talus sheet and talus cone, both landform types were generally classified as “talus slopes” in order to prevent misleading interpretations.

Concerning the material of each landform, the range of the dominant grain size classes is illustrated. For those landforms, where no information on material is available, a special signature for “unspecified” was introduced. Material is also displayed for vegetated landforms if material outcrops were visible during fieldwork. Therefore, the mapped material represents both the surface and (uppermost) subsurface sediments. In contrast to the mapping legend by KNEISEL et al. (1998), no special signature for vegetated material is used.

Finally, the process domains are illustrated as areal signatures in combination with the relevant vegetation cover class. This combination allows a first, relatively general idea of the current activity of the processes operating on the individual landforms. Moreover, the representation of vegetation cover replaces the original signature for vegetated material (filled grain sizes) as provided by KNEISEL et al. (1998). For each process domain, specific colours have been chosen: The gravitational process domain is displayed in brown, the fluvial in green, the slope erosion domain in blue, the cryogenic domain in pink and the glacial domain in purple. Combinations of different process domains (e.g. fluvial-gravitational) are illustrated as striped area with the individual colours of each contributing process domain. Grey areas typify unspecified process domains. Then, depending on vegetation class, the symbols of process domains are shaded in colour intensity based on the following principle: The higher the degree of vegetation cover, the darker is the colour of the process domain. As last step, the geomorphological maps are illustrated at the same scale to allow comparability between the two alpine basins. For purposes of presentation, the original scale of 1:5000 is converted to 1:7000 when printing the maps on DIN A1 and A2.

### 5.3 Inventory and geomorphometric characterisation of landforms

Each study site was analysed for its individual landform types, with regard to their current spatial distribution and their morphometric characteristics. Based on the mapping catalogue, the sediment storage landforms were classified and cartographically illustrated. Each landform type is assigned to a specific colour.

Subsequently, different geomorphometric landform attributes were studied using ArcGIS on the base of the DEMs. The DEMs have been previously smoothed by a moving window routine (3x3 cells) in order to remove small surface irregularities. Referring to DIKAU (1989), primary and secondary landform attributes were determined according to their respective geomorphic relevance (tab. 5.1). While primary attributes (e.g. slope, curvature, aspect) provide morphological characteristics of landforms, the overall aim of secondary attributes is to describe the environmental setting and the relative position within the landscape or – in the context of this study – within the sediment cascades. As primary attributes, slope and aspect have been directly calculated for each raster cell from the DEMs by the appropriate ArcGIS tools. The secondary attributes determined in this study are altitude, distance to the watershed and distance to the stream channel as well as the normed distance to the watershed.

In contrast to primary attributes, the calculation of most of the secondary attributes requires additional processing steps in ArcGIS. While the altitude information for each raster cell was directly extracted from the DEMs, the distance to the watershed and the stream channel have been analysed using the Euclidean distance function of ArcGIS. The Euclidean distance calculates the straight-line distance from each raster cell to a defined source. As a source, the polyline of the watershed as well as the polyline of the stream channel from the geomorphological map were used. However, these values render information only on the absolute distance to the watershed/stream channel. In turn, a direct comparison of the landforms and the analysis of potential neighbourhood relations are not possible. For instance, a talus slope in a relative narrow valley part is in closer distance to the stream channel than a talus slope along an elongated trough.

**Table 5.1:** Primary and secondary landform attributes according to DIKAU (1989) and their geomorphic relevance (DIKAU & SCHMIDT 1999).

| Primary attributes         | Geomorphic relevance                             |
|----------------------------|--|
| Slope                      | Velocity of surface runoff, moisture content     |
| Aspect                     | Insolation intensity, local climate              |
| Curvature                  | Velocity of surface runoff, transport capacity   |
| Secondary attributes       |  |
| Altitude                   | Potential energy, local climate, vegetation      |
| Distance to watershed      | Volume/velocity of surface runoff                |
| Distance to stream channel | Volume/velocity of surface runoff                |
| Normed distance            | <i>Relative position within sediment cascade</i> |

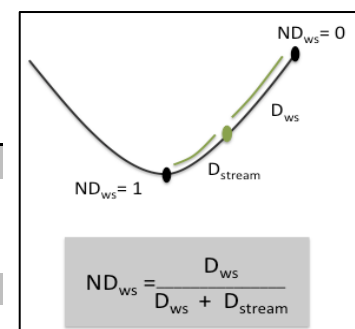


**Fig. 5.1:** Calculation of the normed distance (ND) to the watershed (ws).

For that reason, the normed distance to the watershed, which is the relative position of each landform – or of each raster cell – between the watershed and stream channel, has been calculated (fig. 5.1). The final values can range between 0 and 1. Hence, the higher the value, the closer the landform is located to the valley crest.

#### **5.4 Assessment of toposequences and neighbourhood relationships**

Based on the mapped sediment storage landforms, toposequences from ridge crest to valley bottom were topologically determined in both study sites. Since a quantitative and automatic identification of toposequences in high-mountain terrain often can be problematic (RASEMANN 2004), in this study, toposequences were mapped manually. Previously, to simplify the relatively detailed landform database, some storage types have been summarised. For instance, talus slopes and talus slope/debris flows have been classified as talus slope. Similarly, the combination alluvium/colluvium were summarised with alluvium. Next, beginning from the watershed, each landform was linked with its upper adjacent landform. The individual successions of several storages along a gravitational gradient from ridge crest to valley bottom result in different toposequences. Subsequently, these toposequences were classified into major types based on a systematic grouping of the individual successions (see appendix F-16 and F-17).

In a next step, the functional relationships and neighbourhood characteristics have been evaluated qualitatively. Since such an analysis has not (or rarely) been performed in geomorphologic studies and no standard approach for this procedure exists, a new conceptual framework has been developed for this study (tab. 5.2). This concept is based on three assumptions: *First*, it is supposed that the functional relationship between two neighbouring landforms is determined by the material throughput across the separating boundary. This throughput is defined by both active input and output. The interchange of sediment directly results in a coupling or decoupling of adjacent landforms and therefore, of the complete toposequence. *Second*, this material throughput operates with a specific temporal dynamic, depending on the individual event frequency of the input and output process. Since the focus is on the current landform distribution and neighbourhood characteristics, the time scale of the toposequence analysis is the Holocene. *Third*, it is supposed that the temporally driven material transport between two neighbouring landforms is related to a specific spatial signature as it will affect the position of the separating boundary over time. For instance, the continuous detachment of rock particles cause a gradual backward weathering of the cliff and finally results in a retrogressive displacement of the separating boundary between rockwall and talus slope. This study is based on the idea that decoupling takes place as soon as the second, lower storage type is classified as bedrock or moraine. As described in chapter 2 and examined during fieldwork, these storage types represent buffering element without significant material output. Outcrops or extensive areas of bedrock are natural barriers to the sediment transfer, referring to FRYIRS (2012). Similarly,

the comparatively less inclined moraine deposits represent a break within the relief and stop sediment transport from the hillslope. Moreover, the often densely vegetated moraine material are less capable to transfer sediment, since solifluction – the major reworking process in the SNP – operates at low rates of at most 1 m/year (see CAINE & SWANSON 1986, MATSUOKA 2001).

In the SNP, the temporal dynamics of geomorphic processes can be differentiated into continuous, periodic or episodic, referring to FLAGEOLLET (1996). While rockfall events are continuous processes, constantly occurring as low-magnitude events all over the year, episodic processes mainly include debris flows, which depend on extreme rainfalls or snowmelt. Periodic process activity in the SNP varies seasonally (or diurnally) and is mainly related to fluvial action and glacial/nival processes such as snow avalanches (the major transport process on colluvium), cryogenic creep on moraine valley fills during seasonal freeze-thaw cycles and rampart formation depending on a seasonal snow field along the talus foot. However, the temporal dynamics of the entire material throughput cannot be simply typified as continuous, periodic or episodic as theoretically supposed. Instead, the material transfer across a storage boundary is more complex, as it is a function of both material input and output, each of which may occur due to different geomorphic process. For instance, the material throughput between a talus slope and a debris flow channel is continuous-episodic due to continuous rockfall input into the channel and an episodic depletion via debris flow events. Similarly, the debris cone-alluvium neighbourhood shows an episodic-periodic material throughput due to episodic deposition of the debris cone and periodic fluvial erosion/deposition. Finally, boundaries of all mapped landforms of the study areas were extracted in ArcGIS as polylines and neighbourhood characteristics have been qualitatively evaluated implemented in an attribute table after table 5.2.

**Table 5.2:** Newly created conceptual framework to study the functional relationships between neighbouring landforms.

| Neighbourhood type                               | <i>Storage landform upslope - Storage landform downslope</i>   |  |  |
|--|--|--|--|
| <b>1) Material throughput</b>                    | <ul style="list-style-type: none"> <li>• <b>input and output</b><br/>(coupled)</li> </ul>  | <ul style="list-style-type: none"> <li>• <b>Input or output / either input or output</b><br/>(decoupled)</li> </ul>  |  |
| <b>2) Temporal dynamics of material transfer</b> | <ul style="list-style-type: none"> <li>• <b>Continuous</b><br/>- low magnitude rockfall events</li> </ul>  | <ul style="list-style-type: none"> <li>• <b>periodic</b><br/>- seasonal cryogenic creep/solifluction<br/>- periodic fluvial events<br/>- seasonal snow avalanches<br/>- rampart formation due to seasonal snow field</li> </ul>          | <ul style="list-style-type: none"> <li>• <b>episodic</b><br/>- debris flow events</li> </ul>   |
| <b>3) Displacement of boundary</b>               | <ul style="list-style-type: none"> <li>• <b>retrogressive</b><br/>- rockwall retreat due to rockfalls<br/>- regressive incision of debris flow channel in bedrock (?) and in moraine deposits<br/>- lateral erosion/ undercutting of slope foot by stream</li> </ul> | <ul style="list-style-type: none"> <li>• <b>progressive</b><br/>- elongation of talus slope<br/>- debris flow (cone) deposition<br/>- rampart migration<br/>- rock glacier migration<br/>- colluvial deposition on slope foot</li> </ul> | <ul style="list-style-type: none"> <li>• <b>dynamic</b><br/>- debris cone deposition vs. fluvial erosion<br/>- talus elongation vs. debris flow erosion</li> </ul> |

### 5.5 Analysis of connectivity between hillslopes and the fluvial system

As a next step, the connectivity between the sediment storages along the hillslopes and the stream channel (fluvial system) is examined. For that, a qualitative conceptual approach is developed and tested against a modified GIS-modelling approach developed by BORSELLI et al. (2008).

#### 5.5.1 Qualitative estimation of connectivity

The connectivity degree of the land surface, and more specifically, the connectivity of each storage landform to the stream channel, was studied qualitatively. Based on the geomorphic process comprehension acquired during fieldwork and the determination of toposequences and neighbourhood relationships, a conceptual framework was created. It is assumed the degree of hillslope-channel-connectivity changes with the frequency of material input and output across the storage boundary. Hence, the temporal dynamics of material throughput from one storage landform to its lower neighbour along a toposequence is used as indicator for the degree of connectivity between the sediment storages and the main channel (fig. 5.2). For instance, it is supposed that a continuous material transfer across a storage boundary is related to a permanent and thus, high degree of connectivity. In contrast, a more sporadic sediment throughput, in form of episodic or periodic geomorphic events, results in a lower, inconstant connectivity between a storage landform and the main channel. The interplay of continuous and episodic events might be linked to a medium connectivity. As exception and for simplification, all storage landforms in direct contact to the main channel or alluvium are linked with a high degree of connectivity, regardless of their temporal dynamics of material throughput.

In the case of decoupled neighbouring landforms, where no significant material throughput occurs, the sediment cascade is interrupted at this boundary. Therefore, only the part of the toposequence, which lies lower than the decoupled boundary, represents a sediment cascade that is connected to the stream channel. Hence, all higher located storages are disconnected from the fluvial system.

Finally, it is assumed that the degree of connectivity to the stream cannot increase upslope. Thus, the connectivity degree of each landform represents the maximum degree for the higher situated landforms along the toposequence – even though the frequency of material transfer would imply a higher degree of connectivity. Following these principles, the connectivity of each storage landform to the fluvial system was determined in ArcGIS, beginning from the

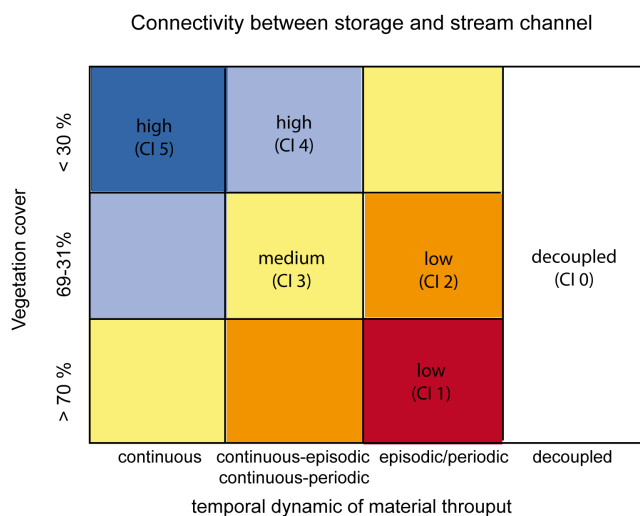


**Fig. 5.2:** Semi qualitative assessment of connectivity between storage landforms and stream, regarding temporal dynamics and vegetation cover.

valley bottom to the ridge crest. Furthermore, the vegetation cover of landforms, as mapped for both study sites, was used as weighting factor for the previously determined connectivity degree. It is supposed that the higher the degree of vegetation coverage, the more it buffers and diminishes the connectivity. As shown in figure 5.2, the combination of connectivity degree and vegetation cover finally results in a specific, qualitative connectivity index (CI). For that, the shapefiles of vegetation and connectivity have been converted to raster files with specific numeral attributes per landform and multiplied with each other using the raster calculator in ArcGIS. In total, five indices can be differentiated as well as one index for decoupled storages. Finally, connectivity maps were created and statistically analysed with respect to spatial variations.

### 5.5.2 Modelling of connectivity index

In addition to the qualitative connectivity study, connectivity was determined quantitatively using the GIS modelling approach by BORSELLI et al. (2008), originally used in the context of soil erosion. The modelling procedure is graphically explained in figure 5.3 by a simple slope with a flow path between a source area A and a local sink B. The underlying question of this topography-based approach is: What is the probability that sediment from a certain source on the hillslope will reach the stream network?

It is assumed that the probability  $p$  that a mass converging in A reaches B is the product of two probabilities: First, the probability  $p_{dn}$  defines the likelihood that sediment arrives at B along the flow line between A and B.  $P_{dn}$  is inversely proportional to the downslope distance. Second, the probability  $p_{up}$  is that sediment reaches the source point A. Therefore, the probability  $p$  (the

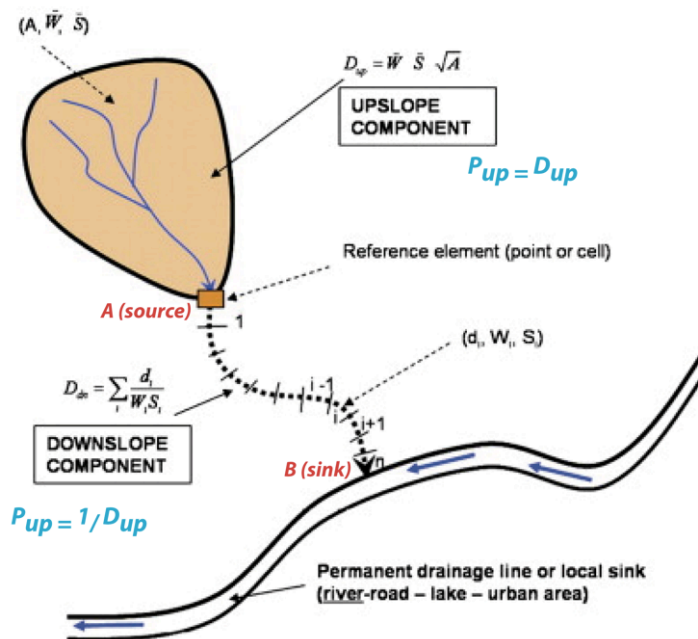


**Fig. 5.3:** Graphic illustration of the numeric GIS-modelling approach. For explanation see text. Source: by BORSELLI et al. 2008 (modified).

connectivity between source A and sink B) is controlled by an upslope and downslope component: The downslope component  $D_{dn}$  represents the downslope length of the flow path between source A and the nearest sink B. It is inversely proportional to  $p_{dn}$ . Furthermore, it is supposed that  $D_{dn}$  depends significantly on local factors such as the slope gradient and – in the context of soil erosion – the type of land use and management. Thus, weighting factors have to be assigned to each flow line segment

between A and B. Beside the slope factor  $S$ , representing the slope gradient of the terrain, BORSELLI et al. (2008) define a weighting factor  $W$ . To calculate  $W$ , they adapt the pre-existing C-factor of the USLE, which is the crop/vegetation and management factor in terms of soil erosion.

The upslope component  $D_{up}$  is the potential for downward routing of the sediment, which is produced upslope.  $D_{up}$  depends on the area draining into A as well as on the same weighting factors  $S$  and  $W$ , as defined for the downslope component. Average values of the two weighting factors over the contributing upslope area are used and multiplied with the square root of the upslope contributing areas (see equation in figure 5.3). Therefore, the upslope component is directly proportional to the probability  $p_{up}$ , as it increases with increasing  $D_{up}$ .

Finally, the probability  $p$  (the product of  $p_{up}$  and  $p_{dn}$ ), that a mass entering A reaches B, can be calculated based on the upslope and downslope component of connectivity, resulting in an index of connectivity (CI). Each raster cell has its own CI-value, which is defined in the range of  $[-\infty, +\infty]$ . Hence, connectivity increases with growing CI.

Since BORSELLI et al. (2008) developed this numeric algorithm for the study of soil erosion in lowlands, it has to reflect about the adaptability of the weighting  $W$  for study in the SNP. While BORSELLI's study area justifies the use of the C-factor of the USLE, where runoff and sediment flux are significantly controlled by vegetation cover and land use management, it can obviously not be applied for high alpine, uncultivated environments. Therefore, in this context, a new weighting factor  $W$  must be defined, which fits the prerequisites of the W-factor, as described by BORSELLI et al. (2008). As major criterion, this factor has to represent an observable and measurable barrier against the sediment transfer due to local conditions controlling the efficiency of sediment delivery to the fluvial system. Finding such a weighting factor is not simple. Referring to CAVALLI et al. (2012), who modified BORSELLI's algorithm for high-alpine regions, the roughness index (RI) seems to be the most suitable weighting factor  $W$  for the study in the SNP. Being a local measure of the topographic surface roughness, the RI is calculated as standard deviation of the residual topography at a scale of just a few meters (see e.g. CAVALLI & MARCHI 2008). Referring to CAVALLI et al. (2012), the residual topography is calculated as the difference between the original DEM (2 m resolution) of each study area and an averaged version of the DEM, which is smoothed by a 5x5 cell moving window using the spatial analyst of ArcGIS. The smoothing avoids the effect of large-scale topography. After calculating the residual topography by means of the raster calculator ( $DEM_{original} - DEM_{smoothed}$ ), the standard deviation is computed using a 5x5 cell moving window over this residual topography raster grid. According to CAVALLI et al. (2012), the RI is defined as (eq. 5.2):

$$RI = \sqrt{\frac{\sum_{i=1}^{25} (x_i - x_m)^2}{25}} \quad (5.1)$$

$$W\text{-factor} = 1 - \left(\frac{RI}{RI_{max}}\right) \quad (5.2)$$

In equation 5.1, 25 specifies the number of processing cells within the 5x5 cells moving window,  $x_i$  the value of the one specific cell of the residual topography and  $x_m$  the mean of the 25 cells value.

Finally, to gain the same variation range as for the  $S$ -factor and to weight them equally with regard to the USLE C-factor, the roughness index was standardised (eq. 5.2). This allows comparability to BORSELLI'S original model. The  $W$ -factor reaches its maximum value in the cases where the deposited sediments are more at risk of mobilisation (minor vegetation cover and less protection) and reaches zero when sediment storage is totally protected from transport (dense vegetation cover). As stated by CAVALLI et al. (2012), using the RI factor has the advantage that its use is objective and based on tabular data such as the C-factor. Furthermore, it allows the modelling of the sediment connectivity solely on a small amount of input data.

The connectivity index for both study sites was calculated by using ArcGIS based on the DTMs and on the weighting factor  $W$ . In order to force the connectivity calculation to close at the border of the stream channel, a raster mask of the stream was created. The modelling procedure is described in more detail in appendix C-8. Finally, the originally calculated connectivity index has been reclassified into five classes (1-2 = low, 3 = medium, 4-5 = high) based on a natural breaks classification. To compare the modelled CI with the semi-qualitative study, the same range/size of classes has been chosen.

### **5.6 Calculation of storage activity and sediment supply potential**

Based on the mapping of storage landforms and the connectivity analyses, "hotspots" within the sediment flux systems of the alpine valleys have been analysed as a last step. While the inventory of sediment storage provides the localisation of available sediment sources within the sediment cascade, the knowledge on the connectivity of sediment sources with the main channel allows estimating the potential for sediment delivery to the fluvial system. It is assumed that the higher the degree of connectivity between a storage and the stream channel, the higher is the efficiency for sediment supply (BRIERLEY et al. 2006, FRYIRS et al. 2007).

Nevertheless, connectivity alone is not the single influencing factor on sediment fluxes in mountain areas. Instead, it is assumed that the efficiency of a storage landform for sediment supply represents a function of both, connectivity and storage activity. In this study, the activity of sediment storages is approximated by two parameters: The degree of vegetation cover and the stream power index (SPI). In addition to the buffering effect, vegetation considerably contributes to the slope stability by minimizing rain-drop impacts and runoff and by stabilising non-consolidated sediments through its dense root systems (THELER et al. 2010). While most of the studies, such as SCHROTT et al. (2003), only use the vegetation cover as activity indicator, in this study, it is assumed that the storage activity might also be controlled by the risk of sediment mobilisation via geomorphic processes. The

stream power index (SPI) serves as measure for the erosive power of overland flow, by combining the slope gradient and the upslope drainage area (eq. 5.3, MOORE et al. 1993):

$$SPI = \text{specific catchment area} * \tan(\text{slope}) \quad (5.3)$$

With a rise in specific drainage area and slope gradient, the amount of water contributing from upslope areas and the velocity of water flow increase. Hence, with increasing SPI, the risk of sediment mobilisation/erosion and storage activity increases (GRUBER & PECKHAM 2008).

Following these considerations, the potential of sediment supply can be determined by using two simple matrices (fig. 5.4), inspired by THELER et al. (2010). The first matrix combines the SPI with the vegetation cover and gives the degree of storage activity to be defined in three classes (high, medium, latent). The SPI was calculated for each raster cell based on the smoothed DTMs (3 x 3 neighbourhood filter) by using the GIS hydrological toolsets and the raster calculator. The specific drainage area was calculated as a function of the flow accumulation and the size of the raster cell. The slope raster grids have been converted to radian. In order to derive specific SPI-values for each storage landform, a new raster grid was created showing the mean SPI per storage.

The SPI was classified into three classes (low, medium, high). Based on the geomorphological mapping, three classes of vegetation cover are distinguished (<30%, 31-69%, >70%). As shown in the first matrix, the classed of vegetation cover and of the SPI are multiplied by using the raster calculator in ArcGIS.

Then, the information from the first matrix is used in the second matrix and multiplied with the degree of hillslope-channel-connectivity by ArcGIS. For that, three classes of activity have been distinguished, while inactive and latent active storages were summarised. The connectivity indices have been classified as low (CI=1-2), medium (CI=3), high (CI=4-5) and, if available, no connection/decoupled. Finally, the matrix allows the evaluation of the potential of basin surface or more specifically, of sediment storages to deliver sediment into the fluvial system. This procedure was performed twice for each valley, by using both the qualitative and numeric connectivity study.

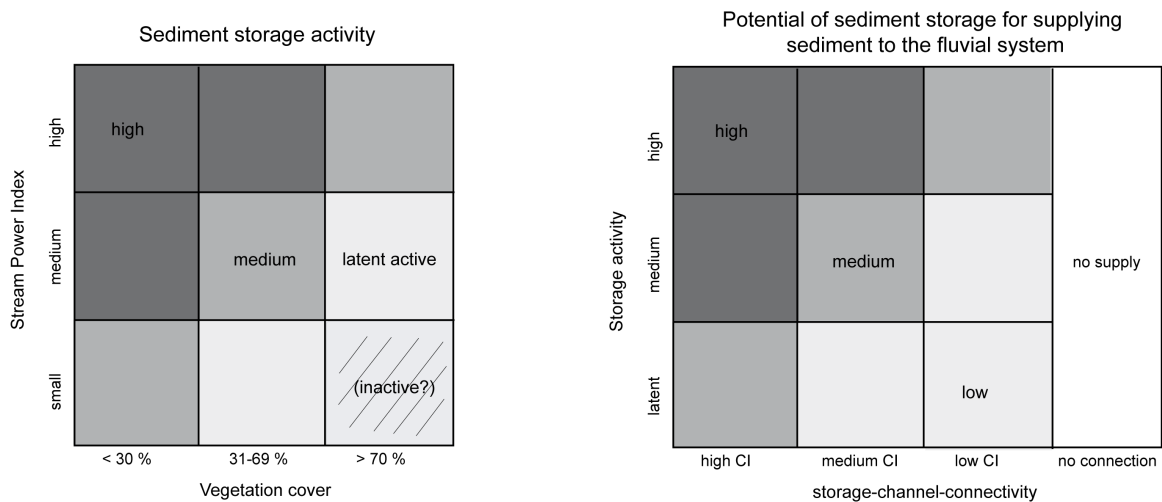


Fig. 5.4: Evaluation of the sediment supply potential. Own graphic, referring to THELER et al. (2010).

## 6 RESULTS

For the following chapter, it is highly recommended to use the supplemented maps (M-1 to M-14), as listed in the titles. They are one of the key outcomes of each analysis. Furthermore, some of the tables and graphics of each sub-chapter are presented within the appendix D to I.

### 6.1 Geomorphological setting of the study areas (*M-1, M-2*)

The geomorphological maps of the study areas at the scale of 1:5000 display active geomorphic processes, singular landforms, geomorphography, hydrology, surface material as well as the combination of process domains and the degree of vegetation cover. On the geomorphological map of **Val dal Botsch** (map M-1), the north-to-south oriented V-shaped valley is primarily dominated by gravitational processes such as low magnitude rockfalls, debris flows and snow avalanches, but also by cryogenic processes and slope erosion. The fluvial process domain is exclusively related to periodic sedimentation, incision and lateral erosion by the stream channel. Hence, extensive alluvial deposits cover the valley bottom with grain sizes ranging from clay up to angular boulders due to the large gravitational influences from hillslopes.

Below the bedrock cliffs, the gravitational process domain controls the steep upper slopes, predominantly along the western slopes near the outlet and along the south-facing slopes of the upper cirque. Continuous low-magnitude rockfalls occur mostly above the upper timberline along the western upper valley and result in the accumulation of extensive talus sheets and cones, summarised as talus slopes. Large failures have not been identified. The talus slopes are mainly composed of angular rock fragments ranging from pebbles to some larger boulders. The dominance of smaller particles might reflect the origin of low-magnitude events. Furthermore, the talus deposits show a distinct fall sorting with a downslope increase in particle size from top to foot, but modification by debris flow action frequently takes place leading to the formation of levees and flow tracks.

Debris flow events are widespread and active processes throughout the valley, mainly occurring along steep hillslopes. Often appearing at the transition between slope foot and valley bottom, major depositional landforms include cones and hillslope debris flows, summarised as debris cones. Grain sizes of those deposits range between boulder and sand depending on the source lithology. In addition, the contemporary deposition by both rockfalls and debris flows result in the formation of talus slopes/debris flows.

While slope-type debris flows mobilise loose talus sediment, torrent bed-type debris flow occur in channels incised within moraine valley fills, especially along the western middle basin. The largest hillslope debris flows in Val dal Botsch, and also one of the most impressive within the SNP, can be found along the western slopes near the outlet (fig. 4.4b). Here, multiple, successive large debris flows have overrun the forest, visible by numerous upright-standing trees within the deposited

debris flow material. Here, STOLZ & HUGGLE (2008) calculated maximal magnitudes of 25,000 m<sup>3</sup> and velocities of 8 m/s.

Although to minor extent, seasonal snow avalanches may be active along the slopes near the outlet. Typical indices of gravitational impact by avalanches are avalanche tracks within the dense vegetated hillslopes, uprooted fallen trees with distinct downslope orientation and typical accumulations of rock fragments that are stacked on top of each other.

The slope erosional process domain can be primarily found within the middle and upper basin, particularly along the sidewalls of incised debris flows tracks and along the slope foots. Here, lateral erosion by debris flows or the stream channel are generating an oversteepening of the fine-grained, mainly sparse vegetated slopes, which in turn, immediately induces extensive sheetwash or linear rill erosion with gullying during seasonal rainfall events (fig. 2.8).

Today, glacier ice cover is absent within the basin. Nevertheless, parts of a moraine ridge, which might be related to the little ice age in 1850, can be found along the cirque within the eastern upper valley. In addition, as the most characteristic feature in Val dal Botsch, vegetated moraine valley fills cover the middle and upper basin, representing an undulating hummocky relief that looks like badlands (fig. 4.4a, fig. 2.8). Nevertheless, they are relatively steeply inclined. Frequently, bed-type debris flow and gullying along sidewalls are retrogressively incising the cohesive material upwards resulting in steep channels. Most of such moraine deposits border on talus slopes located at higher altitudes. However, some of those talus slopes are connected via the retreating debris flow channels. The cryogenic process domain controls the vegetated moraine deposits via solifluction. Seasonal and diurnal thawing of the active layer induces a slow downslope dislocation of the upper, water-saturated sediment cover over the frozen, impermeable underground. In turn, the movement of vegetated surface material becomes immediately visible through the formation of stripes, terraces and garlands, one of the most prominent features in Val dal Botsch. Yet, the cryogenic creep seems to be very slow due to the stabilising effect of vegetation, and thus, it is possibly only of minor importance for sediment transfer within the valley. Interestingly, both the cryogenic creep and the retreating incision appear to be more active in the western than the eastern valley.

Finally, two relatively rare landform types in Val dal Botsch are protalus ramparts along the eastern upper valley (fig. 2.3) and two nivation hollows. Rampart formation might be an active gravitational-nival process within the valley, depending on the existence of a seasonal snowfield at the lower margin of a talus foot and rockfall input of relatively coarse particles. In upper, protected slope positions, nivation hollows are gradually developing under snow patches over time.

The geomorphological map of **Val Mütschans** (map M-2) displays an interesting geomorphic case of an alpine valley that gradually broadens from a V-shaped valley within the lower to a U-shaped valley within the upper basin (fig. 4.4e). One of the most significant characteristics is the large

proportion of bedrock, particularly along the south-facing slopes. Nevertheless, small “pockets” of loose rock fragments or even small talus slopes are frequently embedded within hollows, considerably favoured by the horizontal bedding of the rock layers. Due to the comparatively small scale, those embedded talus slopes have been rarely mapped.

The majority of the valley is dominated by the gravitational process domain. Small-scale rockfall events generate talus slopes of relatively fine, angular rock fragments. Extensive stripe-like deposits cover the upper basin in particular (fig. 4.4e). Particle size often increases from top to foot. Most of the talus slopes are not as elongated as in Val dal Botsch, since they are often bordered by large bedrock outcrops or moraine deposits. In addition, two protalus ramparts are situated along the north-facing talus slopes of the upper trough, indicative for the gravitational-nival process domain.

Some of the most active and dominant geomorphic processes in Val Müschauns are debris flows. In form of hillslope debris flows, they modify talus deposits and leave behind incised tracks with distinct levee systems along the steep talus. At the south-facing slopes of the middle basin, the interplay of episodic hillslope debris flows and continuous rockfall events results in the formation of talus slope/debris flows, some of which are densely vegetated today (fig. 4.4d).

Primarily along the lower and middle basin, torrent bed-type debris flows mobilise sediment fills within steep, deeply incised bedrock channels and transport them downslope to the valley bottom (fig. 2.4b). Thus, debris cones with large boulders, stuck debris flow heads and levee ridges are frequent features at the transition between the lower slopes and the valley bottom in Val Müschauns. Most of the cones are superimposed on fluvial terraces and are being laterally eroded by the stream channel. The largest debris cones occur along the southern slopes, particularly within the Müschauns Dolomite. Since the volume of the individual deposits seems to decrease in upstream direction, lithology might control the sediment capacity of debris flows.

Avalanche tracks within the forest, uprooted trees and imbricated/layered rock fragments along the densely vegetated slopes of the lower basin reveal seasonal impact of snow avalanches. Visible exposures within the colluvium-covered slopes show a subsurface material of grain sizes ranging from gravel to very fine clasts. The (gravitational-)slope erosional domain characterises mainly the south-facing slopes of the lower catchment. Here, debris flows or lateral fluvial erosion gradually lead to overstepping of the slopes, thereby inducing rill erosion (with gullying) and sheetwash, or even new debris flows, within the fine grained, cohesive material.

Similar to Val dal Botsch, there is no glacier ice in Val Müschauns today, but the glacial lake within the upper valley and the bordering moraine ridge indicate former glacial action. Within the uppermost cirque of the basin, there might be an inactive rock glacier. However, it needs to be stressed that the existence and activity degree of the rock glacier is associated with certain degree of uncertainty, because its mapping is based solely on air photo and DEM interpretation.

The cryogenic and gravitational-cryogenic process domains are clearly concentrated within the upper basin. Here, the majority of the lower slopes are covered by coarse to fine grained, relatively compact, sparse vegetated moraine valley fills, influenced by cryogenic creep during seasonal freeze-thaw cycles. In contrast to Val dal Botsch, the typical undulating badland relief with bounded vegetation terraces or stripes (garlands) is not as strongly pronounced. Instead, solifluction stripes are often unbounded. This is possibly related to the lesser inclination and the comparatively thinner vegetation cover that would result in stabilisation. Furthermore, solifluction occurs within talus material thereby generating visible single lobes of relatively fine material (fig. 2.2). The fluvial-cryogenic process domain is exclusively concentrated within the bottom of the upper valley. Here, the wide alluvial plain is structured by a typical geometric ground pattern with circles or polygons of sparse vegetation and rock fragments due to seasonal frost heaving (fig. 4.4f).

Finally, the entire valley bottom of Val Müschauns is dominated by fluvial processes including periodic incision, sedimentation of alluvial plains and high terraces as well as lateral erosion of the deposits along the lower slopes. As typical features, the alluvium is often mixed with coarse, angular slope material originating from debris flows or rockfalls (fig. 2.9).

For a better understanding of the alpine valleys a closer consideration of the process domains appears to be suitable. However, since the main focus of this study will be on the storage landforms, a short characterisation of process domains in both study areas is presented in appendix D.

## **6.2 Spatial distribution and characteristics of storage landforms (M-3, M-4)**

First of all, the altitudinal distribution of the land surface needs to be considered (appendix D-13). The majority of the basin surface of Val dal Botsch is located within the middle altitudinal ranges between 2250 and 2750 m a.s.l., with a significant peak at 2300 m. In contrast, Val Müschauns' surface is largely concentrated at much higher altitudes between 2650 and 2850 m a.s.l.

The detailed information concerning the number of storage landforms, area, altitude and aspect are displayed in appendix E. In figure 6.1, the specific slope gradients, altitudes and normed distances to the watershed of the landforms are presented in the form of boxplots. For each storage, the boxplots depict the minimum, maximum, median as well as the upper and lower quartile of the data.

In total, 137 sediment storage landforms have been mapped in the 3.72 km<sup>2</sup> large alpine valley Val dal Botsch that can be divided into ten different types of storage landforms (map M-3 and appendix E-14). In Val Müschauns (6.18 km<sup>2</sup>), based on 199 mapped objects, twelve different storage types have been identified (map M-4, appendix E-15). In contrast to other geomorphic studies (OTTO 2006, SCHROTT et al. 2003) bedrock is also typified as sediment storage type, since it represents the first sediment source within the cascade. Colluvium generally describes hillslope derived colluvial material of usually less than one meter in thickness. Hence, bedrock often crops out. In Val

Müschauns, the storage type alluvium/colluvium was introduced representing alluvial deposits with large material input from hillslopes. Landforms that have been classified as unspecified will not be mentioned in the subsequent investigations.

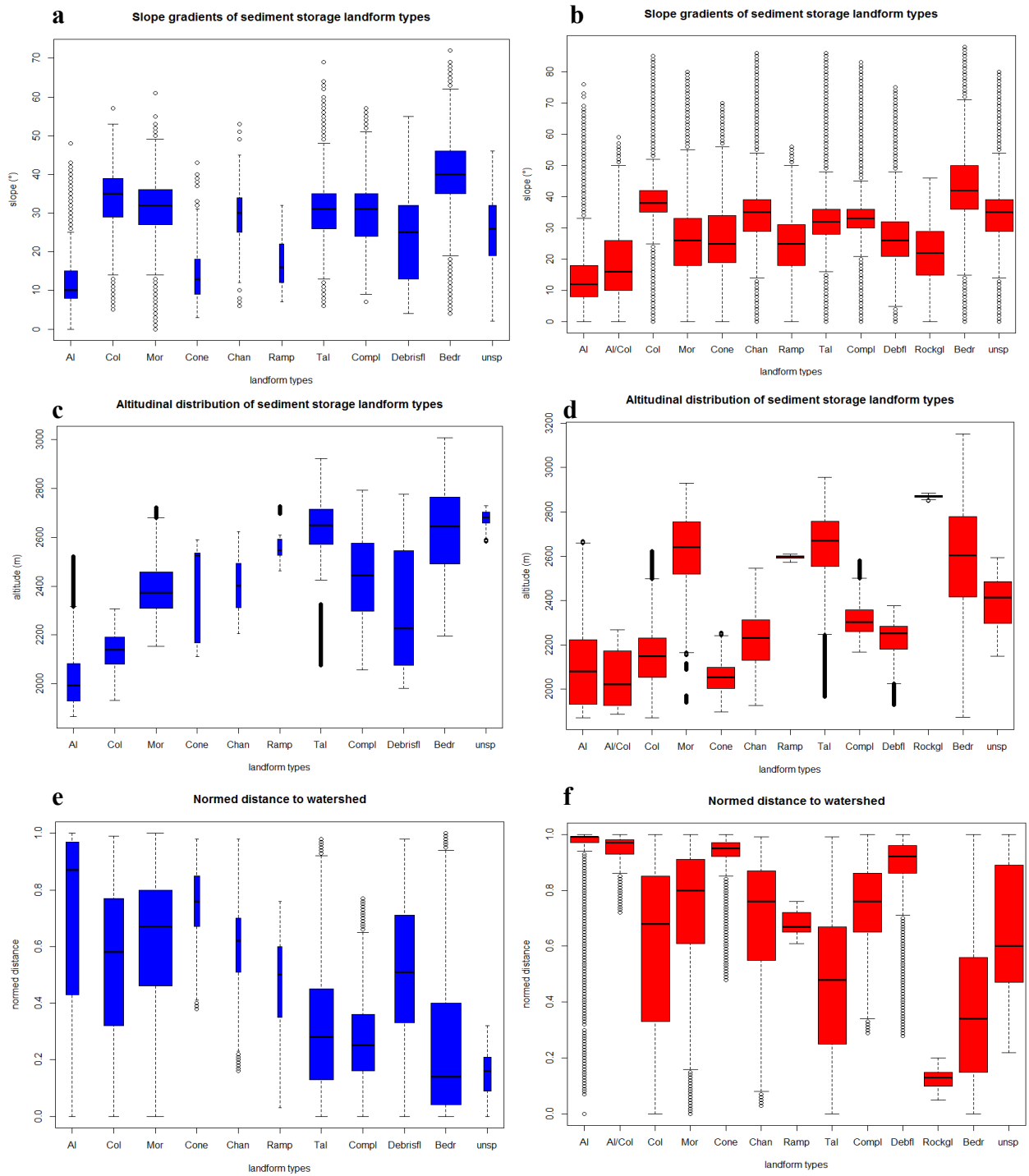
**Val dal Botsch** is characterised by a considerably heterogeneous pattern of storage landform types (tab. 6.1a). Around 22 % of the surface is bedrock – consequently, more than 78 % of the valley is covered by sediments. The catchment is primarily dominated by moraine deposits, which cover more than 25 % of the land surface, largely within the middle and upper basin. Further major sediment storages are rockfall and debris flow deposits such as talus slopes (14 %), talus slope/debris flows (12 %) and hillslope debris flows (9 %). Colluvium and alluvium account for 9 % and 4 % of the basin surface. The relative amount of surfaces made of debris cones, debris flow channels and protalus ramparts are relatively small, with less than 1 %, respectively. While debris flow channels are frequently incised within moraine deposits, the associated cones occur mainly along the western slopes at the transition between to the valley bottom.

More than half of **Val Müschauns**'s surface (59 %) is dominated by bedrock, particularly along the south-facing slopes (tab. 6.1b). Hence, 41 % of the basin area is covered by loose sediment. It is important to remark that small-scale talus slopes, stored within couloirs of the rock faces, were not mapped at the scale of 1:5000. Consequently, the absolute talus surface will be slightly underestimated. Rather similar to Val dal Botsch, the major sediment deposits in Val Müschauns are talus slopes (13 %), particularly within the upper basin.

**Table 6.1:** Absolute and relative area of storage landform types in Val dal Botsch (a) and Val Müschauns (b). For a more detailed description see appendix .

| a) Landform types<br>in Val dal Botsch | Number<br>of<br>objects | relative<br>surface (%)<br>(relative<br>sediment cover) |
|--|-------------------------|---|
| Alluvium                               | 8                       | 3.83 (4.89)   |
| Colluvium                              | 9                       | 9.09 (11.61)  |
| Moraine deposit                        | 37                      | 26.47 (33.80)   |
| Debris cone                            | 3                       | 0.79 (1.00)   |
| Debris flow channel                    | 6                       | 0.69 (0.88)   |
| Protalus rampart                       | 6                       | 0.48 (0.61)   |
| Talus slope                            | 20                      | 14.03 (17.91)   |
| Talus/debris flows                     | 6                       | 12.07 (16.22)   |
| Hillslope debris flows                 | 17                      | 9.45 (12.07)  |
| Bedrock                                | 19                      | 21.69 (-)   |
| unspecified                            | 6                       | 1.40 (1.79)   |
| <i>Total</i>                           | <b>137</b>              |   |

| b) Landform types<br>in Val Müschauns | Number<br>of<br>objects | Relative<br>surface (%)<br>(relative<br>sediment cover) |
|---------------------------------------|-------------------------|---|
| Alluvium                              | 1                       | 0.94 (2.32)   |
| Alluvium/Colluvium                    | 21                      | 0.29 (0.72)   |
| Colluvium                             | 20                      | 11.93 (29.28)   |
| Moraine deposit                       | 17                      | 8.59 (21.08)  |
| Debris flow cone                      | 15                      | 0.45 (1.12)   |
| Debris flow channel                   | 21                      | 0.90 (2.22)   |
| Protalus rampart                      | 1                       | 0.05 (0.12)   |
| Talus slope                           | 36                      | 13.08 (32.09)   |
| Talus /debris flows                   | 6                       | 2.69 (6.59)   |
| Hillslope debris flows                | 9                       | 0.65 (1.58)   |
| Block glacier                         | 1                       | 0.12 (0.30)   |
| Bedrock                               | 44                      | 59.25 (-)   |
| Unspecified                           | 7                       | 1.05 (2.59)   |
| <i>Total</i>                          | <b>199</b>              |   |



**Abbreviations of landforms (also for all subsequent figures displaying boxplots):**

*Al=Alluvium, Col=Colluvium, Al/Col=Alluvium/ Colluvium, Mor=Moraine deposits, Cone= Debris cone, Chan=Channel, Ramp=Rampart, Tal=Talus slope, Compl=Complex or Talus slope/debris flows, Debrisfl=Hillslope debris flows, Rockgl=Rock glacier, Bedr=Bedrock, unsp=unspecified*

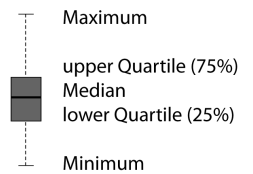


**Fig. 6.1:** Morphometric characteristics of storage landforms in Val dal Botsch: a) Slope gradients, b) altitudinal distribution and c) normed distance to watershed (0= watershed, 1=stream). The boxplots depict the minimum, maximum, median as well as the upper and lower quartile of the data for each landform. The thickness of the boxplots in Val dal Botsch represents the sample size (number of objects/number of raster cells). In Val Müschau, the specific thickness of boxplots is not illustrated, since the sample size of some landforms was tool small.

The relative amount of surfaces consisting of other rockfall and debris flow generated talus deposits is very small with less than 3 %, respectively. Furthermore, despite their small proportion (1 %), debris flow channels are widespread features, primary incised within bedrock – rarely in moraine deposits. Colluvium and moraine valley fills account for 12 % and 9 %. In contrast, alluvial/colluvial deposits as well as the ramparts and the rock glacier represent only minor parts of the basin surface with less than 1 %, respectively.

The **specific slope angles** of each landform type are illustrated in figures 6.1a-b as boxplots. In both valleys, the highest gradients of around 38-51° can be identified for the steep bedrock cliffs, in contrast to the very flat alluvium within the valley bottom (median 10°). In Val dal Botsch, small gradients of 13° (median) characterise debris cones, in contrast to obviously steeper gradients of 24° (median) in Val Müschauns. Here, the GIS-analysis probably depicts the oversteepening of those objects within the DEM (through fluvial erosion). In both valleys, talus slopes and talus/debris cones have inclinations of around 27-35°. The gradients of hillslope debris flows are slightly lower with ca. 22-32° and even lowest in Val dal Botsch. In Val dal Botsch, ramparts are rather flat (16°), whereas in Müschauns, the rock glacier and the ramparts are characterised by median gradients of 24-26°. In both valleys, colluvium is relatively steep (28-42°). Moraine deposits of Val dal Botsch are obviously steeper (median = 33°) than in Val Müschauns (median = 27°). In contrast, debris flow channels are almost in the same order (32-38°), although incised within different landforms.

With regard to the **altitudinal distribution** of landforms (fig. 6.1c-d), in both study areas, there is a dominance of colluvium and alluvium in lower altitudes (1800-2100 m a.s.l.) and bedrock in upper altitudes (2500-2800 m a.s.l.), highest in Val Müschauns. The rock glacier of Val Müschauns is an exception, lying above 2880 m a.s.l. However, in both valleys, the highest sediment deposits occur at altitudes of ca. 2550-2650 m, in form of talus slopes, sometimes bordered by protalus ramparts. In Val Müschauns, moraine deposits are also located in such higher altitudinal ranges. In contrast, the majority of Val dal Botsch's moraine deposits are concentrated at slightly lower altitudes, between 2300-2450 m a.s.l. The medium altitudes (2100 - 2550 m a.s.l.) of the two basins are largely characterised by talus slope/debris flows, hillslope debris flows as well as channels. Debris cones are deposited at altitudes below 2200 m a.s.l. in both valleys.

Contrary to the absolute altitude, the **normed distance** (fig. 6.1e-f) provides information on the relative position of a landform between the ridge crest and stream and therefore on the relative position within a toposequence and a sediment cascade. While bedrock – and as exception the rock glacier in Val Müschauns – represents the first and uppermost sediment source, the lowermost storages close to the stream are alluvium and alluvium/colluvium. In between, a specific landform succession is generally visible: Directly below the cliffs, talus slopes and talus slope/debris flows

largely dominate the uppermost slopes of both valleys, sometimes bordered by a rampart (or rock glacier). In Val Müschauns, talus slopes are situated much higher than in Val dal Botsch. Hillslopes debris flows cover the midslopes, or even the lower slopes as in Val Müschauns. Within the middle and lower slopes, debris flow channels follow, some of which lead to the accumulation of a debris cone at the top or close to the alluvium. Colluvial and moraine deposits are primarily located along the middle and lower slopes.

### 6.3 Major toposequence types (M-5, M-6)

As shown by the boxplots of the normed distance (fig. 6.1e-f), a simple slope classification in homogeneous units is not possible. Instead, there are distinct possibilities in which manner neighbouring storage landforms are topologically organised. All individual landform sequences are presented in appendix F. The classified types are displayed in M-5 and M-6. It needs to be stressed that the line of toposequence does not illustrate the exact position of sediment routing pathway.

In **Val dal Botsch**, 23 different toposequences have been identified in total and classified into seven types (fig. 6.2, M-5). A dominant landform succession along the western slopes near the outlet is toposequence I: Below a steep rock face, hillslope debris flows border on alluvium within the valley bottom. Sometimes, extensive talus slopes are interposed. In that case, they represent important sediment sources for the subsequent debris flow processes.

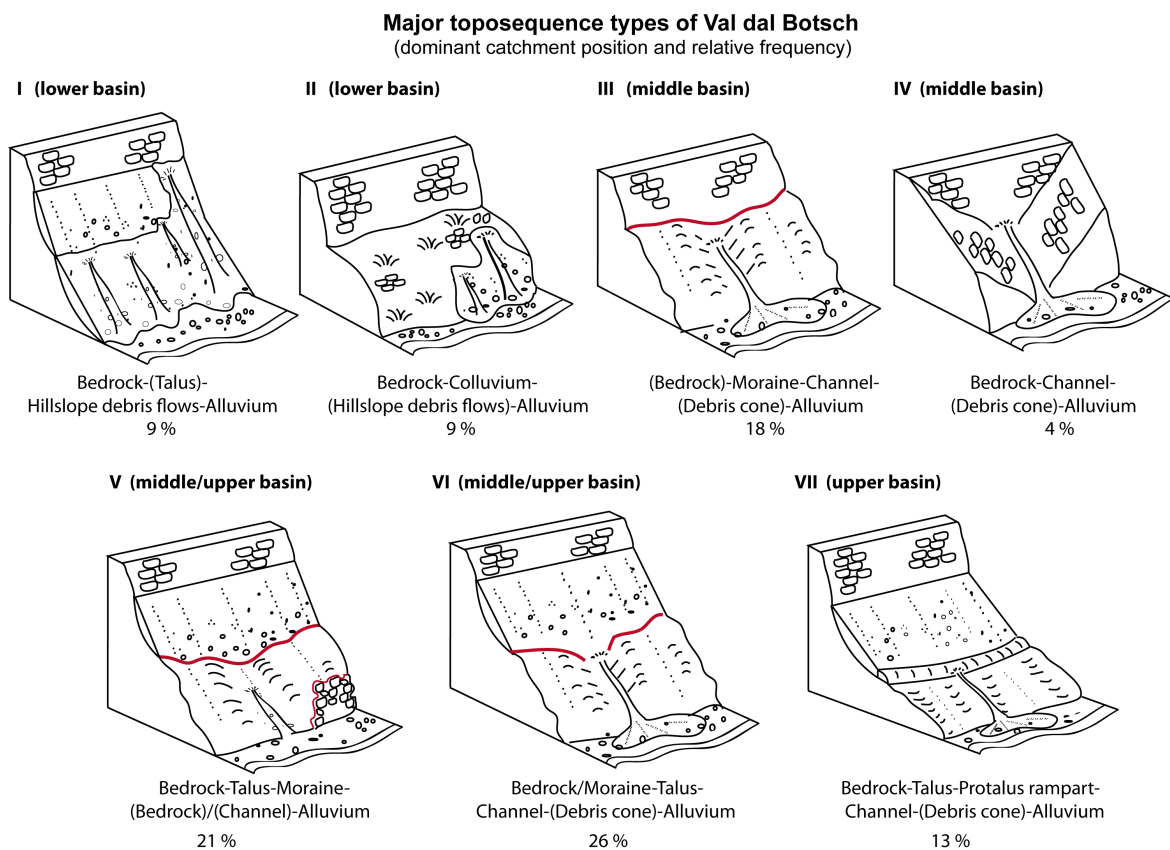


**Fig. 6.2:** Topological sketches of major toposequence types in Val dal Botsch. Relative frequency and major position within the catchment is also displayed. Red lines specify decoupled boundaries, as will be explained in chapter 6.4. The storage type talus slope comprises talus slopes as well as talus slope/debris flows.

The simplest, but also relatively rare topological organisation of landforms is toposequence II, mainly mapped in the lower basin: Located below a rock face, colluvium borders on alluvium, which is periodically influenced by the valley stream. Partially, hillslope debris flows separate colluvium from alluvium.

A major toposequence is type III, typical for the middle (and upper) basin. Here, a debris flow channel is incised within moraine deposits, followed by a debris cone lying above an alluvial plain. The channel is periodically filled with moraine material, primarily via cryogenic creep. With increasing sediment availability within the channel, torrential debris flows can be initiated by large water inputs, for example through heavy rainfall or snowmelt events.

In the course of gradual erosion of the moraine deposits, the underlying bedrock becomes exposed and toposequence III develops into type IV. Now, the surrounding bedrock constitutes the major sediment source for debris flows events. This toposequence occurs only rarely within the basin.

The second major landform succession is toposequence V: A rock face provides the sediment source for a talus slope, which is separated from the alluvium by extensive moraine fill (or rarely, by bedrock outcrops). Most often, a debris flow channel is incised within the moraine material, gradually retreating upslope in direction to the talus.

With continuous retrogressive incision, toposequence V may change to type VI – the most frequent landform succession in Val dal Botsch: In contrast to type IV, the moraine deposits no longer separate the talus slopes. Instead, the talus material is directly transferred downslope by debris flows via a channel and deposited along the slope foot upon the alluvium, most often in form of extensive debris cones. Toposequence types V and VI mainly dominate the middle/upper basin.

Finally, toposequence VII represents a special case, occurring in the upper valley: A rampart borders on a talus foot. Representing an important sediment source, the forefront of the rampart becomes subsequently eroded by debris flows. Sediment is then transferred downstream within a channel and accumulated as a debris cone above the alluvium near the stream.

In **Val Müschauns**, 33 different individual toposequences have been mapped (M-6) and classified into six toposequence types (fig. 6.3). One of the simplest, but contemporarily one of the major types within the lower basin is toposequence I: Lying below a rock face, colluvium directly borders on the alluvial plain, which is influenced by periodic fluvial action. Sometimes, small talus slopes separate the colluvial slope deposits from the alluvium.

In the course of the gradual retrogressive incision by debris flows, toposequence II may develop into type III, where the formerly separated talus slopes border directly on the debris flow channel. Hence, the channel is continuously filled with talus material until it will be depleted by episodic debris flow events. This type is mainly located in the middle basin.

Toposequence IV can be exclusively found along the south-facing slopes of the middle valley. Similar to Val dal Botsch's toposequence VI, hillslope debris flows are in direct contact with the

alluvium. In contrast, the hillslope debris flows are not fed by talus material, because bedrock outcrops separate the higher talus slope from the lower toposequence.

A typical landform succession in the upper valley is toposequence V: Below a steep rock face, an extensive talus slope, sometimes bounded by a protalus rampart, is followed by moraine valley fills in close contact to the alluvium.

Finally, toposequence VI represents a special and rare case of landform organisation within the upper trough. A talus is followed by a rock glacier, which borders on moraine deposits. The glacial lake represents the final sediment sink of this toposequence. Sediment storage within the lake is not considered within this study, because the focus is on the surficial sediment cover.

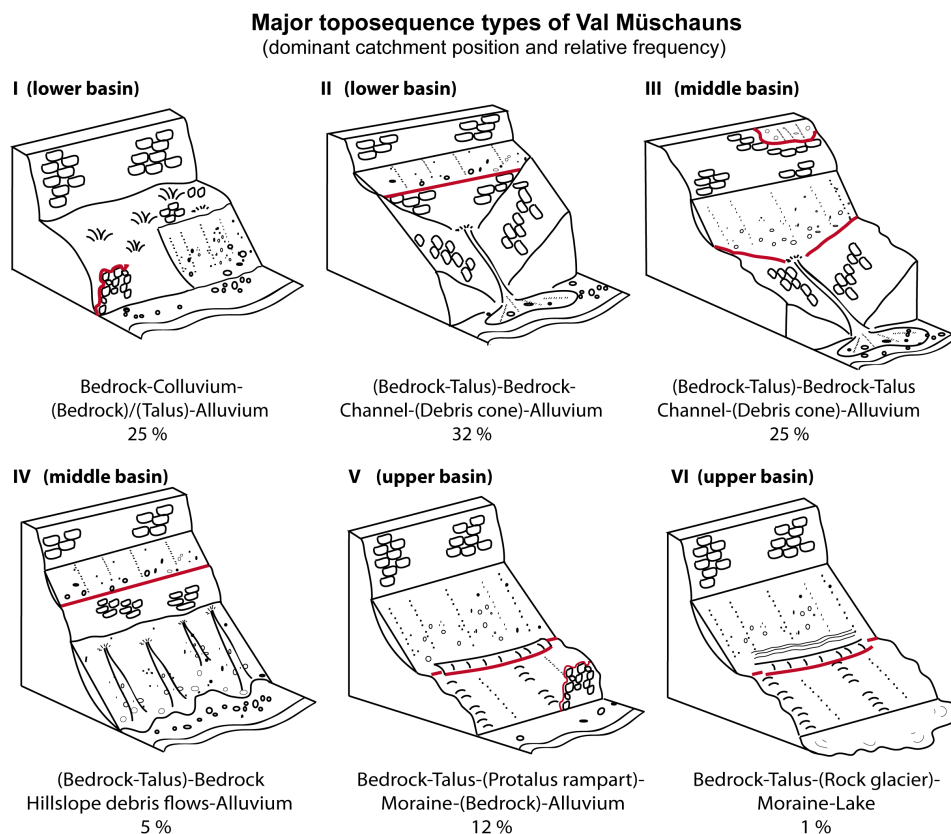


**Fig. 6.3:** Topological sketches of major toposequence types in Val Mütschans. For description see fig. 6.2.

#### 6.4 Functional relationships between neighbouring landforms

In order to relate the different toposequence types to alpine sediment cascades with uninterrupted sediment fluxes, the functional relationships between neighbouring landforms need to be considered. Based on the conceptual approach (chapter 5.4), for each alpine valley, specific storage neighbourhoods have been identified, resulting in different functional characteristics with regard to the material throughput, temporal dynamics and the long-term boundary displacement.

In **Val dal Botsch**, 22 different types of storage neighbourhoods exist. Table 6.1 illustrates all types of neighbourhoods with the temporal dynamics of material throughput (rows) and the displacement

of the separating boundary (columns). Due to the dominance of moraines, bedrock and talus deposits in Val dal Botsch, the most frequent storage relationship exists between bedrock and talus slopes (35 %). Here, sediment throughput across the boundary takes place primarily by continuous rockfall events. Further major neighbourhood types are moraine-talus and moraine-alluvium, which account for 8 % and 6 % of the basin's entire boundary length. Here, periodic cryogenic creep on vegetated moraine deposits during periodic freeze-thaw cycles results in material input to the lower storages. In contrast, rockfall processes or periodic shift of the alluvial plain transport material out of the moraine deposit. Likewise, the episodic material throughput between bedrock and hillslope debris flows constitutes one of the major neighbourhoods in Val dal Botsch, with a relative length of 6 %. All other neighbourhoods account for less than 5 % of the entire boundaries, respectively.

As a consequence, the material transfer across storage boundaries is linked to distinct dynamics. It becomes obvious that Val dal Botsch is particularly affected by a continuous material transfer, as around 35 % of the sediment throughput occurs continuously. This signal can entirely be related to the bedrock-talus neighbourhood. Then, a continuous-episodic (13 %), a continuous-periodic (11 %) as well as a periodic (13 %) and periodic-episodic (10 %) dynamic seem to equally dominate the material transport from storage to storage. The episodic material transfer, primarily controlled by the bedrock-hillslope debris flow neighbourhood, is of comparatively minor importance with 6 %.

The material transport between two storages and its temporal dynamic appears to influence the long-term position of the separating boundary notably. More than the half of the storage boundaries (66 %) of Val dal Botsch behaves retrogressively. The key relationships for this retrogressive displacement are bedrock-talus, moraine-talus, moraine-alluvium and bedrock-hillslope debris

**Table 6.1:** Functional relationships of neighbouring storages in Val dal Botsch. The neighbourhood-types are classified regarding the displacement of the separating storage boundary (columns) and the dynamics of the sediment throughput (rows). “Continuous-episodic” and “continuous-periodic” also operate vis-à-vis as “episodic-continuous” and “periodic-continuous”. The term “channel” defines debris flow channels.

| temporal dynamic \ displacement | retrogressive   | progressive                | dynamic  | unspecified/<br>decoupled  |      |
|---------------------------------|---|----------------------------|--|--|------|
| continuous                      | Bedrock-Talus (35%)   |                            |  |  | 35 % |
| continuous-episodic             |   |                            | Talus-Channel (1%)<br>Talus-Hillslope debris flows (12%)   |  | 13 % |
| continuous-periodic             | Bedrock-Alluvium (1%)<br>Moraine-Talus (8%)                   | Talus-Rampart (2%)         | Talus-Alluvium (<1%)   |  | 11 % |
| periodic                        | Bedrock-Colluvium (3%)<br>Moraine-Alluvium (6%)               |                            | Colluvium-Alluvium (4 %)   |  | 13 % |
| episodic                        | Bedrock-Hillslope debris flows (6%)<br>Bedrock-Channel (2%)   | Channel-Debris cone (< 1%) |  |  | 8 %  |
| periodic-episodic               | Moraine-Channel (4%)<br>Colluvium-Hillslope debris flows (2%) |                            | Channel-Alluvium (<1%)<br>Debris cone-Alluvium (1%)<br>Rampart-Channel (<1%)<br>Hillslope debris flows-Alluvium (3%) |  | 10 % |
| decoupled                       |   |                            |  | Bedrock-Moraine (2%)<br>Moraine-Bedrock (5%)<br>Talus-Moraine (4%) | 10 % |
|                                 | 66 %  | 2 %                        | 22 %   | 10 %   |      |

flows. Despite of the short relative length, the material transfer between moraine and debris flow channels also appears to play a crucial role. Hence, bedrock and moraine deposits gradually retreat as result of continuous rockfall detachment, regressive incision by episodic debris flows and periodic fluvial undercutting. In contrast, the progressive displacement of storage boundaries, for example, in the course of rampart propagation and debris cone deposition, seems to be of minor importance in Val dal Botsch. Instead, 22 % of the catchment's storage boundaries behave dynamically, where retrogressive and progressive displacements balancing each other over time. The dynamic signal is largely related to the close contact to the alluvium. Hence, the periodic shift of fluvial erosion and deposition balance the sediment input from hillslopes over time.

Finally, with regard to the toposequence approach and its transferability to the sediment cascade, one of the most important outcomes is that around 10 % of Val dal Botsch's storage boundaries are decoupled therefore disconnecting the specific toposequences. Hence, all talus-moraine, moraine-bedrock and bedrock-moraine neighbourhood lead to a decoupling of the sediment cascades of Val dal Botsch. As shown as red lines in figure 6.2, toposequences III and V do not represent incessantly coupled sediment cascades from the ridge to the stream. Nevertheless, the majority of Val dal Botsch's toposequences are coupled, generating uninterrupted sediment fluxes along hillslopes. Here, sediment fluxes traverse around five coupled storage landforms on average.

In **Val Müschauns**, 26 different types of storage neighbourhood have been identified in total, as shown in table 6.2. Similar to Val dal Botsch, the most widespread storage neighbourhood exists between bedrock and talus slopes. With a relative length of 27 % it is less frequent than in Val dal Botsch. Instead, there is a particular dominance of the relationship between bedrock and debris flow channels in Val Müschauns (21 %). A further major neighbourhood occurs between bedrock and

**Table 6.2:** Functional relationship of neighbouring storage in Val Müschauns. For description see table 6.1.

| dis-<br>placement<br>temporal<br>dynamic | retrogressive   | progressive                                      | dynamic   | unspecified/<br>decoupled  |      |
|--|---|--|---|--|------|
| continuous                               | Bedrock-Talus (27%)<br>Colluvium-Talus (1%)                     |  |   |  | 28 % |
| continuous-<br>episodic                  |   |  | Talus-Channel (1%)<br>Talus-Hillslope debris flows (<1%)                                    |  | 1 %  |
| continuous-<br>periodic                  | Bedrock-Alluvium (3%)   | Talus-Rock glacier (<1%)<br>Talus-Protalus (<1%) | Talus-Alluvium (1%)   |  | 5 %  |
| periodic                                 | Bedrock-Colluvium (11%)<br>Moraine-Alluvium (2%)                |  | Colluvium-Alluvium (2%)<br>Moraine-Lake (1%)  |  | 14 % |
| episodic                                 | Bedrock-Channel (21%)<br>Bedrock-Hillslope debris<br>flows (1%) | Channel-Debris cone<br>(<1%)                     |   |  | 22 % |
| periodic-<br>episodic                    | Moraine-Channel (2%)  |  | Debris cone-Alluvium (2%)<br>Channel-Alluvium (<1%)<br>Hillslope debris flows-Alluvium (1%) |  | 4 %  |
| decoupled                                |   |  |   | Colluvium-Bedrock (5%)<br>Bedrock-Moraine (5%)<br>Talus-Moraine (3%)<br>Rock glacier-Moraine (<1%)<br>Moraine-Bedrock (3%)<br>Talus-Bedrock (9%)<br>Protalus-Moraine (<1%) | 26 % |
|  | 66 %  | 1 %  | 7 %   | 26 %   |      |

colluvium (11 %), where sediment throughout takes place largely in form of periodic snow avalanches. With a relative length of 9 % and 5 %, two of the major storage neighbourhood types are decoupled, including talus-bedrock and colluvium-bedrock. All other storage relationships account for less than 5 % of the basin's storage boundary, respectively.

The material transfer between adjacent storages in Val Müschauns is dominated by a notable continuous event frequency. Mainly due to the bedrock-talus relationship, 28 % of the material throughput occurs continuously. Nevertheless, in contrast to Val dal Botsch, there is also a considerable episodic (22 %) and periodic (14 %) signal, due to the leading relationships bedrock-debris flow channel and bedrock-colluvium.

Similar to Val dal Botsch, around 66 % of the landform boundaries in Val Müschauns are dominated by a retrogressive displacement. Key drivers of this retreat are continuous rockfall events (bedrock-talus), episodic bedrock erosion by debris flows (bedrock-channel) as well as periodic snow avalanches (bedrock-colluvium). In contrast, the progressive (1 %) and dynamic displacement (7 %) of storage boundaries play a minor role.

Finally, due to the specific landform organisation and the resulting storage neighbourhoods, around 26 % of the storage boundaries are decoupled, interrupting the sediment trajectories. In particular, the specific relationships between talus and bedrock, comprising all embedded talus slopes within the rock face, as well as the neighbourhood bedrock-moraine and colluvium-moraine are major decoupling neighbourhoods within the sediment cascades of Val Müschauns. Hence, the majority of the toposequences contains a decoupling storage neighbourhood and does not represent a sediment cascade uninterrupted from the valley ridge to bottom (as shown in figure 6.3 as red lines). As a consequence, sediment cascades with unceasing fluxes are relative short, on average crossing three coupled storage landforms until sediment flux stops or enters the stream channel.

## **6.5 Strength of connectivity between storage landforms and stream**

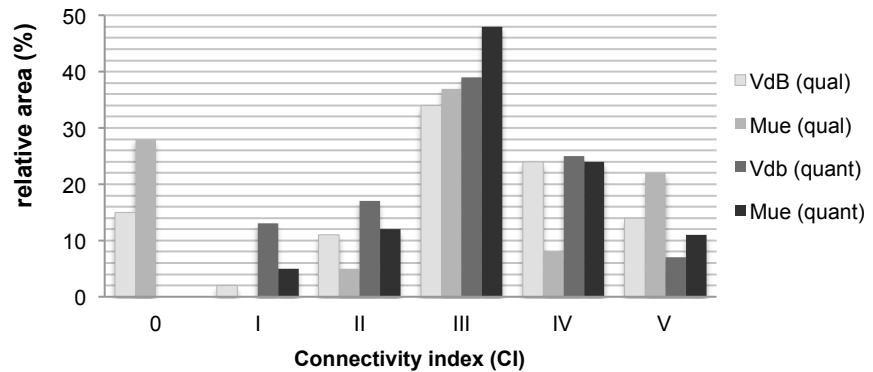
Next, the results of the qualitative and quantitative connectivity studies will be presented. The correlation between the results of both procedures is extremely weak with a correlation coefficient ( $R^2$ ) of 0.14 in Val dal Botsch and 0.23 in Val Müschauns (see appendix G-22).

### **6.5.1 Connectivity degree based on conceptual approach (M-7, M-8)**

Following the idea that the connectivity between storage landforms and the stream channel is controlled by the temporal frequency of material throughput between neighbouring landforms, qualitative connectivity maps with connectivity indices (CI) ranging from 0 (decoupled) to V (high) have been created for both alpine basins (map M-7, M-8). As first visible trend, the overall connectivity of the basin surface to the fluvial system ranges from medium to relatively high in both basins (fig. 6.4). While in Val dal Botsch, the mean CI is 2.92 (std. dev. = 1.51), Val Müschauns is

Hillslope-channel connectivity within the study areas

**Fig. 6.4:** Comparison of overall qualitative (qual.) and quantitative (quant.) connectivity degree in Val dal Botsch (VdB) and in Val Müschauns (Mue).



characterised by a slightly lower mean CI of 2.62. With a value of 1.89, the standard deviation is even higher. This might point out a more pronounced spatial variability within the basin compared to Val dal Botsch. While both valleys are dominated by a medium CI (III) with 34 % in Val dal Botsch and 37 % in Val Müschauns, the relative surface with a high CI (V) is much greater in Val Müschauns (22 %) than in Val dal Botsch (14 %). In turn, only 15 % of Val dal Botsch's surface is determined as decoupled (CI 0). In Val Müschauns this value is nearly twice as high (28 %).

Looking at the map M-7, **Val dal Botsch** shows a heterogeneous spatial connectivity pattern. Areas with (very) high connectivity (CI IV-V) are concentrated mainly near the outlet and in the eastern upper basin. Moreover, tributary channels as well as the valley bottom are highly connected. The eastern lower/middle basin is characterised by a medium connectivity. Most of the decoupled areas are concentrated within the upper, western valley.

For **Val Müschauns**, the map M-8 illustrates that the majority of the upper valley is decoupled, except of some of the lower slopes that have CI values between I and IV. In contrast, the valley bottom and the tributary channels are the best-connected areas with a CI VI and V. Likewise, strongly connected areas (CI IV-V) are extensive along the south-facing slopes of the lower and medium valley. A CI value of III largely dominates the higher slopes of the lower and middle basin. Weakly connected areas are frequently scattered within the lower basin (CI I-II).

The variation of the qualitative connectivity index within the study sites depending on altitude, slope position (normed distance) and slope gradient are illustrated as boxplots in appendix G-21 (in comparison to the results of the numeric approach). In both study sites, the qualitative connectivity index appears quite unaffected by the slope gradient and altitudinal zonation. Areas of low and high connectivity can be equally found in each altitude or in each longitudinal distance to the basin outlet. Nevertheless, the decoupled areas of both alpine valleys are clearly concentrated within the higher altitudes (ca. > 2600 m a.s.l.), thereby in the upper valleys. In Val Müschauns, decoupled storages are situated even much higher (median = 2780 m). Concerning the lateral variation, the connectivity degree slightly weakens upslope with a contemporarily increasing tendency of decoupling.

However, this leads to the question how strong the specific storage types are connected to the fluvial system. Tables 6.3 and appendix G-18 illustrate the connectivity degree of each storage type in Val

**Table 6.3:** Connectivity degree of the sediment storage types in Val dal Botsch. Results of the qualitative study approach and numeric modelling. “0” signifies decoupling. See also appendix G-18.

|                               |       | relative surface (%) |       |       |       |       |       | mean | std. dev. | median |
|-------------------------------|-------|----------------------|-------|-------|-------|-------|-------|------|-----------|--------|
|                               |       | 0                    | I     | II    | III   | IV    | V     |      |           |        |
| <b>Alluvium</b>               | qual  | 0.00                 | 0.00  | 0.00  | 62.09 | 0.00  | 37.91 | 3.76 | 0.97      | 3      |
|                               | quant |                      | 31.01 | 7.92  | 12.14 | 24.65 | 24.28 | 3.03 | 1.59      | 3      |
| <b>Colluvium</b>              | qual  | 4.08                 | 4.58  | 0.00  | 90.45 | 0.00  | 0.90  | 2.80 | 0.74      | 3      |
|                               | quant |                      | 6.44  | 11.30 | 41.67 | 36.57 | 4.03  | 3.2  | 0.92      | 3      |
| <b>Moraine deposit</b>        | qual  | 6.65                 | 2.04  | 33.40 | 38.93 | 10.81 | 8.17  | 2.70 | 1.17      | 3      |
|                               | quant |                      | 7.92  | 13.30 | 39.98 | 30.71 | 8.09  | 3.18 | 1.02      | 3      |
| <b>Debris cone</b>            | qual  | 0.00                 | 0.00  | 0.00  | 0.00  | 0.00  | 100.0 | 4.99 | 0.14      | 5      |
|                               | quant |                      | 34.00 | 14.20 | 21.27 | 19.88 | 10.65 | 2.59 | 1.4       | 3      |
| <b>Debris flow channel</b>    | qual  | 0.00                 | 0.00  | 0.00  | 19.36 | 0.00  | 80.64 | 4.59 | 0.81      | 5      |
|                               | quant |                      | 5.80  | 8.34  | 21.52 | 30.55 | 33.79 | 3.78 | 1.17      | 4      |
| <b>Protalus rampart</b>       | qual  | 0.00                 | 0.00  | 0.00  | 37.21 | 28.81 | 33.98 | 3.97 | 0.84      | 4      |
|                               | quant |                      | 33.99 | 17.32 | 26.56 | 17.52 | 4.61  | 2.41 | 1.24      | 2      |
| <b>Talus slope</b>            | qual  | 57.59                | 0.00  | 9.36  | 18.92 | 10.37 | 3.76  | 1.38 | 1.70      | 0      |
|                               | quant |                      | 12.01 | 21.61 | 42.87 | 19.65 | 3.85  | 2.82 | 1         | 3      |
| <b>Talus/ Debris flows</b>    | qual  | 1.49                 | 0.00  | 0.00  | 10.60 | 81.70 | 6.21  | 3.90 | 0.63      | 4      |
|                               | quant |                      | 11.70 | 12.28 | 37.02 | 30.43 | 8.57  | 3.12 | 1.11      | 3      |
| <b>Hillslope debris flows</b> | qual  | 0.00                 | 0.00  | 0.00  | 45.31 | 5.26  | 49.42 | 4.04 | 0.97      | 4      |
|                               | quant |                      | 23.27 | 19.94 | 30.01 | 20.44 | 6.34  | 2.67 | 1.22      | 3      |
| <b>Bedrock</b>                | qual  | 18.54                | 5.93  | 3.83  | 20.30 | 40.30 | 11.09 | 2.91 | 1.67      | 4      |
|                               | quant |                      | 12.95 | 22.63 | 43.50 | 17.25 | 3.67  | 2.76 | 1         | 3      |

dal Botsch. Debris cones and debris flow channels represent the landforms that are best-connected to the stream. Likewise, most of the talus/debris flows have a CI IV (81 %), even though 1.4 % of them are decoupled. The connectivity degree of the hillslope debris flow is very high (CI V, 49 %) to medium (CI III, 45 %). Furthermore, the majority of bedrock has a CI IV (40 %), but around 18.5 % is decoupled. Colluvium and moraine deposits as well as the majority of alluvial plains (near the outlet) are controlled by a weaker connection (CI III), respectively. This is mainly due to the dense vegetation cover. However, around 6.6 % of moraine deposits and 4 % of colluvium are decoupled because they border on bedrock. Table 6.3 also indicates that the lowest connectivity is related to talus slopes. Less than 25 % of them have a CI that is higher than III. Instead, 57.5 % of the talus slopes, mainly located along the western upper valley, are decoupled due the neighbourhood to moraine deposits.

As shown in table 6.4 and appendix G-19, the highest CI values in Val Müschauns are related to debris cones and channels but also to alluvium. Around 88 % of the debris cones and 69 % of the channels have a CI of V. Likewise, more than 70 % of the hillslope debris flows and talus slope/debris flows have a CI V, respectively, due to the close proximity to the stream. In contrast, the lowest CI values in Val Müschauns are related to talus slopes, predominantly located within the upper valley where the bedrock or vegetated moraine deposits stop the sediment transfer. Around 75 % of the talus slopes as well as all ramparts and the single rock glacier are decoupled from the stream, largely due to buffering bedrock outcrops. The median connectivity of colluvium and moraine valley fills is CI II. However, due the neighbourhood to bedrock, particularly within the upper basin, 47.8 % of the moraine deposits are decoupled from the stream. Finally, while around half of the rock faces has a CI I, 23.1 % are decoupled due to the adjacency to moraine deposits.

**Table 6.4:** Connectivity degree of sediment storage types in Val Müschauns. See also appendix G-19.

|                               |       | relative surface (%) |       |       |       |       |       | mean | std. dev. | median |
|-------------------------------|-------|----------------------|-------|-------|-------|-------|-------|------|-----------|--------|
|                               |       | 0                    | I     | II    | III   | IV    | V     |      |           |        |
| <b>Alluvium</b>               | qual  | 0.00                 | 0.00  | 0.00  | 0.00  | 0.00  | 100   | 4.99 | 0.17      | 5      |
|                               | quant |                      | 1.32  | 1.22  | 13.93 | 53.32 | 30.22 | 4.10 | 0.77      | 4      |
| <b>Al/Col</b>                 | qual  | 0.00                 | 0.00  | 0.00  | 0.00  | 15.15 | 84.85 | 4.84 | 0.41      | 5      |
|                               | quant |                      | 7.87  | 7.65  | 23.76 | 28.26 | 32.47 | 3.70 | 1.22      | 4      |
| <b>Colluvium</b>              | qual  | 0.00                 | 2.84  | 35.53 | 17.11 | 44.30 | 0.21  | 3.03 | 0.96      | 3      |
|                               | quant |                      | 0.93  | 7.60  | 57.64 | 27.31 | 6.53  | 3.31 | 0.74      | 3      |
| <b>Moraine</b>                | qual  | 47.81                | 0.00  | 0.00  | 38.23 | 7.68  | 6.27  | 1.77 | 1.76      | 3      |
|                               | quant |                      | 17.81 | 18.05 | 41.84 | 15.91 | 6.39  | 2.75 | 1.12      | 3      |
| <b>Debris cone</b>            | qual  | 0.00                 | 0.00  | 0.00  | 0.00  | 11.46 | 88.54 | 4.88 | 0.34      | 5      |
|                               | quant |                      | 2.48  | 5.29  | 27.66 | 30.63 | 33.94 | 3.88 | 1.02      | 4      |
| <b>Debris flow channel</b>    | qual  | 0.00                 | 0.00  | 0.00  | 22.51 | 7.98  | 69.51 | 4.48 | 0.84      | 5      |
|                               | quant |                      | 0.27  | 4.09  | 28.39 | 22.46 | 44.79 | 4.07 | 0.96      | 4      |
| <b>Protalus rampart</b>       | qual  | 100                  | 0.00  | 0.00  | 0.00  | 0.00  | 0.00  | 0.00 | 0.00      | 0      |
|                               | quant |                      | 31.97 | 28.79 | 30.83 | 5.73  | 2.68  | 2.18 | 1.03      | 2      |
| <b>Talus slope</b>            | qual  | 75.08                | 0.00  | 0.00  | 8.35  | 0.57  | 16.00 | 1.07 | 1.92      | 0      |
|                               | quant |                      | 9.88  | 18.54 | 46.05 | 17.41 | 8.12  | 2.95 | 1.04      | 3      |
| <b>Talus/ Debris flows</b>    | qual  | 0.00                 | 0.00  | 0.00  | 0.00  | 19.57 | 80.43 | 4.80 | 0.40      | 5      |
|                               | quant |                      | 1.97  | 11.59 | 49.82 | 24.32 | 12.30 | 3.33 | 0.90      | 3      |
| <b>Hillslope debris flows</b> | qual  | 0.00                 | 0.00  | 5.64  | 0.00  | 23.21 | 71.15 | 4.60 | 0.77      | 5      |
|                               | quant |                      | 2.11  | 9.57  | 38.35 | 29.07 | 20.91 | 3.57 | 0.99      | 3      |
| <b>Rock glacier</b>           | qual  | 100                  | 0.00  | 0.00  | 0.00  | 0.00  | 0.00  | 0.00 | 0.00      | 0      |
|                               | quant |                      | 42.79 | 21.18 | 25.49 | 7.40  | 3.14  | 2.07 | 1.12      | 2      |
| <b>Bedrock</b>                | qual  | 23.11                | 0.24  | 0.03  | 50.71 | 2.51  | 23.40 | 2.79 | 1.73      | 3      |
|                               | quant |                      | 2.87  | 11.31 | 48.87 | 24.60 | 12.35 | 3.32 | 0.93      | 3      |

### 6.5.2 Quantitative connectivity index based on numeric approach (M-9, M-10)

Compared to the qualitative connectivity study, the numeric GIS modelling displays a different connectivity pattern in both valleys. In **Val dal Botsch** (map M-9), the connectivity degree originally ranges from -1.81 (very low) to 5.35 (very high), with a mean CI of 1.57 (std. dev. = 0.69). Given the pixel-based histogram in appendix G-20, the lowest and highest modelled CI values represent only outlier with a frequency of less than 1 %. Therefore, the original raster grid was reclassified into five new classes (I-V). Thus, the mean (reclassified) CI for the entire catchment of Val dal Botsch is 2.97 (std. dev. = 1.09), almost similar to the qualitative approach. The comparison of both approaches (fig. 6.4) with regard to the connectivity of land surface immediately displays that the numeric algorithm is not capable to calculate decoupled areas within the basin. Instead, considerably more areas with a CI I (13 %) and CI II (17 %) have been modelled.

In **Val Müschauns**, the GIS-modelling results in surface connectivity indices that range from -4.69 to 5.55 (map M-10). The mean CI is 1.82 (std. dev. 0.68). After reclassification of the original raster grid (appendix G-20), the mean CI is 3.24 (std. dev. 0.97). Hence, in contrast to the qualitative results, the average quantitative CI is considerably higher in Val Müschauns than in Val dal Botsch, since the modelling does not display decoupled areas. Instead, more areas that are moderately (III, 48 %) and highly connected (IV, 24 %) have been modelled (fig. 6.4).

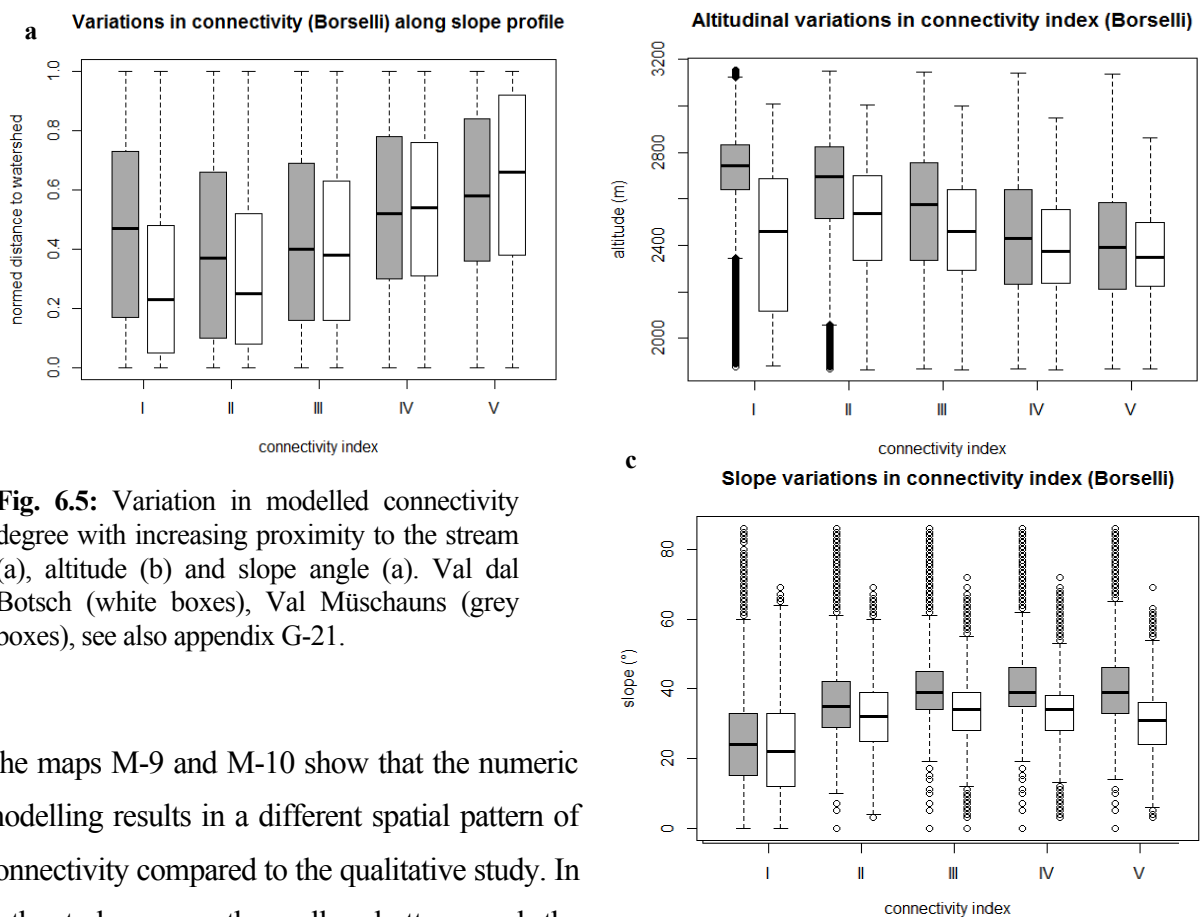


**Fig. 6.5:** Variation in modelled connectivity degree with increasing proximity to the stream (a), altitude (b) and slope angle (a). Val dal Botsch (white boxes), Val Müschauns (grey boxes), see also appendix G-21.

The maps M-9 and M-10 show that the numeric modelling results in a different spatial pattern of connectivity compared to the qualitative study. In both study areas, the valley bottom and the incised hillslope channels display the highest connectivity to the stream network. Furthermore, the connectivity clearly increases with increasing proximity to the stream and with growing steepness of relief (fig. 6.5a,c). Moreover, longitudinal variations in connectivity become visible on both maps as indicated by figure 6.5b. Particularly in Val Müschauns, there is an obvious trend showing a weakening of connectivity in upstream direction. In contrast, the upstream decrease of connectivity in Val dal Botsch is only less pronounced, even though some of the slopes of the upper valley are related to a low CI value. Here, the CI values of the slopes near the outlet are diminished by a high surface roughness despite of their proximity to the stream/outlet. Interestingly, in Val dal Botsch, the east-facing slopes are related to slightly higher CI values relative to the west-facing slopes.

These general trends are well reflected within the connectivity of the different storage types. In Val dal Botsch (tab. 6.3, see also small map in M-9), the average connectivity degree of talus slopes (CI III) is obviously higher compared to the qualitative study. Moreover, with regard to the deposits within the cirque of the eastern upper valley (e.g. hillslope debris flows, debris cones, ramparts), the modelling evidently incorporates the decreasing inclination of these convex landforms and the rise in surface roughness. Concerning alluvium, colluvium and moraine deposits, the median CI is III, almost comparable to the qualitative study. Similar to the qualitative study, debris flow deposits such as debris flow channels and cones, hillslope debris flows and talus slope/debris flows are modelled as the best-connected landforms with a median CI value of IV-V. However, the high CI is no longer concentrated to the incised channels within the western middle basin, but also to

surrounding areas of moraine deposits. Finally, even though the algorithm is not capable of modelling any decoupling, the talus slopes and cliffs of the western upper valley, which have been qualitatively defined as decoupled, display relatively low CI value of I-III.

In Val Müschauns, alluvium, debris flow channels and cones are modelled as best connected landforms – similar to the qualitative method (tab. 6.4 and small map in M-10). However, the median CI of IV is slightly lower and the majority of debris flow channels and debris cones have a CI ranging between III and V. The modelling also resulted in slightly lower CI values for hillslope debris flows and talus slope/debris flows (median CI III). The connectivity degree of the bedrock cliffs is similar to the qualitative study (median CI III). Likewise, the median CI value of moraine and colluvium of III is quite similar to the values of the qualitative analysis. Although decoupled areas cannot be modelled, most of the protalus ramparts and the rock glacier in the upper trough have a CI I and nearly half of the talus slopes has a CI of III. Interestingly, the numeric approach also factors in the somewhat higher connectivity for the moraine deposits within the upper basin, compared to the surrounding slopes that are weakly connected (or even decoupled).

### **6.6 Activity of sediment storages (M-11, M-12)**

Based on the vegetation cover and the risk of erosion the recent degree of activity can be calculated. The maps M-11 and M-12 display an overall higher mean activity in Val Müschauns (mean = 3.50, std. dev. = 0.99) than in Val dal Botsch (mean = 2.80, std. dev. = 1.12). This trend matches to the vegetation cover and erosion risk in both valleys, as the mean vegetation cover of 39 % is much higher in Val dal Botsch than in Val Müschauns (17 %). Similarly, the general erosion risk with a mean SPI of 1.75 is much lower in Val dal Botsch compared to Val Müschauns (2.37). Hence, 76 % of Val Müschauns' land surface is typified as highly active, twice as much as in Val dal Botsch (35 %). In turn, a relative area of 17 % in Val dal Botsch and 10 % in Val Müschauns are classified as inactive.

The maps M-11 and M-12 present a considerably comparable lateral pattern in both alpine valleys. Activity of land surface increases with increasing altitude (fig. 6.6a) and with growing proximity to the watershed (fig. 6.6b). Highest activity occurs in higher altitudes (2800-2400 m a.s.l.) above the treeline, immediately below the valley crest. In contrast, the less active or inactive areas can largely be found along the foot of slopes near the stream and in lower altitudes (ca. 2200 m a.s.l.), where vegetation cover is dense. Additionally, activity rises to some extent with increasing slope angle (fig. 6.6c), with highest activity at inclinations of ca. 38° (median in Val Müschauns). Moreover, the activity slightly increases in upstream direction, particularly in Val Müschauns, with the lowest activity in the lower basin relative to the activity of the upper basin. As an exception, the hillslope debris flows near the outlet of Val dal Botsch are highly active. The middle basins of both valleys represent an intermediate position, where highly active areas alternate with inactive zones.

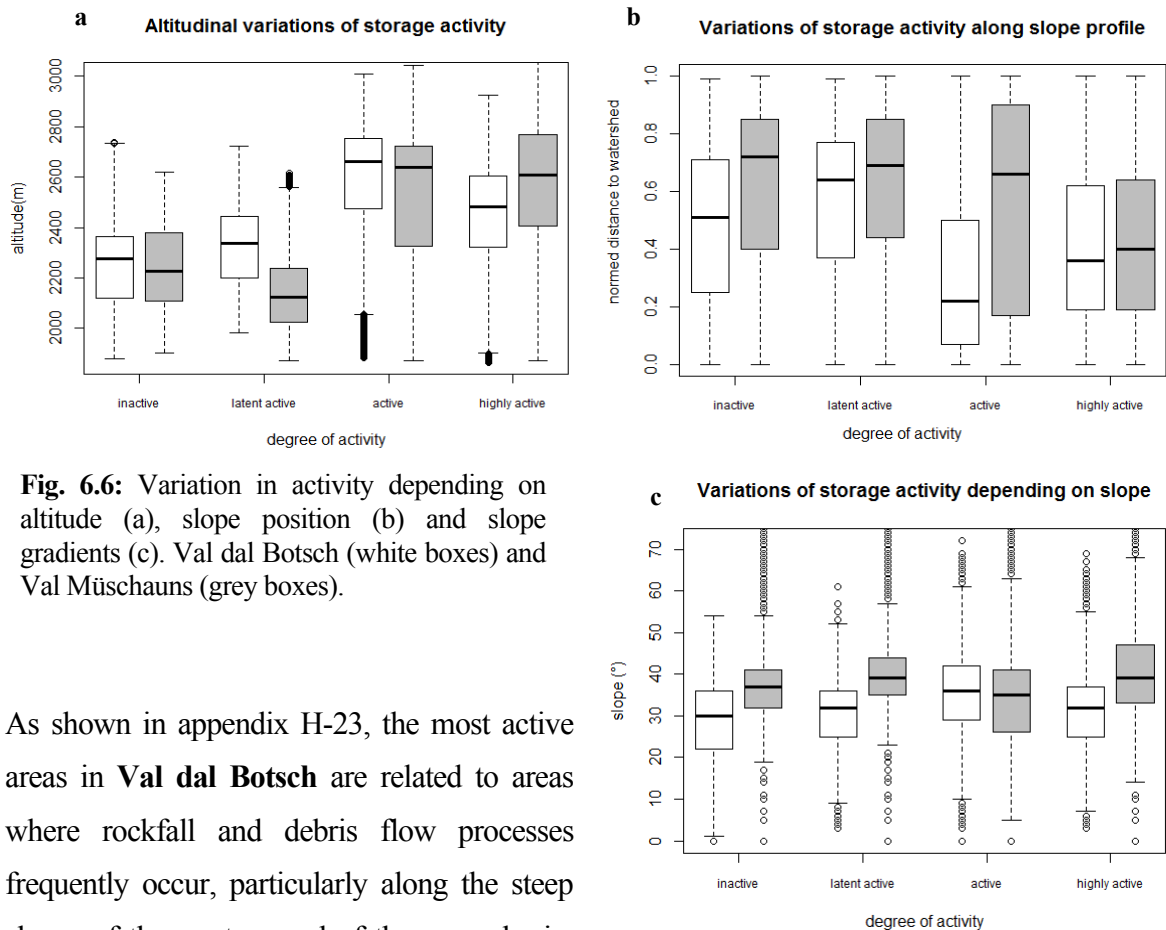


**Fig. 6.6:** Variation in activity depending on altitude (a), slope position (b) and slope gradients (c). Val dal Botsch (white boxes) and Val Müschauns (grey boxes).

As shown in appendix H-23, the most active areas in **Val dal Botsch** are related to areas where rockfall and debris flow processes frequently occur, particularly along the steep slopes of the western and of the upper basin.

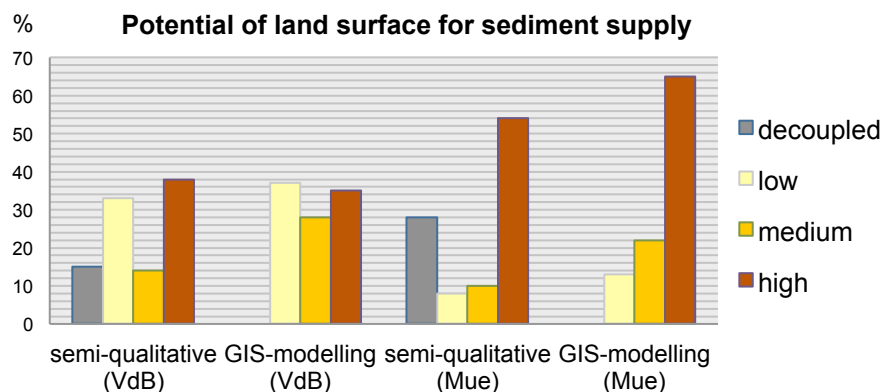
Here, vegetation cover is relatively sparse or not-existent (< 30 %) and the SPI is medium to high. Therefore, debris flow channels, debris cones as well as talus slopes, talus slope/debris flows and hillslope debris flows are the most active landforms in the valley. Nevertheless, some of the hillslope debris flows (7 %) and talus slopes (9 %) are inactive due to the buffering effect of dense vegetation. Furthermore, the eastern slopes of the lower/middle basin show a comparatively lower degree of activity. Consequently, the majority of colluvium and moraine deposits, which is mainly located in that position, is inactive (66 % and 33%) or only latently active (28 % and 43 %). Finally, 62 % and 32 % of the steep, non-vegetated rock faces are (highly) active.

In **Val Müschauns**, almost all upper slopes of the catchment are highly active. The erosion risk is highest along the south-facing slopes of the valley. Predominantly located above the treeline or/and characterised by steep gradients, the most active storage landforms in Val Müschauns are bedrock, debris channels and cones as well as talus slopes, talus slope/debris flows, hillslope debris flows (see also appendix H-24). Nevertheless, some of the vegetated hillslope debris flows (9 %) and talus slope/debris flows (7 %) along the northern valley are classified as inactive due to the dense vegetation cover and the relatively low SPI. The moraine deposits and colluvium along the lower slopes near the stream channel and within the lower basin are only latently active or even inactive, despite of a medium SPI. Here, the comparatively dense vegetation cover reduces the activity state.

### 6.7 Potential for sediment supply to the fluvial system (M-13, M-14)

Finally, based on the recent degree of activity and connectivity of storage landforms, the potential of individual storage landforms for supplying sediment into the fluvial system can be evaluated. As shown in map M-13 and M-14, the delivery potential considerably varies in space. In addition, obvious differences exist depending on the specific connectivity approach that is used. Both the semi-qualitative and quantitative approach calculate a much higher general sediment supply potential in Val Müschauns than in Val dal Botsch. Whereas in Val Müschauns, the mean potential equals 1.90 (semi-qual.) and 2.52 (GIS), much lower mean values have been calculated for Val dal Botsch: 1.77 (semi-qual.) and 1.97 (GIS). The standard deviations range from 1.11 to 1.31 (semi-qual.) and from 0.71 to 0.85 (GIS). The use of the qualitative connectivity study generates an obvious higher scattering of supply potential-values (fig. 6.7). In Val Müschauns, there is a clear dominance of areas with high potential (54 % semi-qual. and 65 %, GIS). As shown in figure 6.7, much more high-potential areas are calculated by the GIS-modelling, mainly to the disadvantage of the decoupled areas. In contrast, in Val dal Botsch, the supply potential appears to be equally distributed throughout the catchment, particularly illustrated by the numeric results.

**Fig. 6.7:** Sediment supply potential of the land surface of Val dal Botsch and of Val Müschauns. Comparison between the qualitative and the quantitative assessment.



The potential for sediment supply in **Val dal Botsch** is substantially heterogeneous in space. Figure 6.8a indicates for both approaches that the sediment supply potential increases with rising altitudes. Yet, the decoupled storages are situated at the highest positions of the study sites. The variations along the slope profile are shown in appendix I-25. Except for the decoupled areas, the potential is slightly higher along the middle and upper slopes, but this trend is not as good expressed. Looking at map M-13, both methods display all incised channels and its upper zones as the most potent sediment sources within the sediment flux system. Likewise, the western slopes, particularly near the outlet, and the upper basins have a high potential. In comparison, the lowest potential for sediment supply occurs along of the eastern valley side. Some areas of the western middle basin are characterised by a medium to low potential in both approaches.

Consequently, the specific storage types of Val dal Botsch are distinguished by a different sediment supply potential as shown in appendix I-26. In both approaches, the highest potential is primarily related to the majority of debris flow channels and cones as well as talus slope/debris flows.

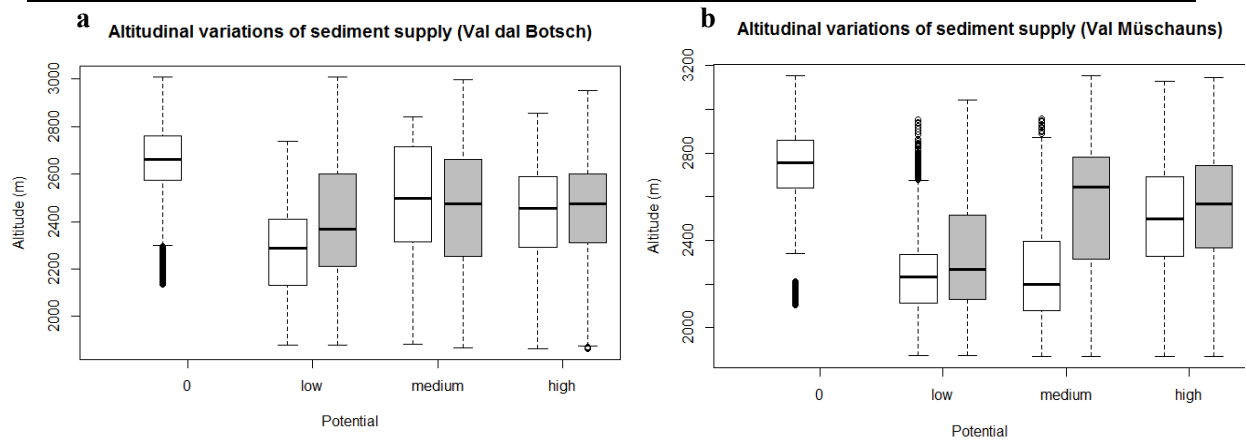


**Fig. 6.8:** Altitudinal variations of sediment supply potential in Val dal Botsch (a) and Val Müschauns (b). White boxplots (semi-qual.), grey (quant.). Variations on slope profile are illustrated in appendix I-25.

The supply potential of hillslope debris flows is noticeably variable in both analyses. Only half of them have a high potential, while the rest has a minor activity or/and is less connected. In contrast, both studies result in a very low sediment supply potential for the majority of colluvial and moraine deposits. However, most significant difference exists concerning the talus slopes. While the numeric approach calculates a medium potential for most of those storages, the semi-qualitative approach relates talus slopes to relatively low values. Hence, the geomorphic system comprehension implies that almost two thirds of the talus deposits (57 %) as well as large parts of the rock faces (18 %) might not be capable recently to transfer sediment into the fluvial system. Similarly diverging results are visible for colluvium and moraine deposits.

In contrast, **Val Müschauns** shows a more regular spatial pattern concerning the potential for sediment being delivered into the fluvial system, visible in both approaches. The altitudinal variations are much more pronounced than in Val dal Botsch (fig. 6.8b). While the lower basin has the lowest potential, the middle valley is characterised by the highest potential for sediment supply. Furthermore, appendix I-25 indicates that the upper hillslopes are most potential to deliver sediment. Map M-14 displays that the incised bedrock channels as well as the majority of the upper slopes of the basin are characterised as high-potential. Nevertheless, by comparing both approaches, considerable differences become visible, particularly for the upper basin. Whereas the majority of sediment storages within the upper basin have been determined qualitatively as decoupled being therefore incapable of transferring material into the channel, the quantitative method displays those areas with a medium sediment supply potential (median). Furthermore, in both approaches, the lower slopes of Val Müschauns, particularly within the lower and middle basin, are controlled by a comparatively low potential, primarily due to the low activity. In contrast to the numeric approach, the semi-qualitative study reveals that the south-facing slopes of the lower/middle catchment might have a greater potential for supplying sediment to the stream than the north-facing slopes.

Consequently, the potential for sediment supply of the individual storage types in Val Müschauns differs noticeably as shown in appendix I-27. In both approaches, the majority of debris flow

channels and cones as well as most of the talus slope/debris flows and hillslope debris flows are highly potential, respectively. Likewise, a high supply potential is qualitatively and quantitatively calculated for all alluvial and alluvial/colluvial storages. In both studies, colluvial landforms have a medium to low potential. The steep rock faces are related to a high potential (median) in both approaches, but 23 % of the cliffs are qualitatively determined as decoupled. However, the most significant differences are visible for rockfall generated storage landforms. Given the qualitative study, only 25 % of the talus slopes are highly potent to deliver sediment to the stream, while the majority (75 %) is decoupled from the sediment cascade. In contrast, the quantitative study classifies around 63 % of the talus slopes as highly potential. Similarly, almost half of the moraine deposits is determined qualitatively as decoupled, whereas the majority of them is modelled with a medium potential in the quantitative approach.

## 7 DISCUSSION

After a presentation of potential error sources and limitations of the basic assumptions, the results of this study will be discussed with regard to other geomorphological studies. One of the major aims is to verify or falsify the hypotheses of this thesis.

### 7.1 Potential error sources of the study and limitations of basic assumptions

Before interpreting and discussing the presented results, it has to be stressed that some specific sources of errors and uncertainties exist, which therefore demand a critical evaluation. First of all, the quality of the basic input data might influence the final results. Depending on the creation procedure, the DEMs of the study areas contain systematic errors, whose effects are yet difficult to quantify. Consequently, all geomorphometric parameters, and in particular the second derivatives, reflect these errors (SCHMIDT & DIKAU 1999). More specifically, the roughness of vegetation cover is removed only insufficiently within the DEM of Val dal Botsch. While the DEM of Val Müschauns is almost excellent displaying even micro-scale variation in relief (e.g. levees), the DEM of Val dal Botsch does not represent homogeneously the altitude of terrain, but partially the roughness of vegetation canopy surface. This has to be kept in mind when comparing the geomorphometric results of both study areas.

In addition, the smoothing performed a priori of the DEMs by a 3x3 window routing could have produced some basic errors. Even though the smoothing allows an extraction of spurious irregularities within the raster data, the procedure may also delete micro-scale variation in topography, which could be important for morphometric analysis.

Furthermore, it must be emphasised that the temporal validity of the results is limited and that the maps provide solely an instantaneous image of the current geomorphic system. The mapping campaign shows that some land surface features have changed already in comparison with the aerial

photos of 2011. For instance, some debris cones or talus sheets are recently more extensive or more eroded by the channel stream. Even though this error might be relatively small, this already indicates that the valleys are high-dynamic systems.

Likewise, the assessment of landform activity and hence, the deriving potential for sediment supply have to be evaluated critically. Since the state of activity was difficult to observe during fieldwork, representative indicators were used including the vegetation cover and the stream power index (SPI). However, both indicators may provide errors. Even though the calculation of the SPI has the advantage of being a quantitative measure, it highly depends on the quality of the input DEM. Additionally, the mapping of vegetation cover, based on air photo interpretation and fieldwork (in summer!), is rather subjective and temporally limited in its representativeness. Thus, it is important to bear in mind that vegetation cover has strong temporal and spatial dynamics depending on seasonal, climatic extremes and climate change or – in other alpine regions – land use.

Some uncertainties might also be related to the geomorphological mapping and the identification of storage landforms. As stated by OTTO & DIKAU (2004), the two-dimensional map has obvious restrictions regarding the representation of the complex nature of alpine systems. For instance, microforms such as levees or surface rills have been generalised in the geomorphological maps and have not been considered in subsequent landform analyses. Nevertheless, the relatively small scale of 1:5000 already displays the geomorphic system of both alpine valleys in detail.

Moreover, the mapping of some regions was sometimes hampered by the mountain relief and the limited accessibility or by the dense vegetation cover. Instead, those areas have been mapped on the base of the hillshades and slope angle map. Hence, some mapping errors could occur in such areas, particularly in combination with the partially poor DEM quality in Val dal Botsch. Finally, it is obvious that manual mapping is affected by the subjectivity and field experience of the cartographer (VAN ASSELEN & SEIJMONSBERGEN 2006). Therefore, the geomorphological maps and the landform classification map might be to some degree subjective with respect to the interpretation, selection of criteria and position of landform boundaries.

Further sources of errors may also stem from of the performed (GIS-)analyses. For instance, the interpretation of results concerning the normed distance to the watershed has to be treated carefully. This attribute was calculated on the basis of the Euclidian distance, which is the straight/shortest distance of a pixel to a defined source. This makes sense since the focus of the study is on the relative position of a landform along the slope profile between valley ridge and stream channel. In turn, the normed distance represents the relative position along the sediment routing pathway only partially. For a more exact assessment, the use the flow direction instead of the Euclidean distance would have been more suitable.

Furthermore, the study of toposequences is also related to a certain degree of subjectivity, despite of its obvious advantages. Even though the classification of the individual toposequences was

performed by a consistent scheme, it depends on a certain degree of personal judgment. Similarly, the results of the quantitative connectivity modelling need to be interpreted suspiciously. One critical point is the reclassification procedure of the original raster grid into five classes. The raster was classified by the natural breaks method, which represents a visually logical and rather subjective grouping. However, even though this seems quite ambiguous, it may be the best way to compare both connectivity approaches based on an identical range of classes. Furthermore, a considerable limitation of BORSELLI's modelling approach may be the use of the single flow direction to calculate the contributing area. This algorithm only insufficiently displays the real sediment routing in mountain environments, where divergent flow dominates. For future work, the multiple flow D-infinity approach would be more suitable, as performed by CAVALLI et al. (2008). Additionally, based on the 2m-resolution of the DEMs, the single flow algorithm possibly underestimates the real width of some debris flow channels.

Finally, it needs to be stressed that no sensitivity analysis of the connectivity modelling has been performed due to the restricted time of this study. Even though the connectivity modelling might provide reliable initial outcomes for this thesis, a sensitivity analysis is obligatory for future work to better understand the influence of some parameters on the modelling results.

Moreover, it is obvious that the qualitative (and often subjective) conceptual assumptions underlying the methods are possibly linked to some uncertainties. Particularly, the assessment of the functional relationships between neighbouring landforms as well as the qualitative connectivity study, which have not been applied in such a manner until now, might engender criticism. For example, it might appear as idealistic or simplified to typify bedrock and moraine deposits as buffering/decoupling landforms in general. Even though the geomorphological field work in the SNP indicates that those two landforms considerably obstruct most of the sediment transfer from the upper slopes, additional small-scale sediment routing pathways (e.g. along layered rock sheets) have been identified, which might be crucial for the sediment transfer. However, at the scale of 1:5000, those small corridors have not been mapped and therefore, the simplification of this basic assumption seems to be adequate on the scale of storage landforms.

Another limitation is that the qualitative connectivity degree is solely based on the frequency characteristics of geomorphic events. Hence, the event magnitude is being neglected entirely, but it might be crucial for the behaviour of connectivity. For instance, debris flows occur only episodically and less frequent than small-scale rockfalls, but the magnitude of a debris flow event may be of greater dimension. Hence, it is the question if this episodic material input possibly generates a temporarily stronger coupling than continuous rockfall events. Additionally, the study is based on the assumption that all landforms that directly border on alluvium have a very high connectivity to the fluvial system. The periodic shift of the alluvial plain, leading to temporary coupling or decoupling, is neglected. A potential limitation of the method also derives from the

vegetation that is used as a buffering factor, because the type of vegetation was neglected. However, the type might play a crucial role for connectivity, since bushes and trees have different root depths and provide varying stabilisation or, conversely, loading to the sediment stored on slope.

Finally, the high standard deviation values of some results – particularly of the qualitative connectivity study – need to be considered. Since they indicate a large scattering of data, the precision of those results is partially restricted, largely due to random errors (e.g. inaccuracy by the cartographer). In such case, it is more suitable to use the median value instead of the arithmetic average (mean), since it is less affected by outlier and is more representative of the data set.

## **7.2 Spatial organisation of sediment storages in meso-scale alpine systems**

In alpine geosystems, the spatial and temporal interaction of diverse geomorphic processes generates a specific pattern of nested sediment storages that is unique in each valley. The knowledge on the spatial arrangement and the morphometric characteristics of these storages is a key prerequisite to understand the typical signal of sediment cascades within alpine basins. The investigations in the Swiss National Park reveal that sediment storages are not randomly distributed within alpine valleys. Instead, a certain spatial regularity becomes evident determined by different, catchment-specific mechanisms.

Firstly, the number of individual storage landforms within an alpine basin is obviously a function of the catchment size. The 6.18 km<sup>2</sup> large Val Müschauns hosts considerably more individual landforms and types than Val dal Botsch, which is with 3.47 km<sup>2</sup> half as large in size. Additionally, geomorphic mapping reveals that the growth in valley size is accompanied by a rising spatial complexity, significantly complicating the linkage between process and form. The nesting and overlapping of landforms is appreciably more pronounced in Val Müschauns.

Likewise, the distinctive bedrock-sediment ratio in both basins might indicate that the spatial landform pattern is influenced by the altitudinal extent of a valley. While in Val dal Botsch, 78 % of the land surface is covered by loose sediment, around 60 % of Val Müschauns' surface represents steep bedrock cliffs or outcrops. Interestingly, in both basins, the highest sediment deposits extend to maximum altitudes of ca. 2600 m a.s.l. Looking at the altitudinal distribution of the catchment surface, it becomes obvious that the majority of Val dal Botsch's surface is largely located at ca. 2300 m a.s.l.. Hence, most of the basin is covered by sediment. In contrast, the majority of the land surface of Val Müschauns is situated higher up, at altitudes between 2650-2850 m a.s.l., and therefore lies largely above the uppermost sediment deposits. Nevertheless, it would be wrong to deduce that Val Müschauns stores considerably less sediment. Instead, the role of bedrock as effective intermediate storage needs to be considered, as it might hold considerable amounts of fine-grained sediment. In the Reintal catchment, for example, SASS & KRAUTBLATTER (2007)

demonstrated that the depletion of such short-term storage by secondary processes might exceed the usual annular rockfall deposition by 0.5 to 50 times.

Furthermore, the number and location of debris flow channels might be evidence for the significant control of the basins' lithology on the spatial organisation of landforms. Even though the relative surface of debris flow channels is very small (1 %) in both study areas, noticeably more channels exist in Val Müschauns. Here, the majority of those bed-type debris flows are incised within the rock faces of the lower basin that is built up of a contrasting lithology compared with the middle/upper basin as well as the entire basin of Val dal Botsch. The stratified limestone of the Ortler nappe appears to favour the incision of debris flows, in contrast to the banked dolomites of the Quattervals nappe (TRÜMPFY et al. 1997). These findings correspond with the study by BRARDINONI et al. (2012), who highlight the influence of lithological characteristics of bedrock on debris flow dynamics in northeastern Italy.

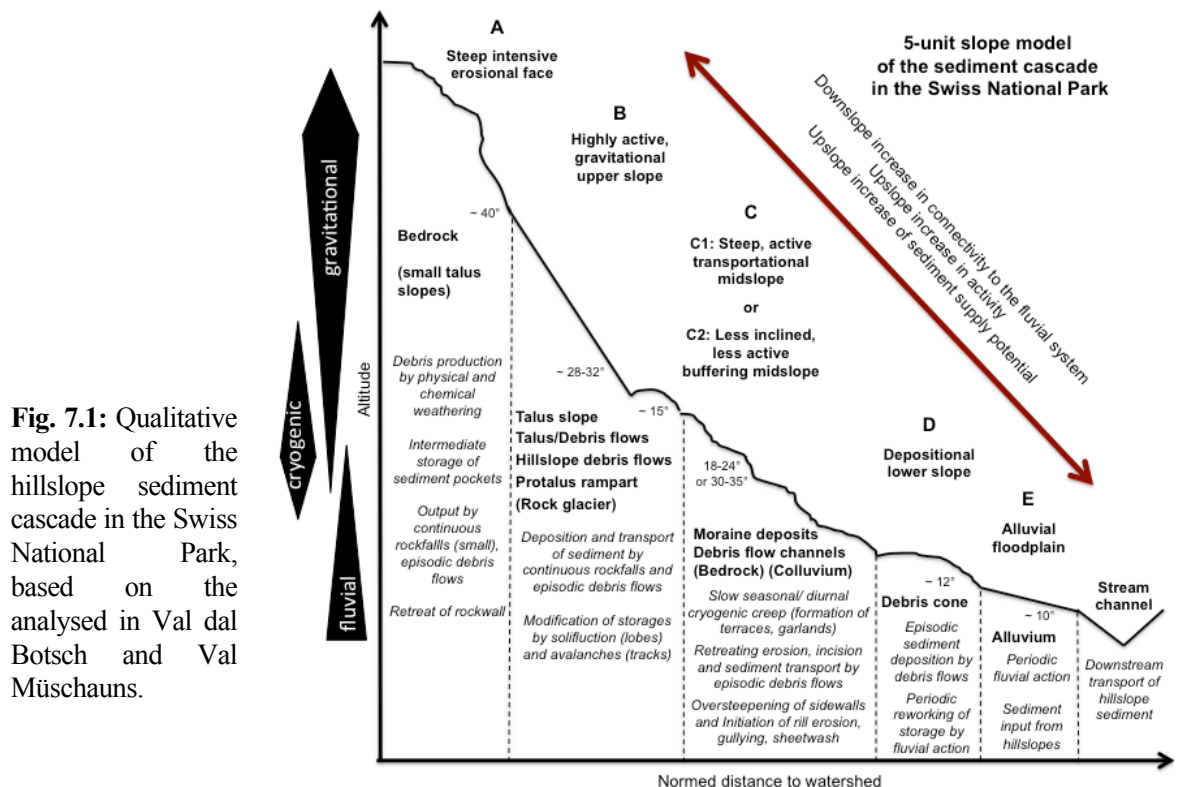
However, besides some discrepancies, Val dal Botsch and Val Müschauns show a similar regularity of sediment storages in both the lateral/vertical and longitudinal/horizontal directions. On a catchment scale, colluvial slope deposits dominate mainly the lower basins, whereas cryogenic and gravitational processes and storages frequently occur within the upper parts of the valleys. This longitudinal zonation of landforms is evidently linked to topography. In upstream direction, the rise in altitude and slope gradients – accompanied by a thinning of vegetation cover due to the interplay of climatic and topographic factors – increasingly favours the occurrence of gravitational and frost-related processes (see also CAINE 1974).

Moreover, the morphometric analysis of storage landforms reveals a noticeable lateral organisation on a hillslope scale. In both alpine basins, each storage type is characterised by nearly the same specific morphometry concerning the slope gradient, altitudinal range and distance to the watershed. As a consequence, each landform type appears to be linked to a specific position on the hillslope between the valley ridge and channel stream. Referring to the 9-unit slope model by DALRYMPLE et al. (1968) and CONACHER & DALRYMPLE (1977), figure 7.1 systemises this lateral zonation of storage landforms in the Swiss National Park. According to this model, a hillslope can generally be divided into five units, all of which are typified by distinct slope gradients, altitudes and slope position. Due to the interrelationship between hillslope morphometry and climate-ecological conditions, each unit hosts a unique set of various neighbouring and overlapping storages that are deposited and reworked by different geomorphic processes. This model illustrates, even though in a purely semi-qualitative way, the lateral alpine sediment cascade of the Swiss National Park in the sense of CHORLEY & KENNEDY (1971).

The uppermost slope unit A (ca. > 2600 m a.s.l.) in Val dal Botsch and Val Müschauns is built up by a steep rock face (40°), providing fresh debris through physical and chemical weathering. Similar to the study by CAINE (2001), the rock faces frequently store sediment particles within couloirs,

which will be channelled by snow and water further downslope. The bedrock cliffs represent therefore both, the first sediment source as well as an intermediate storage of sediment. Above a height of ca. 2400 m a.s.l., a relatively steeply inclined slope unit B (28-32°) follows. Gravitational processes, mainly continuous rockfall and episodic slope-type debris flows, result in the deposition of talus deposits. Sometimes, a protalus rampart is formed along the downslope margin. The morphology of talus deposits is significantly controlled by the height and lithology of adjacent cliffs (RAPP 1960a,b) as well as by the depletion of intermediate storages via secondary processes (SASS & KRAUTBLATTER 2007). In turn, the height of the talus slope controls the efficiency of the adjacent rock face in providing weathered material. Modification and redistribution frequently occurs through cryogenic creep or debris flows as described by LUCKMAN (1988), who emphasises the particular role of snow avalanches in the Canadian Rocky Mountains.

The midslopes (ca. 2200-2400 m a.s.l.) are primarily covered by moraine deposits (rarely by colluvium or bedrock) often reworked by seasonal cryogenic creep. This is particularly pronounced in Val dal Botsch, which is characterised by a typically hummocky landscape with slowly creeping vegetation stripes. However, this slope unit is probably of major importance within the sediment cascades in the Swiss National Park, since the inclination of the moraine deposits control the initiation of episodic debris flows. Hence, slope unit C can be either very steep, active-transportational (C1), as in Val dal Botsch, or relatively flat and less active, even buffering (C2), as in Val Müschauns. In Val dal Botsch the steep gradients (30-25°) of the moraine deposits favour the active regressive incision of debris flows. Since the channels are largely filled by rockfall material, they represent mainly transport-limited systems (STINY 1910), where debris flow triggering depends on rainfall events. In contrast, due the more gentle inclines (18-24°) and the occurrence of stabilising



permafrost, debris flow initiation is hampered in Val Müschauns. Consequently, the debris flow channels are largely weathering or supply-limited systems, where sediment input is the limiting factor (STINY 1910). Then, with increasing proximity to the valley bottom (1800-2100 m a.s.l.) and decreasing slope gradients ( $12^\circ$ ), the footslope in unit D is often dominated by the episodic deposition of debris cones. Finally, the lowermost slope unit E is the almost flat alluvial floodplain ( $10^\circ$ ), where periodic fluvial activity interacts with stochastic inputs from the hillslope. In a comparable model, SLAYMAKER (1993) identifies similar contrasts between high-, mid- and low-altitude slopes of the coastal mountains of Western Canada.

Finally, the findings in Val dal Botsch and Val Müschauns underline very well that a holistic analysis of all geomorphic processes and valley characteristics such as catchment size, altitudinal extent, lithology and topography is needed to understand the spatial pattern of landforms. For that, the geomorphic mapping on 1:5000 has proven to be an excellent base for the morphometric study.

### **7.3 Evidence of paraglacial activity in the deglaciated alpine basins?**

The temporal variability of storage landforms needs to be considered, as one of the major controls on the cascading sediment fluxes in alpine systems. Although only the current state of the alpine systems has been mapped in this study, the landform pattern and the vegetation cover might allow some hypothetical assumptions concerning the temporal dynamics of the sediment storages.

The landform inventory demonstrates that both Val dal Botsch and Val Müschauns are dominated primarily by gravitational processes. Particularly favoured by the steep, highly active rock faces in both valleys, masses of loose sediment are frequently stored in the form of talus deposits. This is in good accordance to other studies performed in meso-scale alpine catchments. For instance, RAPP (1960a,b), CAINE (1986) and SCHROTT et al. (2003) correspondingly observed a dominance of talus processes and storages in valleys smaller than  $30 \text{ km}^2$ . In contrast, (glacio-)fluvial processes especially characterise larger basins ( $4000\text{-}5000 \text{ km}^2$ ) as shown, for example, by JÄCKLI (1957) and JORDAN & SLAYMAKER (1991). The study in the Turtmann valley ( $110 \text{ km}^2$ ) by OTTO et al. (2009) bridges the gap between meso-scale and macro-scale alpine valleys. Interestingly, the authors found a prevailing occurrence of glacial and glacio-fluvial deposits. Referring to OTTO et al. (2009), this shift of process domains from gravitational to (glacio-)fluvial might reflect the propagation of paraglacial impulses from upland to lowland as described by CHURCH & SLAYMAKER (1989).

In addition, the strong assumption arises that the paraglacial evolution of alpine systems is not only dominated by the catchment size and position, but also appreciably influenced by valley morphometry. By comparing the relative proportion of moraine deposits in Val dal Botsch and Val Müschauns, significant divergences become obvious. In the U-shaped Val Müschauns, moraine deposits account for less than 9 % of the basin surface. Here, the reworking of Pleistocene moraine fills through solifluction or debris flows might be almost completed. Today, there is a pronounced

dominance of gravitational processes and storages. This corresponds very well with BALLANTYNE'S (2003) model of paraglacial landform succession, where sediment is routed through different sediment storages from the initial glacial landforms to post-paraglacial sediment deposits. In the V-shaped Val dal Botsch, around 25 % of the surface is covered by glacial material, shaped by cryogenic creeping and debris flows. Based on these findings, it can possibly be assumed that U-like shaped valleys might adjust faster to non-glacial conditions whereas V-like valleys are still in progress to work over the paraglacial impulse.

Furthermore, in both study sites, the activity of storage landforms appears to increase progressively in an upstream direction. The colluvium and the extensive alluvial plain (in Val dal Botsch) of the lower basins are densely vegetated and seem to be inactive today. In contrast, an overall higher degree of activity can be assigned to the upper basins (talus slopes), where vegetation cover is relative sparse or non-existent. This longitudinal pattern of vegetation could imply a temporal variability that is a product of the climatic and ecological fluctuations since deglaciation of the alpine valleys. During the Pleistocene, both study sites were covered by ice up to a height of ca. 2800 m (ROESCH 1937, TRÜMPFY et al. 1997). With the retreat of the Würm ice, ca. 10,000 years ago, the lower basins probably became ice-free much earlier than the upper basins, which might still have been covered by local glacier systems until the Younger Dryas/End of the Little Ice age. In theory, the sediment deposits within the lower basins could therefore be much older, as their accumulation started shortly after the onset of the deglaciation. This suggestion might be confirmed when looking at the middle basins that appear to take up an intermediate position. Particularly in Val Müschauns, highly active hillslope debris flows are located immediately adjacent to partly vegetated debris flow deposits, which might be relict features without noticeable recent debris flow activity (fig. 4.4d). Analogous findings have been reported in the Reintal by SCHROTT et al. (2003) also inferring a paraglacial origin. Similarly, other studies in formerly glaciated regions, for example in Great Britain (CURRY & MORRIS 2004, WILSON 2009), particularly in Scotland (HINCHLIFFE & BALLANTYNE 2009), or in New Zealand (HALES & ROERING 2005) interpret such horizontal zonation throughout a catchment as paraglacially conditioned landform evolution.

Nevertheless, it needs to be warned about mono-causal explanations and thus, the paraglacial interpretation have to be treated critically, as recently advocated by MCCOLL (2012). Vegetation cover is probably a restricted indicator for the long-term variability of landform activity. The study by HÖRSCH (2001) clearly demonstrates that the spatial pattern of vegetation in alpine basins is directly controlled by topography, which in turn determines the spatial distribution of precipitation, radiation, air and ground temperature and moreover, geomorphologic processes. As shown in figure 7.1, the progressive steepening of the relief with rise in altitude generates a simultaneous thinning of the vegetation cover and change of vegetation type to low-growing shrubs and grasses. In turn,

activity of geomorphic processes is considerably enhanced. Hence, the talus deposits above the timberline are some of the most active storages in alpine valleys. In contrast, the high vegetation density/high activity of the lower slopes (colluvium, moraine deposits) and thus, of the lower basin is probably just a product of the current relief, and not due to long-term climatic fluctuations.

Finally, although the spatial distribution of storage landforms in combination with the spatial vegetation pattern provide evidence to assume a long-term variability since deglaciation, the interpretations remain undeniably hypothetical and even critically for this moment. To prove these initial assumptions, further studies would be necessary in other deglaciated, meso-scale valleys of contrasting morphometry, especially by performing geophysical surveys for volumetric information.

#### 7.4 Understanding sediment trajectories and the role of functional storage relationships with respect to time and space

As stated by SLAYMAKER (1991), the knowledge of sediment pathways from individual sources to a sink is crucial to understand alpine sediment cascades. In the sense of CHORLEY & KENNEDY (1971), it is important to stress that sediment is not directly transferred from a source, e.g. a rock face, to the channel network/outlet. Instead, sediment trajectories occur along various storage landforms, which are themselves filled and exhausted by various processes operating over different spatial and temporal scales. The toposequence analysis in the Swiss National Park demonstrates that various possibilities exist, in which manner sediment storage landforms can be topologically organised along hillslopes. Nevertheless, the toposequences cannot simply be related to uninterrupted sediment fluxes from valley ridge to stream channel (OTTO 2006). Instead, the functional relationships between neighbouring storage landforms need to be considered, as intermediate decoupling or coupling can occur. The first interesting outcome of this analysis is that the specific toposequence type and its strength of internal coupling vary distinctly longitudinally throughout the catchments (fig. 7.2). The upstream increase of the number of storages and

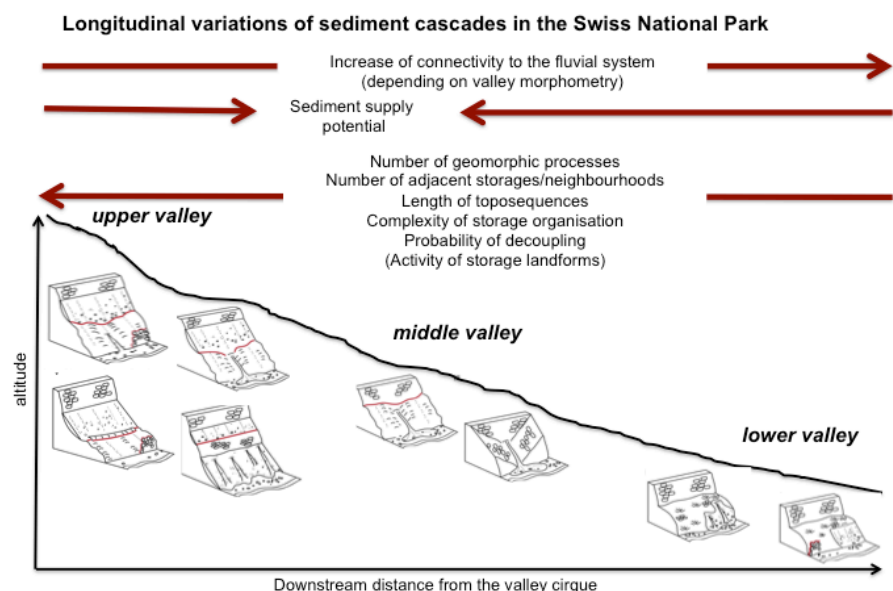


**Fig. 7.2:** Longitudinal variability of sediment cascades in the Swiss National Park due to spatial variations in storage pattern and neighbourhoods, connectivity, activity and sediment supply.

neighbourhoods of different storage types is accompanied by a rise in complexity of storage organisation and the probability of decoupling through a buffering element. Concurrently, the length of slopes, particularly in Val Müschauns, increases upstream favouring the decoupling of sediment trajectories.

Nevertheless, the comparison of the two alpine basins reveals significant discrepancies. While in Val dal Botsch, 23 individual landform successions have been identified, 33 toposequences exist in the larger basin Val Müschauns. Additionally, the toposequences in Val dal Botsch are with six successive storages on average shorter when compared to Val Müschauns, where up to eight storages can be neighbored laterally. By considering the storage relationships, it becomes obvious that the majority of the toposequences of Val dal Botsch represents connected sediment trajectories, as 90 % of the storage boundaries are coupled. On average, sediment is transferred across five coupled consecutive storages along a cascade. In contrast, around 26 % of the storage boundaries of Val Müschauns are decoupled. Here, almost all toposequences are interrupted in-between resulting in sediment cascades of only three consecutive storages. Hence, even though the toposequences are longer in Val Müschauns, the lengths of coupled sediment trajectories are significantly longer in Val dal Botsch, comprising around five coupled, successive storages.

The question arises whether the sediment cascades along the hillslopes are generally better coupled in Val dal Botsch than in Val Müschauns. A major controlling mechanism might be the unique arrangement of storage landforms within the valleys. In Val Müschauns, the sediment cascades are notably affected by the large proportion of bedrock and the frequent neighbourhood to bedrock. Nearly all toposequences are buffered by the existence of bedrock outcrops in-between. Around 62 % of the toposequences begin with a bedrock-talus-bedrock succession. However, the high coupling degree of the toposequences in Val dal Botsch might even be more surprising with regard to the large proportion of buffering moraine deposits (26 %) within the basin. Therefore, further factors have to influence the length and effectiveness of sediment trajectories in alpine valleys.

The results give reason to assume that the specific hillslope geomorphometry is a key driver for the internal coupling along the sediment cascades. The relatively flat and elongated slopes in Val Müschauns, particularly within the upper basin, seem to enhance the decoupling between neighbouring landforms. In particular, the midslopes (fig. 7.1) intensify the buffering between the talus slopes of the upper slopes and the lower footslopes. In contrast, the steep midslopes in Val dal Botsch strengthen the internal coupling between the individual storages within the cascades.

Moreover, it is noticeable that specific slope gradients have a direct influence on the activity of debris flows. The moraine deposits on the midslopes in Val dal Botsch are heavily incised by bed-type debris flow, so that these buffering elements are intersected in most of the toposequences (III, V, VI, VII, fig. 6.2). The majority of Val dal Botsch's debris flow channels are fed directly by the

higher located talus or rampart material. In contrast, the lower gradients of the midslopes in Val Müschauns largely hamper the incision by debris flows. As shown in toposquence type V and VI (fig. 6.3), the debris flow channels do not currently reach high enough to couple the rockfall material, embedded within cliff irregularities, with the lower footslopes or even with the stream.

Furthermore, time plays a crucial role for the operation of alpine sediment trajectories. The findings of this study reveal that the specific functional relationships between neighbouring storages crucially control the temporal variability of sediment routing with regard to both the event time scale and the multi-millennial time scale. Sediment trajectories are temporally variable as the sediment throughput between adjacent landforms operates at different event frequencies. The effectiveness of this dynamic material transfer clearly depends on the length of the separating boundary as calculated in table 6.1 and 6.2. In both valleys, more than 28 % of the current sediment transport across the storage boundaries occurs continuously, mainly driven by the bedrock-talus neighbourhood. Hence, the constant coupling between steep rock faces and talus slopes via continuous low-magnitude rockfall events is a key control on the currently active sediment fluxes in the Swiss National Park. The geomorphic importance of the constant coupling between rock faces and talus slopes has, though indirectly, been mentioned by e.g. JÄCKLI (1957), RAPP (1960a,b), JOHNSON & WARBURTON (2002) and KRAUTBLATTER et al. (2012), who all highlight the particular contribution of small-magnitude rockfalls. Interestingly, due to most abundant neighbourhood between bedrock and debris flow channels in the lower part of Val Müschauns – accounting for 21 % of the entire storage boundaries – the sediment trajectories of the lower/middle basin are greatly controlled by an episodic dynamic. It is likely that this episodic sediment transfer will have significant impacts of the sediment budget in Val Müschauns, as shown by BENDA & DUNNE (1987) and BENDA (1990).

Additionally, the findings of the neighbourhood analysis gives reason to assume that sediment trajectories are characterised by a long-term variability that possibly ranges from numerous centuries to millennia. The sediment throughput between neighbouring landforms might be accompanied by a displacement of the separating boundary over time. This basic assumption of this thesis is confirmed by various geomorphic studies in mountain environments. For instance, SASS & WOLLNY (2001), SASS (2005) and CURRY & MORRIS (2004) investigate long-term rockwall retreat rates ranging between 0.06-0.37 mm/year – or even higher during the Lateglacial – particularly through the work of continuous low-magnitude rock fall events. Likewise, ZIMMERMANN (1990) and KNEISEL et al. (2007) show that the episodic incision of debris flows in unconsolidated sediments is linked to a gradual retrogressive erosion and upslope migration of the initiation site.

However, none of those studies has mentioned explicitly the consequences for the internal coupling behaviour of alpine sediment cascades. Instead, the findings of this thesis might indicate that the long-term storage coupling will affect the evolution of the hillslope morphometry that has in turn, long-term consequences for the cascading sediment fluxes in mountain basins. With 66 % of the

entire storage length, both study sites are mainly controlled by a retrogressive displacement of storage boundaries over time. A key driver is the coupling between bedrock and talus slopes. Consequently, it might be possible that the talus slopes embedded within the rockwall will coalesce over time in the course of a gradual retreat of the separating bedrock boundary (fig. 6.2, 6.3). Hypothetically, the currently decoupled talus slopes (e.g. in Val Müschauns) will become coupled one day. In turn, the upward growth of the talus would have significant influence on the adjacent rock face, since its efficiency in providing fresh debris will gradually be reduced as the cliff height decreases. STATHAM (1976) describes this interplay of talus accumulation, talus morphometry and rockwall height in his famous “scree slope rockfall model”.

Likewise, the long-term regressive erosion and migration of debris flow channels within the cohesive moraine deposits will probably overcome the buffering element and generate a connection between the upper slopes and the stream channel. Theoretically, the toposequence type V of Val dal Botsch, could develop into the type VI over time. In Val Müschauns, debris flows are largely incised in bedrock. Here, it is not clear if toposequence II will gradually develop into III. Even though STOCK & DIETRICH (2003, 2006) describe the active incision of debris flows in bedrock, there is no information on a retreating migration in this type of lithology. The geomorphic mapping in Val Müschauns give evidence to presume that secondary processes at the source area, such as rockfalls, might favour regressive incision. However, this assumption needs further validations.

With regard to the first hypothesis this chapter highlights the particular role of debris flows in alpine sediment cascades. Their channels represent important sediment transport pathways and operate as major connecting linkages between storages along hillslopes. Particularly, by modifying the mountain relief over long time scales, debris flows might control the long-term coupling between neighbouring sediment storages notably, and thereby, the entire connectivity to the fluvial system. Consequently, **the first hypothesis can be confirmed**, but will be taken up later.

Finally, this chapter demonstrates very well the great value of the toposequence concept for studying alpine sediment cascades. In combination with the analysis of functional relationships, which have not been applied in such a manner until now, the methods presented here allow a topological systematisation of hillslopes into several neighbouring storages and offer a valuable qualitative evaluations of sediment trajectories and their internal short- and long-term coupling.

### **7.5 The role of alpine sediment cascades within the sediment flux system**

The role of alpine sediment cascades within sediment flux systems of formerly glaciated, meso-scale basins is still insufficiently understood (GÖTZ & SCHROTT 2007). The comprehension is complicated most noticeably by the fact that transport, storage and release of sediment occur on different temporal and spatial scales due to diverse controlling factors, varying activity states and reaction times (see e.g. CAINE 1986, WALLING 1983, SLAYMAKER 2003). Considerable

uncertainties also exist over the linkages between storage landforms and the fluvial system (see HARVEY 2001, 2002, BEEL et al. 2011). Referring to REID & DUNNE (1996), after localising and analysing all storage landform and major sediment routing pathways in Val dal Botsch and Val Müschauns, the focus is finally on the potential of the two valleys for delivering sediment to the fluvial system. In this study, the sediment supply potential is defined as a function of the hillslope-channel connectivity as well as the state of activity, approximated by the vegetation cover and erosion risk. This way of proceeding differs obviously to other studies (e.g. BEEL et al. 2011, CAVALLI et al. 2012), which do not consider the recent activity and use solely the connectivity as proxy to evaluate sediment fluxes.

Both, the qualitative and quantitative analyses imply that both valleys play a distinct role in the sediment flux system of the Swiss National Park. The average potential is highest in Val Müschauns, even in the qualitative study. This discrepancy can be explained by the different degree of geomorphic activity within the catchments buffering the overall connectivity degree. The surface of Val Müschauns is considerably more active (mean 3.5) on average compared to Val dal Botsch (mean 2.8). As a first suggestion, this could be explained by the specific glacial history of the valleys, as described by CHURCH & SLAYMAKER (1989) and BALLANTYNE (2002). Due to the lower altitudes and the smaller catchment size, the last deglaciation possibly started earlier in Val dal Botsch, therefore leading to an earlier decline of activity of sediment fluxes than in Val Müschauns. This idea might be confirmed by the overall vegetation coverage, which is denser and more extensive in Val dal Botsch, stabilising most of the sediment storages today. Nevertheless, as already stated, the paraglacial hypothesis requires a critical review (MCCOLL 2012). Thus, as a second assumption, it might be more likely that the overall activity degree and therefore the potential for sediment supply is the result of the alpine topography and especially of the bedrock-sediment ratio. Given the higher erosion risk in Val Müschauns, particularly along the northern valley side, the large portion of steep cliffs probably enhances the geomorphic activity in contrast to the more convex, depositional storage landforms in Val dal Botsch (see also CAVALLI et al. 2012).

However, by comparing the results of the qualitative and quantitative connectivity assessment, significant discrepancies become apparent concerning the relative land surface that finally contributes sediment to the fluvial system. The quantitative method implies a higher (mean) degree of connectivity in Val Müschauns than in Val dal Botsch. In contrast, the qualitative study illustrates precisely the opposite with an obvious higher mean connectivity in Val dal Botsch. Hence, one of the most striking differences of the two methods is the capability to display decoupling or disconnectivity. Nevertheless, based on systemic comprehension and confirmed by geomorphic field mapping, the results of the qualitative study appear to be more reliable in this context.



**Fig. 7.3:** Upper basin of Val dal Botsch. In total, 15 % of the valley is decoupled by moraine deposits, e.g. the talus slopes shown at the right side of the photo.



**Fig. 7.4:** Decoupled talus slopes in Val Müschauns. Nearly the entire upper valley is decoupled through moraine deposits and bedrock outcrops.

Nearly one third of Val Müschauns' basin, which is in fact the entire upper basin, is decoupled through the buffering by moraine deposits and bedrock outcrops (fig. 7.4). Hence, only two thirds of the sediment deposited within the basin recently contributes to the sediment flux system. This is obviously less than in Val dal Botsch. Here, only 15 % of the surface is decoupled from the fluvial system (fig. 7.3). Interestingly, the large amount of moraine valley fills in Val dal Botsch would actually imply a generally higher buffering effect. However, due to the frequent incision of debris flow channels, most of the higher-situated talus slopes are strongly connected to the stream channel.

With regard to the contrasting size of both valleys, these findings appear to contradict to common studies such as by CHURCH & SLAYMAKER (1998) and OWENS & SLAYMAKER (1992), observing a rise in yield with increasing catchment size in formerly glaciated valleys, due to the enhanced remobilisation of (paraglacial) sediment storages. Yet, those studies differ from the Swiss National Park as the authors investigated much larger valleys within an order of up to  $3 \times 10^4 \text{ km}^2$ . Instead, there is strong evidence to presume that in alpine basins, smaller than  $10 \text{ km}^2$ , the specific valley geomorphometry determines the potential of how any part within a catchment is involved in the sediment flux system. The steep and narrow valley morphometry of Val dal Botsch noticeably favours comparatively short toposequences, but stronger coupling between neighbouring storages and finally to the stream channel. In contrast, within the U-shaped upper trough of Val Müschauns, the elongated, gently inclined slopes increase the length of toposequences but, at the same time, impede the activity of the coupling geomorphic processes such as debris flows. Therefore, it can be hypothesised that the sediment delivery problem in alpine headwater regions is likely to be a consequence of the valley morphometry rather than of the catchment size, as originally described by WALLING (1983). The control of the relict glacial topography on sediment connectivity has also been stressed by BRARDINIONI & HASSAN (2006) in the Canadian Rocky Mountains. In the same region, HOFFMANN et al. (submitted) compared fluvially and glacially dominated basins and underline the particular effect of glacial erosion on the decoupling of headwater basins from the fluvial system due to the decrease of the rivers' transport capacity.

Moreover, assuming that U-shaped cross profiles reflect a higher degree of glacial erosion (MONTGOMERY 2002), this study might indicate that the varying influence of Pleistocene glacial erosion affects the current degree of decoupling in small alpine basins differently. The overall buffering effect and the possibility of decoupling consequently appear to be higher in trough valleys, where glacial erosion was more effective compared to rather V-shaped valleys. This emphasises the path dependence of small, meso-scale alpine cascading systems comprehensively (SCHUMM 1991, BALLANTYNE 2002). Hence, the current strength of coupling and connectivity in alpine basins appears still to be a response of their specific glacial history. This might be closely linked to the valley sensitivity (see e.g. BRUNSDEN & THORNES 1997, USHER 2001). It is reasonable to assume that due to the higher degree of connectivity, V-shaped valleys will generally be more sensitive to upstream disturbance of future climate change, such as an increase of geomorphic activity and mobilisation of sediment deposits, in comparison with trough valleys, where the weak connectivity will diminish those effects and further propagation to lowland basins for the moment.

Concerning the third hypothesis, the qualitative analysis indicates that the two study areas differ substantially in their capacity to deliver sediment to the basin's outlets. Val Müschauns is characterised by a higher potential for supplying sediment to the stream network, only two thirds of surface currently takes part within the sediment flux system. The highly active talus slopes within the upper trough are contemporarily decoupled, implying thereby that most of the sediment produced since the retreat of the Pleistocene ice masses is probably still stored within the basin. Despite of the lack of volumetric information, the thickness of these talus slopes is assumed to be very high (SASS & WOLLNY 2001). Thus, it is likely that a large volume of loose sediment does not presently reach the basin outlet. In contrast, the majority of the sediment stored within Val dal Botsch has a connection to the stream and therefore contributes to the sediment yield. Hence, **the third hypothesis can be verified in the case of the U-shaped Val Müschauns, but needs to be falsified for the V-shaped Val dal Botsch, underlining the role of basin morphometry.**

Additionally, despite of some weaknesses of the numeric approach, which will be discussed in the next chapter, the results of the connectivity modelling demonstrate clearly that sediment delivery varies spatially throughout catchments. These spatial variations are also confirmed by field investigations and systemic knowledge, making these specific quantitative results reliable. On a hillslope scale (fig. 7.1), the connectivity to the fluvial system weakens noticeably upslope with growing proximity to the stream. At the same time, the geomorphic activity increases upslope with rising altitude and slope inclination. Consequently, the mid and upper slopes might have the highest potential within the sediment flux system of the alpine basins. On a catchment scale, the longitudinal behaviour of sediment fluxes appears to depend on valley morphometry. As shown by both connectivity assessments, the overall connectivity pattern of Val dal Botsch is relatively

homogeneous in space. Due to the reduced degree of activity within the lower and middle basin, the upper regions probably play the main role for the sediment flux system. In contrast, connectivity weakens markedly in an upstream direction for Val Müschauns, as indicated by the quantitative GIS-modelling. Here, the elongated slopes of the upper trough and the longer trajectories favour the opportunity of decoupling relative to the steeper lower/middle basin. Similarly, CAVALLI et al. (2012) investigated an upstream decrease in connectivity within a U-shaped alpine valley by using BORSELLI's modelling approach. Hence, as activity also decreases upstream, the middle basin of Val Müschauns can be considered as the most effective in terms of sediment flux.

In this context, the role of debris flows as major driver of the temporal variability of the cascading sediment fluxes needs to be highlighted. In the course of the long-term regressive incision of the channels, the internal storage coupling of the hillslope cascade increases, directly influencing the connectivity to the stream. This might be accompanied by substantial effects on the long-term sediment delivery potential. Likewise, debris flows can lead to short-term interruptions of the hillslope-channel connection, which might affect even the long-term sediment fluxes. The geomorphological mapping within the Swiss National Park bears evidence that the deposition of debris cones near the channel stream might cause a temporary decoupling between the hillslope storages and the fluvial system. Moreover, remnants of debris cones at the valley side opposite to the initiation slope probably indicate that the deposition of very large cones can even cause a transient damming of the stream and thus, a complete decoupling of the valley's upper parts. It seems likely that during the subsequent fluvial erosion, breaking through the damming material, sediment yields would increase drastically, even beyond those from the time of the actual

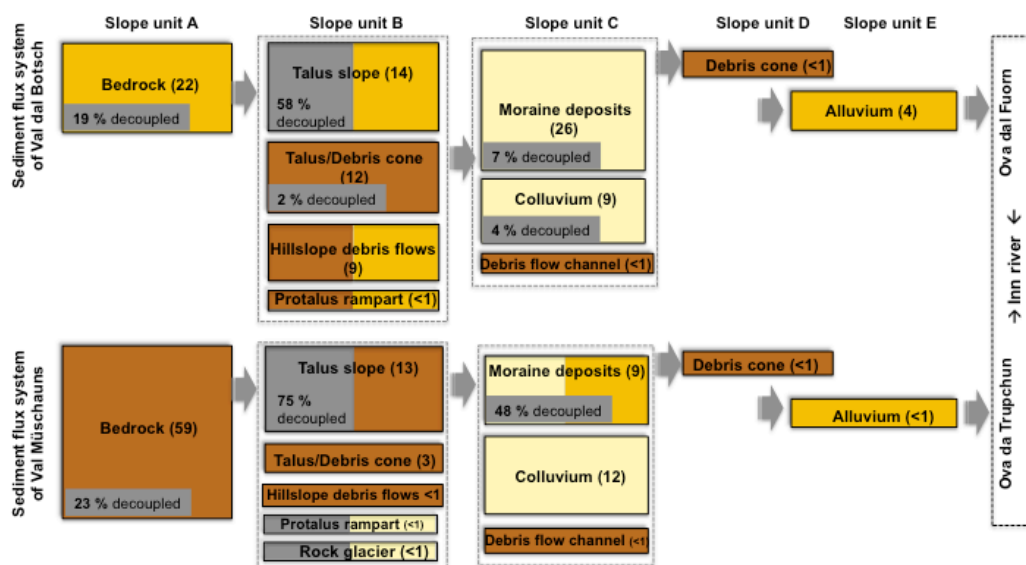


**Fig. 7.5:** Illustration of the sediment fluxes systems of Val dal Botsch and Val Müschauns. The size of boxes correlates to the relative size of storage landform. The relative storage surface is given as percentage n brackets. The median sediment supply potential is displayed for the qualitative (left hand side box colour) and quantitative analysis (right hand side box colour). Colour of average potential: Brown = high, orange = medium, light yellow = low. The percentage of decoupled fraction of each storage is shown in grey.

decoupling event. Corresponding to the study by HAAS et al. (2004) in the Northern Limestone Alps, these findings again point out the role of debris flows, both as key driver for hillslope-channel connectivity and as major contributing process within alpine sediment budgets. **Once again, the first hypothesis can be verified.**

Finally, one of the greatest values of this study – particular with regard to sediment budget studies – is the identification of “sediment hotspots”. As shown in figure 7.5, the sediment flux systems of the two alpine valleys can ideally be divided into five slope units, all comprising a unique set of sediment storages varying in surface area. Depending on the specific connectivity approach, each sediment storage landform is characterised by a different potential to deliver sediment to the stream network. Both study areas can be regarded as open systems, as their valley floors represent only temporary sinks due to the high dynamic nature of the stream.

The role of rockfall-generated talus slopes is quite interesting. With a relative surface of 13-14 %, they are among the dominant and most active storages in both basins. This corresponds with the study by KRAUTBLATTER et al. (2012), emphasising the geomorphic work of continuous low-magnitude rockfalls. They probably contribute 18 % of the total rockfall sediment yield in alpine basins. In the Swiss National Park, however, most of the talus slopes within the upper basins might be currently decoupled. Assuming a talus thickness of ca. 5-13 m (SASS & WOLLNY 2001), it becomes obvious that a large volume of available sediment does not contribute to the cascading fluxes. Likewise, colluvial and moraine deposits cover relatively large areas in both valleys (21-35 %), but their supply potential is comparatively low. Moreover, with regard to the frequent bedrock outcrops indicating a relatively thin sediment cover, colluvial and moraine deposits appear to be less effective within the sediment flux systems. In contrast, in both valleys, the highest potential can be assigned to those sediment storage landforms that have been created by debris flows. They have one of the highest levels of connectivity as well as activity within the basin. Despite their small surface area, the deposited material can reach heights of up to 10 m (RICKENMANN 2001). This underlines the importance of debris flow action for the sediment budget of alpine systems.

For the moment, some of the findings remain semi-quantitative, since no information on the storage volume is available. The comparison between the qualitative and quantitative results additionally highlights the need of a profound systemic knowledge, since the modelling would probably overestimate the sediment delivery potential in both valleys. Nonetheless, with regard to the methodological framework, the overlay of the sediment connectivity and activity generally appears to be a good proceeding to evaluate the sediment flux system of alpine basins. Moreover, based on the sediment storage inventory and the identification of sediment trajectories (toposequences), this approach gives a semi-quantitative and cartographic estimation of the sediment hotspots that can potentially be mobilised in alpine basins, particularly as response to future climate change.

## **7.6 Can conventional geomorphological mapping be replaced by numeric methods to explain the complexity of alpine geosystems?**

Geomorphological field mapping represents a classical tool to analyse the complexity of alpine environments (see e.g. SMITH et al. 2011). Regional examples of geomorphological maps on a scale of 1:5000 to 1:200,000 are summarised by BARSCH & LESER (1987). Based on the map legend of KNEISEL et al (1998), OTTO & DIKAU (2004) created a detailed map of the Turtmann Valley on a scale of 1:25,000, providing the essential foundation for a comprehensive geophysical survey.

To study the geomorphic systems of the Swiss National Park, the geomorphic mapping on a scale of 1:5000 offers a synthesised way of showing the arrangement and distribution of all sediment storage landforms and currently active geomorphic processes. With regard to the choice of legend, the use of the legend by KNEISEL et al. (1998) has proven to be very suitable to show the wide range of geomorphic transfer and storage processes occurring in alpine basins in detail. The two maps of the study areas provided an excellent basis to increase the comprehension of the geomorphic system and to proceed with further (morphometric) analyses in ArcGIS.

However, the fieldwork in the Swiss National Park highlighted some obvious limitations of classical geomorphic mapping. To name only a few of them: The mapping was time consuming, particularly due to the steep relief, the difficult accessibility of some regions and the dense vegetation cover. The final maps of Val dal Botsch and Val Müschauns are obviously affected by a certain degree of subjectivity of the cartographer and ultimately just a momentary snap shot of the complex and dynamic surface of the earth. Likewise, VAN ASSELEN & SEIJMONSBERGER (2006) and BISHOP et al. (2012) discuss further restrictions that might be linked to the traditional geomorphic mapping.

As a consequence, there are reasons to assume that modern, quantitative approaches have the greater potential in the analysis of (alpine) geosystems compared to classical field mapping. The recent development of GIS and the availability of high-resolution digital terrain models, for instance via airborne LiDAR surveys, seem to improve the understanding of geosystems profoundly (HENGL & REUTER 2009). BISHOP et al. (2012: 5) go even further and claim that the new “geocomputational algorithms and approaches now permit Earth scientists to go far beyond the traditional mapping”.

Has classical geomorphic field mapping become dispensable today? To pursue this question, the sediment connectivity in the Swiss National Park has been analysed by a new conceptual approach, based on classical field mapping, and has been tested against the numeric GIS-algorithm by BORSELLI et al. (2008). First of all, the application of BORSELLI’s numeric approach highlights very well that the method stands out particularly due to its simplicity and rapid spatial characterisation of connectivity by means of available GIS routines (see also CAVALLI et al. 2012). Moreover, the index is topography-based, displaying real flow pathways of sediment particles between a source and sink as well as the influencing effects of topography (slope, drainage size, surface roughness). For instance, the modelling in Val dal Botsch reveals that some of the talus slopes along the right

upper basin have a weaker connectivity due to their low gradients, even though they are in close proximity to the stream network. Additionally, the use of quantitative weighting factors derived from the DEM allows a comparability of the findings in the Swiss National Park with studies in other alpine regions that use BORSELLI's approach. Furthermore, while the minimum scale of the qualitative connectivity assessment is the storage landform, the numeric method is pixel-based. This permits to work out small-scale variations of the connectivity index within a single storage landform or narrow corridors of sediment routing. For example, the modelling results of Val dal Botsch display some highly connected areas within the less connected moraine deposits, which are in direct proximity to the intersected debris flow channels. Particularly, with regard to the spatial variability of connectivity, the results of BORSELLI's method are quite promising and in good accordance with qualitative investigations such as the longitudinal decrease of connectivity towards the upper, U-shaped basin of Val Mütschans.

Nevertheless, the final results of the numeric approach depend noticeably on the quality and resolution of the input data. Although the pixel-based information appears to be quite advantageous, working on a micro-scale within DEMs might also be linked to an increase in uncertainties. For instance, by using DEM resolutions larger than 2x2 m, important sediment routing pathways will possibly be neglected and the channel width of debris flows can be underestimated. It also needs to be stressed that the possibility to update a map by means of numeric analyses is limited, since it depends on the continuous update of input data itself, which is obviously rather expensive.

Therefore, given the very weak correlation coefficients between both connectivity procedures, their results and especially, their reliabilities differ substantially. A crucial disadvantage of the numeric study is that it cannot display the variety of geomorphic processes in alpine environments. The method is rather focused on channelised sediment transport (CAVALLI et al. 2012). More process-oriented GIS-approaches (particularly for alpine regions) have been developed by WICHMANN et al. (2009) and THIEL et al. (2011). Thus, it must be assumed that BORSELLI's algorithm cannot model the sediment connectivity in high-alpine systems adequately. In contrast, the qualitative framework implements the type and, particularly, the event frequency of geomorphic processes. The comprehensive mapping includes the wide range of depositional and reworking processes within the study areas, which clearly represents a strong advantage of the qualitative study.

Therefore the key strength of the qualitative connectivity assessment becomes evident, proving its superiority over the numeric method: The qualitative framework is based on a fundamental systemic comprehension of the alpine valleys. The realisation of the sediment cascade concept and the analysis of functional relationships between storages enable the identification of obstructions within the sediment transport and thus, decoupled areas within the alpine basins. In contrast, BORSELLI's GIS-approach – and possibly various other pixel-based methods – does not consider potential decoupling. Even though, the numeric method displays a lower degree of connectivity within the

upper basin of Val Müschauns, the use of BORSELLI's algorithm would result in a significant overestimation of the capacity of the land surface that delivers sediment to the stream network, as indicated by the contrasting mean values. As a consequence, the modelling would to a certain degree fail to provide a basis for sediment budgets in alpine systems where decoupling occurs frequently. Recently, a first, more promising numeric approach based on systemic knowledge has been developed by HECKMANN & SCHWANGHART (2012). They applied the graph theory to investigate network structures of alpine cascading systems and considered storage (de)coupling. However, such approaches are considerably rare and still in the early stages of development.

Finally, the findings of this thesis demonstrate that it is not possible to display highly dynamic alpine systems accurately by a single numerical algorithm. It needs therefore to disagree with the statement by BISHOP et al. (2012: 5), for the reason that Earth scientists do still depend on heuristic, knowledge-based geomorphic mapping – even in or precisely because of our modern, pixel-based world. Thus, the traditional geomorphic field mapping still remains an indispensable basis for a profound and accurate systemic comprehension of geomorphic systems and consequently, for the validation of numeric investigations. Accordingly, **the last hypothesis needs to be verified.**

Nonetheless, the great potential of numeric methods for future work has to be stressed as some of the modelling results, such as the spatial pattern of connectivity or the lower strength of connectivity in the upper basin of Val Müschauns, are very reliable. Therefore, in combination with the classical field mapping, pixel-based modelling approaches continue to be important tools to characterise and understand the highly dynamic operation of sediment cascades in (alpine) geosystems.

## 8 CONCLUSION AND OUTLOOK

In alpine environments, the transport of sediments from hillslopes to the fluvial system follows a cascading way, as described by CHORLEY & KENNEDY (1971). Different geomorphic processes transfer sediment along various storage landforms, which are themselves filled and depleted over varying spatial and temporal scales. A profound understanding of alpine sediment cascades is important even more today, because it has a major significance for sediments budgets and the sensitivity of alpine systems to environmental and anthropogenic disturbances. The main aim of this master thesis was to gain further insights regarding the highly spatio-temporal dynamic nature of sediment cascades and their role within the sediment flux systems of alpine basins. By a combination of classical geomorphic mapping in the field and various geomorphometric analyses in ArcGIS, two meso-scale, alpine valleys of contrasting valley morphometry – Val dal Botsch and Val Müschauns – have been studied in the Swiss National Park (Graubünden, Switzerland).

This study demonstrated that the two alpine catchments are characterised by a unique spatial pattern of sediment storage types, which is a result of a complex interplay of individual catchment-specific factors including basin size, lithology, slope morphometry as well as climate and ecology. However,

both study sites are primarily dominated by gravitational storage landforms and the majority of sediment throughput between adjacent landforms occurs continuously via low-magnitude rockfall events. This was interpreted – but with a high degree of caution – as a typical evolution stage of meso-scale alpine basins within the paraglacial cycle. As one of the most important outcomes, this study indicated that the two alpine valleys play a markedly different role within the sediment flux system of the Swiss National Park. In Val Mütsch, one thirds of the surface, which is nearly the entire upper trough, is currently decoupled from the fluvial system. In Val dal Botsch, the majority of stored sediment presently makes its way to the outlet. The analysis of the sediment trajectories gave reason to assume that in alpine headwater basins, the sediment delivery problem, as described by WALLING (1983), might be a result of the specific valley morphometry (U-shape or V-shape) rather of the valley size. These findings underline the path dependence of alpine systems as the varying degree of the Pleistocene glacial erosion probably still influence the strength of coupling and connectivity of mountain basins. Furthermore, the significant role of debris flows within alpine cascading systems became evident in this study. Their channels represent major connecting linkages between the hillslopes storages and the stream network and might control the short- and long-term degree of coupling and connectivity, particularly due to the influence on the hillslope topography.

Finally, this study demonstrated that numeric algorithms, such as the one by BORSELLI et al. (2008), still insufficiently explain the sediment connectivity in alpine systems, since the decoupling of land surface cannot be displayed. Hence, even in a modern, pixel-based world, the traditional field mapping remains indispensable for a holistic comprehension of alpine systems.

However, it needs to be stressed that some outcomes are still subjected to a certain degree of uncertainty. For instance, the reworking of the paraglacial impulse in the two alpine valleys can be just speculatively explained based on the spatial variation of the vegetation degree. Similarly, it can only be assumed for this moment that the regressive incision of debris flows will affect the long-term operation of the cascading sediment fluxes. Likewise, the influence of the valley shape on the strength of coupling/connectivity and hence, on the sediment delivery problem needs additional investigations. And finally, the evaluation of “hotspots” within the sediment flux systems remains semi-quantitative, since no information on the storage volume exists. Therefore, the future tasks will be to perform geophysical surveys in the study sites in order to quantify the sediment volume stored within the catchments. Moreover, to bring further light in the dispute of “U-shaped valley versus V-shaped valley” additional investigations in comparable alpine basins of contrasting morphometry will be necessary. Nevertheless, the methodological approaches of this master thesis have proven to be very encouraging for a further understanding of sediment storages, routing pathways and internal relationships within alpine cascading systems. Consequently, the performance of similar analyses in populated, more vulnerable alpine regions could make a valuable contribution to identify areas that will be sensitive to anthropogenic influences and future global warming.

---

## 9 REFERENCES

- ANDRÉ, M.F. (1997): Holocene rockwall retreat in Svalbard: a triple-rate evolution. In: *Earth Surface Processes and Landforms* 22: 423-440.
- BALLANTYNE, C.K. (2002a): A general model of paraglacial landscape response. In: *The Holocene* 12: 371-376.
- BALLANTYNE, C.K. (2002b): Paraglacial Geomorphology. In: *Quaternary Science Reviews* 21: 1935-2017.
- BALLANTYNE, C.K. (2003): Paraglacial landform succession and sediment storage in deglaciated mountain valleys: theory and approaches to calibration. In: *Zeitschrift für Geomorphologie, Suppl.* 132: 1-18.
- BALLANTYNE, C.K. (2008): After the Ice: Holocene Geomorphic Activity in the Scottish Highlands. In: *Scottish Geographical Journal* 124 (1): 8-52.
- BALLANTYNE, C.K. & C. HARRIS (1994): *The Periglaciation of Great Britain.* (Cambridge University Press) Cambridge.
- BALLANTYNE, C.K. & D.I. BENN (1994): Glaciological constraints on proglacial rampart Development. In: *Permafrost and Periglacial Processes* 5: 145-153.
- BARSCH, D. (1977): Nature and importance of mass-wasting by rock glaciers in alpine permafrost environments. In: *Earth Surface Processes* 2: 231-245.
- BARSCH, D. (1996): *Rocklacers, indicators for the present and former geocology in high mountain environments.* (Springer) Berlin.
- BARSCH, D. & C.T. CAINE (1984): The nature of mountain geomorphology. In: *Mountain Research and Development* 4(4): 287-298.
- BARSCH, D. & H. LESER (eds.) (1987): Regionale Beispiele zur geomorphologischen Kartierung in verschiedenen Maßstäben (1:5000 bis 1:200000). Beiträge zum GMK-Schwerpunktprogramm VI. *Berliner Geographische Abhandlungen, Heft 42.*
- BEEL, C., ORWIN, J.F. & P.G. HOLLAND (2011): Controls on slope-to-channel fine sediment connectivity in a largely ice-free valley, Hoophorn Stream, Southern Alps, New Zealand. In: *Earth Surface Processes and Landforms* 36: 981-994.
- BENDA, L. (1990): The influence of debris flows on channels and valley floors in the Oregon Coast Range, USA. In: *Earth Surface Processes and Landforms* 15: 457-466.
- BENDA, L. & T. DUNNE (1997): Stochastic forcing of sediment supply to channel networks from landsliding and debris flow. In: *Water Resources Research* 33(12): 2849-2863.

- BENN, B.I. & D.J. EVENS (2010<sup>2</sup>): *Glaciers & Glaciation*. (Arnold) London.
- BEYLICH, A.A. (2011): Mass transfers and sedimentary budgets in geomorphologic drainage basin studies. In: *Advanced Topics in Mass Transfer*, Chapter 18, 399-422. INTECH Book Publication.
- BEYLICH, A.A. & C. KNEISEL (2009): Sediment budget and relief development in Hrafnadalur, subarctic oceanic eastern Iceland. In: *Arctic, Antarctic and Alpine Research* 41 (1): 3-17.
- BISHOP, M.P, JAMES, L.A, SHRODER JR., J.F. & S.J. WALSH (2012): Geospatial technologies and digital geomorphological mapping: Concepts, issues and research. In: *Geomorphology* 137: 1-26.
- BISHOP, M.P. & J. F. SHRODER (eds.) (2004): *Geographic Information Science in Mountain Geomorphology*. (Springer) Heidelberg.
- BORSELLI, L., CASSI, P. & D. TORRI (2008): Prolegomena to sediment and flow connectivity in the landscape: a GIS and field numerical assessment. In: *Catena* 75: 268-277.
- BRACKEN, L. J. & J. CROKE (2007): The concept of hydrological connectivity and its contribution to understanding runoff-dominated geomorphic systems. In: *Hydrological Processes* 21: 1749-1763.
- BRARDINONI, F. & M.A. HASSAN (2006): Glacial erosion, evolution of river long profiles and the organization of process domains in mountain drainage basins of coastal British Columbia. In: *Journal of Geophysical Research* 111, F01013.
- BRARDINONI, F., CHURCH, M., SIMONI, A. & P. MACCONI (2012): Lithologic and glacially conditioned controls on regional debris-flow sediment dynamics. In: *Geology*. doi: 10.1130/G33106.1.
- BRIERLEY, G.J., FRYIRS, K. & V. JAIN (2006): Landscape connectivity: the geographic basis of geomorphic applications. In: *Area* 38(2): 165-174.
- BRUNSDEN, D. (1993): The persistence of landforms. In: *Zeitschrift für Geomorphologie Suppl.–Bd. 93*: 13-28.
- BRUNSDEN, D. (1996): Geomorphological events and landform change. In: *Zeitschrift für Geomorphologie N.F.* 40(3): 273-288.
- BRUNSDEN, D. (2001): A critical assessment of the sensitivity concept in geomorphology. In: *Catena* 24 (2): 99-123.
- BRUNSDEN, D. & D.B. PRIOR (eds.) (1984): *Slope Instability*. (Wiley and Sons) London.
- BRUNSDEN, D. & J. THORNES (1979): Landscape sensitivity and change: In: *Transactions Institute of British Geographers (New Series)* 4 (4): 463-484.

- BÜDEL (ed.) (1981<sup>2</sup>): *Klima-Geomorphologie*. (Borntraeger) Berlin.
- CAINE, N. (1974): The geomorphic processes of the alpine environment. In: IVES, J.D. & R.G. BARRY (eds.): *Arctic and Alpine Environments*. (Methuen) London: 721-748.
- CAINE, N. (1980): The rainfall intensity-duration control of shallow landslides and debris flows. In: *Geographiska Annaler* 62A: 23-27.
- CAINE, N. (1986): Sediment movement and storage on alpine slopes in the Colorado Rocky Mountains. In: ABRAHAMS, A.D. (ed.) *Hillslope processes*. (Allan and Unwin) London: 115-137.
- CAINE, N. (2001): Geomorphic systems of Green Lakes Valley. In: BOWMAN, W.D. & T.R. SEASTEDT (eds.): *Structure and Function of an Alpine Ecosystem*. (Oxford University Press) Oxford: 45-74.
- CAINE, N. & F.J. SWANSON (1989): Geomorphic coupling of hillslope and channel systems in two small mountain basins. In: *Zeitschrift für Geomorphologie* 33(2): 189-203.
- CAVALLI, M. & L. MARCHI (2008): Characterisation of the surface morphology of an alpine alluvial fan using airborne LiDAR. In: *Natural hazards and Earth Systems Science* 8: 232-333.
- CAVALLI, M. TREVISANI, S., COMITI, F. & L. MARCHI (2012): Geomorphometric assessment of spatial sediment connectivity in small alpine catchments. In: *Geomorphology* (in press). doi:10.1016/j.geomorph.2012.05.007.
- CHORLEY, R.J. (1962): *Geomorphology and general systems theory*. US Geological Survey Professional Paper, 500-B.
- CHORLEY, R.J. & B.A. KENNEDY (eds.) (1971): *Physical geography - A systems approach*. (Prentice-Hall International) London.
- CHORLEY, R.J., SCHUMM, S.A. & D.E. SUDGEN (1984): *Geomorphology*. (Routledge) London, New York.
- CHURCH, M. & J. RYDER (1972): Paraglacial sedimentation: a consideration of fluvial processes conditioned by glaciation. In: *Geological Society of America Bulletin* 83: 3059-3071.
- CHURCH, M. & O. SLAYMAKER (1989): Disequilibrium of Holocene sediment yield in glaciated British Columbia. In: *Nature* 337(2): 452-454.
- CONACHER, A.J. & J.B. DALRYMPLE (1977): The nine-unit landsurface model: an approach to pedogeomorphic research. In: *Geoderma* 18 (1-2): 1-154.
- COROMINAS, J., REMENDO, J., FARIAS, P., ESTEVAO, M., Z'ZERE, J. DÍAZ DE TERÁN, J, DIKAU, R., SCHROTT, L, MOYA, J. & A. GONZÁLEZ (1996): Debris flow. In: DIKAU,

- R. & D. BRUNSDEN (eds.): *Landslide recognition. Identification, movement and causes.* (John Wiley & Sons) Chichester.: 161-181.
- COSTA, J. E. (1984): Physical geomorphology of debris flows. Developments and applications of geomorphology. In: COSTA, J.E. & P. J. FLEISHER (eds): *Developments and Applications of Geomorphology.* (Springer) Berlin: 268-317.
- CROOKE, J., MOCKLER, M., FOGARTY, P. & I. TAKKEN (2005): Sediment concentration changes in runoff pathways from a forest road network and the resultant spatial pattern of catchment connectivity. In: *Geomorphology* 68: 257-268.
- CURRY, A.M. & C.J. MORRIS (2004): Lateglacial and Holocene talus slope development and rockwall retreat on Mynydd Du, UK. In: *Geomorphology* 58(1-4): 85-106.
- DALRYMPLE, J. B., BLONG, R.J. & A.J. CONACHER (1968): An hypothetical nine unit landsurface model. In: *Zeitschrift für Geomorphologie N.F.*, 12: 60-76.
- DIETRICH, W.E. & T. DUNNE (1978): Sediment budget for a small catchment in mountainous terrain. In: *Zeitschrift für Geomorphologie, Suppl. Bd. 29*: 191-206.
- DIETRICH, W.E., DUNNE, T., HUMPHREY, N.F. & L.M. RIED (1982): Construction of sediment budgets for drainage basins. In: F.J. SWANSON, R.J. JANDA, T. DUNNE & D.N. SWANSTON (eds.): *Sediment Budgets and Routing in Forested Drainage Basins.* United States Department Agriculture Forest Service: 5-23.
- DIKAU, R. (1989): The application of a digital relief model to landform analysis in geomorphology. In: RAPER, J. (ed.): *Three Dimensional Application in Geographic Information Systems.* (CRC Press) London: 51-77.
- DIKAU, R. (1996): Geomorphologische Reliefklassifikation und -analyse. In: *Heidelberger Geographische Arbeiten* 104: 15-36.
- DIKAU, R. (2006): Oberflächenprozesse - ein altes oder ein neues Thema? In: *Geographica Helvetica*, Heft 3: 170-180.
- DIKAU, R. & J. SCHMIDT (1999): Georeliefklassifikation. In: SCHNEIDER-SLIWA, R., SCHAUB, D. & G. GEROLD (eds.): *Angewandte Landschaftsökologie – Grundlagen und Methoden*: 217-244. (Springer) Heidelberg.
- DOLDER, W. & U. DOLDER (1997): *Der Schweizerische Nationalpark. Reihe Nationalparke, Band 10.* (Kilda-Verlag) Greven.
- ECK, H. (1994): *Graubünden und Tessin. Von den Gipfeln Rätians bis in die Sonnenstube der Schweiz.* (Kohlhammer) Stuttgart u.a.
- EVANS, S.G. & J.J. CLAGUE (1994): Recent climatic change and catastrophic geomorphic processes in mountain environments. In: *Geomorphology* 10: 107-128.

- FLAGEOLLET, J.-C. (1996): The time dimension in the study of mass movements. In: *Geomorphology* 15: 185-190.
- FRANCOU, B. & C. MANTÉ (1990): Analysis of the segmentation in the profile of alpine talus slopes. In: *Permafrost and Periglacial Processes* 1:53-6.
- FRYIRS, K. (2012): (Dis)Connectivity in catchment sediment cascades: a fresh look at the sediment delivery problem. In: *Earth Surface Processes and Landforms* (in press). DOI: 10.1002/esp.3242
- FRYIRS, K., BRIERLEY, G.J., PRESTON, N.J. & M. KASAI (2007): Buffers, barriers and blankets: the (dis)connectivity of catchment-scale sediment cascades. In: *Catena* 70: 49-67.
- GÄRTNER-ROER, I. & M. NYENHUIS (2010): Volume Estimation, Kinematics and Sediment Transfer Rates of Active Rockglaciers in the Turtmann Valley, Switzerland. In: OTTO, J.C. & R. DIKAU (eds.): *Landform – Structure, Evolution, Process Control. Lecture Notes in Earth Sciences* 115. (Springer) Berlin, Heidelberg: 185-198.
- GLADE, T. (2005): Linking debris-flow hazard assessments with geomorphology. In: *Geomorphology* 66 (1-4): 189-213.
- GÖTZ, J. & L. SCHROTT (2007): A comparison of recent and Postglacial sediment fluxes in a paraglacial context - a scale-based approach (Reintal, Bavarian Alps). In: *Geomorphologie, Suppl.-Bd.* 127: 175-196.
- GÖTZ, J., GEILHAUSEN, M. & L. SCHROTT (2010): Zur Interpretation rezenter Sedimentflüsse in einem paraglazialen Kontext. *Salzburger Geographische Arbeiten, Band 46*: 43-63.
- GOUDIE, A.S. (ed.) (2004): *Encyclopedia of Geomorphology*. (Routledge) London.
- GREENWAY, D.R. (1987): Vegetation and slope stability. In: ANDERSON, M.G. & K.S. RICHARDS (eds.): *Slope Stability*. (Wiley) Chichester: 187-230.
- GRUBER, S. & S. PECKHAM (2008): Land surface parameters and objects specific to hydrology. In: HENGL, T. & H. REUTER (eds): *Geomorphometry - Concepts, Software, Applications. Developments in Soil Science*, vol. 33. (Elsevier) Amsterdam: 227-254.
- GRUBER, S. & W. HEABERLI (2007): Permafrost in steep bedrock slopes and its temperature-related destabilisation following climate change. In: *Journal of Geophysical Research*. 112. F02S18, doi:10.1029/2006JF000547.
- GUZZETTI, F., S. PERUCCACCI, M. ROSSI, & C.P. STARK (2008): The rainfall intensity–duration control of shallow landslides and debris flows: an update. In: *Landslides* 5(1): 3-17.

- HAAS, F., HECKMANN, T., WICHMANN, V. & M. BECHT (2004): Change of fluvial sediment transport rates after a high magnitude debris flow event in a drainage basin in the Northern Limestone Alps, Germany. *IAHS Publication 288*: 37-43.
- HAEBERLI, W. (1985): Creep of mountain permafrost: internal structure and flow of alpine rock glaciers. In: *Mitteilungen der Versuchsanstalt für Wasserbau, Hydrologie und Glaziologie 77*.
- HAEBERLI, W. & M. BENISTON (1998): Climate change and its impact on glaciers and permafrost in the Alps. In: *Ambio 27*: 258-265.
- HALES, T.C. & J.J. ROERING (2005): Climate controlled variations in scree production, Southern Alps, New Zealand. In: *Geology 33*: 701-704.
- HARTMANN-BRENNER, D.C. (1973): Ein Beitrag zum Problem der Schutthaldenentwicklung an Beispielen des Schweizerischen Nationalparks und Spitzbergens. PhD theses, University of Zürich.
- HARVEY, A.M. (2001): Coupling between hillslopes and channels in upland fluvial systems: implications for landscape sensitivity, illustrated from the Howgill Fells, northwest England. In: *Catena 42*: 225-250.
- HARVEY, A.M. (2002): Effective timescales of coupling within fluvial systems. In: *Geomorphology 44*: 175-201.
- HECKMANN, T. & W. SCHWANGHART (2012): Geomorphic coupling and sediment connectivity in an alpine catchment - exploring sediment cascades using graph theory. In: *Geomorphology* (2012), doi: 10.1016/j.geomorph.2012.10.033.
- HECKMANN, T., THIEL, M., HAAS, F. & M. BECHT (2009): Towards a quantification of sedimentary connectivity in a Central Alpine catchment. In: *Geophysical Research Abstracts 11 EGU2009-9129*.
- HENGL, T. & H.I REUTER (2009): *Geomorphometry: Concepts, Software, Applications. Developments in Soil Science, vol. 33.* (Elsevier) Amsterdam.
- HINCHLIFFE, S. & C.K. BALLANTYNE (1999): Talus accumulation and rockwall retreat, Trotternish, Isle of Skye, Scotland. In: *Scottish Geographical Journal 115*: 53-70.
- HINCHLIFFE, S. & C.K. BALLANTYNE (2009): Talus structure and evolution on sandstone mountains in NW Scotland. In: *Holocene 19* (3): 477-486.
- HINDERER, M. (2012): From gullies to mountain belts: A review of sediment budgets at various scales. In: *Sedimentary Geology 280*: 21-59.
- HOFFMANN, T. (2006): Modelling the Holocene sediment budget of the Rhine system. PhD theses, University of Bonn.

- HOFFMANN, T. & L. SCHROTT (2002): Modelling sediment thickness and rockwall retreat in an Alpine valley using 2D-seismic refraction (Reintal, Bavarian Alps). In: *Zeitschrift für Geomorphologie, Suppl.-Bd. 127*: 153-173.
- HOFFMANN, T., MÜLLER, T., JOHNSON, E.A. & Y. MARTIN (submitted): Postglacial adjustment of steep, low-order drainage basins, Canadian Rocky Mountains: Field and numerical modeling investigations.
- HOOKE, J. (2003): Coarse sediment connectivity in river channel systems: a conceptual framework and methodology. In: *Geomorphology* 56: 79-94.
- HÖRSCH, B. (2002): Zusammenhang zwischen Vegetation und Relief in alpinen Einzugsgebieten des Wallis (Schweiz). Ein multiskaliger GIS- und Fernerkundungsansatz. PhD theses, University of Bonn.
- HUNGR, O. (2005): Classification and terminology. In: JAKOB, M. & O. HUNGR (eds.): *Debris-flow hazards and related phenomena*. (Springer) Berlin: 9-23.
- INNES, J.L. (1983): Debris flows. In: *Progress in Physical Geography* 7: 469-501.
- IPCC (2001a): Report: Climate change – The scientific basis. In: HOUGHTON, J.T., DING, Y., GRIGGS, D.J., NOGUER, M., VAN DER LINDEN, P.J., DAI, X., MASKEL, K. & C.A. JOHNSON (eds.). (Cambridge University Press) Cambridge, UK.
- IPCC (2001b): Report: Climate change-impacts, adaptations and vulnerability. In: MCCARTHY, J.J., CANZIANI, O.F., LEARY, N.A., DOKKEN, D.J. & K.S. WHITE (eds.). (Cambridge University Press) Cambridge, UK.
- ITURRIZAGA, L. (2011): Paraglacial landform transformation In: SINGH, V.P., SINGH, P. & U.K. HARITASHYA (eds.): *Encyclopedia of Snow, Ice and Glaciers*. (Springer) Netherlands: 817-824.
- IVERSON, R.M. (1997): The physics of debris flows. In: *Reviews of Geophysics* 35(3): 245-296.
- JÄCKLI, H. (1957): *Gegenwartsgeologie des bündnerischen Rheingebiets. Ein Beitrag zur exogenen Dynamik alpiner Gebirgslandschaften*. Geotechnische Serie, 36. (Kümmerle & Frey) Bern.
- JAIN, V. & S.K. TANDON (2010): Conceptual assessment of (dis)connectivity and its application to the Ganga River dispersal system. In: *Geomorphology* 118: 349-358.
- JOHNSON, R.M. & J. WARBURTON (2002): Annual sediment budget of a UK mountain torrent. In: *Geografiska Annaler - Series A: Physical Geography* 84: 73-88.
- JORDAN, P. & O. SLAYMAKER (1991): Holocene sediment production in Lillooet river basin, British Columbia: a sediment budget approach. In: *Géographie Physique et Quaternaire* 45(1): 45-57.

- KIRKBY, M.J. & I. STATHAM (1975): Surface stone movement and scree formation. In: *Journal of Geology* 833: 349-362.
- KNEISEL, C., LEMKUHLE, F., WINKLER, S., TRESSEL, E. & H. SCHRÖDER (1998): Legende für geomorphologische Kartierungen in Hochgebirgen (GMK Hochgebirge). In: *Trierer Geographische Studien* 18.
- KNEISEL, C., ROTHENBÜHLER, C., KELLER, F. & W. HAEBERLI (2007): Hazard Assessment of Potential Periglacial Debris Flows based on GIS-based Spatial Modelling and Geophysical Field Surveys: A Case Study in the Swiss Alps. In: *Permafrost and Periglacial Processes*: 18: 259-268.
- KRAUTBLATTER, M. & R. DIKAU (2007): Towards a uniform concept for the comparison and extrapolation of rockwall retreat and rockfall supply. In: *Geografiska Annaler* 89 A (1): 21-40.
- KRAUTBLATTER, M., MOSER, M., SCHROTT, L., WOLF J. & D. MORCHE (2012): Significance of rockfall magnitude and carbonate dissolution for rock slope erosion and geomorphic work on Alpine limestone cliffs (Reintal, German Alps). In: *Geomorphology* 167-168: 21-34.
- LABHART, T.P. (1992): *Geologie der Schweiz*. (Ott Verlag Thun) Switzerland.
- LUCKMAN, B.H. (1988): Debris Accumulation Patterns on Talus Slopes in Surprise Valley, Alberta. In: *Géographie physique et Quaternaire* 42 (3): 247-278.
- LUCKMAN, B.H. (2007): Talus slopes In: Elias, S.A. (ed.): *Encyclopedia of Quaternary Science*. Elsevier Science: 2242-2249.
- MACMILLAN, R.A. & P.A. SHARY (2009): Landforms and landform elements in geomorphometry. In: HENGL, T. & H. REUTER (eds): *Geomorphometry - Concepts, Software, Applications*. Developments in Soil Science, vol. 33. (Elsevier) Amsterdam: 227-254.
- MARSTON, R.A. & M.E. PEARSON (2004): Sediment budget. In: GOUDIE, A.S. (ed.): *Encyclopedia of Geomorphology*. (Routledge) London. 927-930.
- MATSUOKA, N. (2001): Solifluction rates, processes and landforms: a global review. In: *Earth-Science Reviews* 55: 107-134.
- MCCOLL, S.T. (2012): Paraglacial rock-slope stability. In: *Geomorphology* 153–154: 1–16.
- METEOSCHWEIZ (2009): Klimabericht Kanton Graubünden. Arbeitsberichte der MeteoSchweiz 228. - Available online: [www.gr.ch/DE/institutionen/verwaltung/ekud/anu/projekte/Dokumente\\_Luft/klima\\_gr\\_meteo.pdf](http://www.gr.ch/DE/institutionen/verwaltung/ekud/anu/projekte/Dokumente_Luft/klima_gr_meteo.pdf). (Last access: 12.09.12).

- METEOSCHWEIZ (2012): Standardnormwerte 1961-1990: Lufttemperatur 2m. Available online: [www.meteoschweiz.admin.ch/web/de/klima/klima\\_schweiz/tabellen.Par.0004.DownloadFile.ext.tmp/temperaturmittel.pdf](http://www.meteoschweiz.admin.ch/web/de/klima/klima_schweiz/tabellen.Par.0004.DownloadFile.ext.tmp/temperaturmittel.pdf). (Last access: 12.09.12).
- MILLIMAN, J.D. & R.H. MEADE (1983): World-wide delivery of river sediment to the oceans. In: *Journal of Geology* 91(1): 1-21.
- MILLIMAN, J.D. & P.M. SYVITSKI (1992): Geomorphic/Tectonic Control of Sediment Discharge to the Ocean: The Importance of Small Mountainous Rivers. In: *The Journal of Geology* 100(5): 525-544.
- MILNE, G. (1935): Some suggested units of classification and mapping particularly for East African soils. In: *Soil Research* 4: 183-198.
- MONTGOMERY, D. R. (2002): Valley formation by fluvial and glacial erosion. In: *Geology* 30: 1047-1050
- MONTGOMERY, D.R. & E. FOUFOULA-GEORGIU (1993): Channel network source representation using digital elevation models. In: *Water Resources Research* 29(12): 3925-3934.
- MONTGOMERY, D.R. & J.M. BUFFINGTON (1998): Channel processes, classification and response. In: NAIMAN, R. & R. BILBY (eds.): *River ecology and management*. (Springer) New York: 13-42.
- MOORE, I.D., GESSLER, P.E., NIELSEN, G.A. & G.A. PETERSON (1993): Soil attribute prediction using terrain analysis. In: *Soil Science Society of American Journal* 57: 443-452.
- MÜLLER, U. & M. KOLLMAIR (2004): Die Erweiterung des Schweizerischen Nationalparks. Der Planungsprozess 1995–2000, betrachtet aus partizipationstheoretischer Sicht. In: *Dokumente und Informationen zur Schweizerischen Orts-, Regional- und Landesplanung*, Jg. 40, Heft 4: 44-51.
- MUNRO-STASIUK, M. & D. SJOGREN (2006): The erosional origin of hummocky terrain, Alberta, Canada. In: KNIGHT, P.G. (ed.): *Glacial science and environmental change*. Blackwell Publishing Company.
- OTTO, J.C. (2006): Paraglacial sediment storage quantification in the Turtmann Valley, Swiss Alps. PhD theses, University of Bonn.
- OTTO, J.C. & L. SCHROTT (2010): Quantifizierung von rezenten und postglazialen Sedimentspeichern und Sedimentflüssen – Konzeptionelle Ansätze und aktuelle Studien aus den Ostalpen. In: *Salzburger Geographische Arbeiten* 46: 1-13.

- OTTO, J.C. & O. SASS (2006): Comparing geophysical methods for talus slope investigations in the Turtmann valley (Swiss Alps). In: *Geomorphology* 76(3-4): 257-272.
- OTTO, J.C. & R. DIKAU (2004): Geomorphologic system analysis of a high mountain valley in the Swiss Alps. In: *Zeitschrift für Geomorphologie, N.F.* 48(3): 323-341.
- OTTO, J.C., SCHROTT, L., JABOYEDOFF, M. & R. DIKAU (2009): Quantifying sediment storage in a high alpine valley (Turtmanntal, Switzerland). In: *Earth Surface Processes and Landforms* 34: 1726-1742.
- OWENS, P.N. & O. SLAYMAKER (1992): Late Holocene sediment yield in small alpine and subalpine drainage basins, British Columbia, Erosion, Debris Flows and Environments in Mountain Regions (Proceedings of the Chengdu Symposium, July 1992). IAHS publ.: 147-154.
- OWENS, P.N. & O. SLAYMAKER (2004): An introduction to mountain geomorphology. In: OWENS, P.N. & O. SLAYMAKER (eds.): *Mountain Geomorphology*. (Edward Arnold Publishers Limited) London: 3-33.
- OWENS, P.N. & O. SLAYMAKER (eds.) (2004): *Mountain Geomorphology*. (Edward Arnold Publishers Limited) London.
- PENNOCK, D.J., ZEBARTH, B.J. & E. DE JONG (1987): Landform classification and soil distribution in hummocky terrain, Saskatchewan, Canada. In: *Geoderma* 40: 297-315.
- PHILIPPS, J.D. (1992): Nonlinear dynamical systems in geomorphology: revolution or evolution? In: *Geomorphology* 5: 219-229.
- PHILIPPS, J.D. (2003): Sources of nonlinearity and complexity in geomorphic systems. In: *Progress in Physical Geography* 27(1): 1-23.
- RAPP, A. (1960a): Recent Development of mountain slopes in Kaerkevagge and surroundings, Northern Scandinavia. In: *Geografiska Annaler A* 42(2-3): 1-200.
- RAPP, A. (1960b): Talus slopes and mountain walls at tempelfjorden, Spitsbergen. A geomorphological study of the denudation of slopes in an arctic locality. (Distributed by the Oslo University Press) Oslo.
- RASEMANN, S. (2004): Geomorphometrische Struktur eines mesoskaligen alpinen Geosystems. *Bonner Geographische Abhandlungen*, Bd. 111. (Asgard-Verlag) Sankt Augustin.
- RASEMANN, S., SCHMIDT, J., SCHROTT, L. & R. DIKAU (2004): Geomorphometry in mountain terrain. In: BISHOP, M.P. & J. F. SHRODER (eds.): *Geographic Information Science in Mountain Geomorphology*. (Springer) Heidelberg: 101-145.

- REID, L. & T. DUNNE (eds.) (1996): Rapid evaluation of sediment budgets. GeoEcology paperback. (Catena Verlag, GeoScience Publisher) Reiskirchen.
- RICKENMANN, D. (1995) Beurteilung von Murgängen. In: Schweiz. Ingenieur und Architekt 113 (48): 1104-1108.
- RICKENMANN, D. (2001): Murgänge in den Alpen und Methoden zur Gefahrenbeurteilung. Proceedings of the 31st Internationales Wasserbau-Symposium (IWASA), Aachen.
- ROESCH, H. (1937): Geologische Skizze des Schweizerischen Nationalparkes. Sonderabzug aus St. Brunies, der Schweizerische Nationalpark. 4. Auflage. (Benno Schwabe & Co Verlag) Basel.
- RUHE, R.V. & P.H. WALKER (1968): Hillslope models and soil formation : open systems. In: Proceedings of 9th Congress of the International Soil Science Society, vol. 4. International Soil Science Society, Adelaide, Australia: 551-560.
- RYDER, J.M. (1971): The stratigraphy and morphology of paraglacial alluvial fans in south central British Columbia. In: Canadian Journal of Earth Sciences 8: 279-298.
- SASS, O. (2005): Spatial patterns of rockfall intensity in the northern Alps. In: Zeitschrift für Geomorphologie NF. Suppl.-Bd. 138: 51-65.
- SASS, O. & K. WOLLNY (2001): Investigations regarding alpine talus slopes using ground penetration radar (GPR) in the Bavarian Alps, Germany. In: Earth Surface Processes and Landforms 26: 1071-1086.
- SASS, O. & M. KRAUTBLATTER (2007): A nonlinear model coupling rockfall and rainfall intensity based on a four year measurement in a high Alpine rock wall (Reintal, German Alps). In: Geomorphology 86: 176-192.
- SASS, O., KRAUTBLATTER, M. & H. VILES (submitted): Short and long term measurements of rockwall retreat over the Holocene in Nant Ffrancon, Snowdonia, Wales. In: Earth Surface Process and Landform.
- SCHLUNEGGER, F., BADOUX, A., MCARDELL, B.W., GWERDER, C., SCHNYDRIG, D., RIEKE-ZAPP, D., & P. MOLNAR (2009): Limits of sediment transfer in an alpine debris-flow catchment, Illgraben, Switzerland. In: Quaternary Science Reviews 28 (11-12): 1097-1105.
- SCHMIDT, J. & R. DIKAU (1999): Extracting geomorphometric attributes and objects from digital elevation models - Semantics, methods, future needs. In: DIKAU, R. & H. SAURER (eds.): GIS for Earth Surface Systems: 153-174.

- SCHROTT L., GÖTZ J., GEILHAUSEN M. & D. MORCHE (2006): Spatial and temporal variability of sediment transfer and storage in an Alpine basin (Bavarian Alps, Germany). In: *Geographica Helvetica* 3: 191-201.
- SCHROTT L., HUFSCHEMIDT G., HANKAMMER M., HOFFMANN T. & R. DIKAU (2003): Spatial distribution of sediment storage types and quantification of valley fill deposits in an alpine basin, Reintal, Bavarian Alps, Germany. In: *Geomorphology* 55: 45-63.
- SCHROTT, L. & T. ADAMS (2002): Quantifying sediment storage and Holocene denudation in an Alpine basin, Dolomites, Italy. In: *Zeitschrift für Geomorphologie N.F. Suppl.-Bd.* 128: 129-145.
- SCHROTT, L., NIEDERHEIDE, A., HANKAMMER, M., HUFSCHEMIDT, G. & R. DIKAU (2002): Sediment storage in a mountain catchment: geomorphic coupling and temporal variability (Reintal, Bavarian Alps, Germany). In: *Zeitschrift für Geomorphologie* 127: 175-196.
- SCHUMM, S.A. (1979): Geomorphic thresholds: the concept and its applications. In: *Transactions of the Institute of British Geographers* 4: 485-515.
- SCHUMM, S.A. (1998): *To Interpret the Earth: Ten ways to be wrong.* (Cambridge University Press) Cambridge.
- SCHWAB, M., RIEKE-ZAPP, D., SCHNEIDER, H., LINIGER, M. & F. SCHLUNEGGER (2008): Landsliding and sediment flux in the Central Swiss Alps: A photogrammetric study of the Schimbrig landslide, Entlebuch. In: *Geomorphology* 97: 392-406
- SELBY, M.J. (1993): *Hillslope Materials and Processes.* (Oxford University Press) Oxford.
- SHAKESBY, R.A. (1997): Pronival (protalus) ramparts: a review of forms, processes, diagnostic criteria and palaeoenvironmental implications. In: *Progress in Physical Geography* 21: 394-418.
- SHAKESBY, R.A., MATTHEWS, J.A. & D. MCCARROLL (1995): Pronival ('protalus') ramparts in the Romsdalsalpane, southern Norway: forms, terms, subnival processes, and alternative mechanisms of formation. In: *Arctic and Alpine Research* 27: 271-282.
- SHRODER, J.F & M.P. BISHOP (2004): Mountain geomorphic systems. In: BISHOP, M.P. & J. F. SHRODER (eds.): *Geographic Information Science in Mountain Geomorphology.* (Springer) Heidelberg: 34-73.
- SLAYMAKER, O. (1988): The distinctive attributes of debris torrents. In: *Hydrological Sciences Journal* 33 (6): 567-573.
- SLAYMAKER, O. (1991): Mountain geomorphology: a theoretical framework for measurement programs. In: *Catena* 18: 427-437.

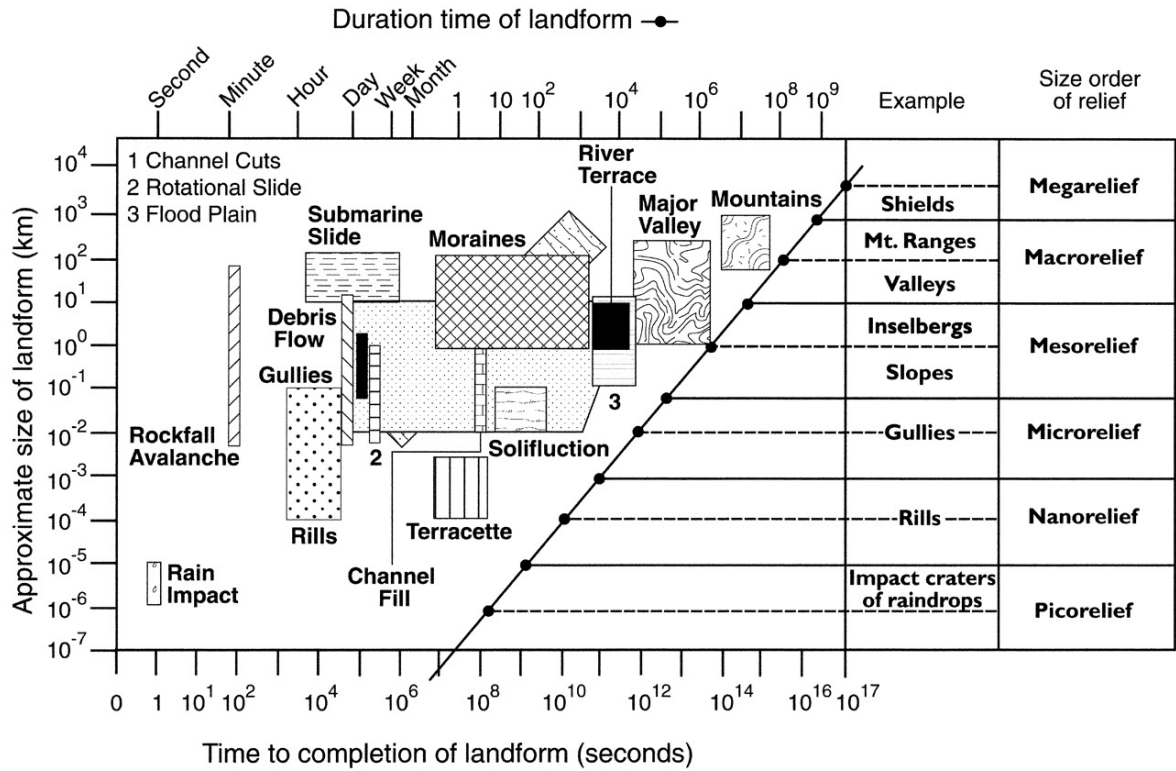
- SLAYMAKER, O. (1993): Cold mountains of Western Canada. In: FRENCH, H.M. & O. SLAYMAKER (1993): Canada's cold environments. (McGill Queen's University Press) Montréal.
- SLAYMAKER, O. (2003): The sediment budget as conceptual framework and management tool. In: *Hydrobiologia* 494: 71-82.
- SMITH, M.J., PARON, P. & J.S. GRIFFITHS (2011): *Geomorphological Mapping: Methods and Applications*. (Elsevier) Amsterdam.
- SOUGNEZ, N., VAN WESEMAEL, B., & V. VANACKER (2011): Low erosion rates measured for steep, sparsely vegetated catchments in southeast Spain. In: *Catena* 84: 1-11.
- SPEIGHT, J. G. (1974): A parametric approach to landform regions. In: *Progress in Geomorphology*, Institute of the British Geographers Special Publication 7: 213-230.
- SPEIGHT, J.G. (1990): Landform. In: McDONALD, R.C., ISBELL, R.F., SPEIGHT, J.G., WALKER, J. & M.S. HOP (eds.): *Australian Soil and Land Survey Field Handbook*. (Inkata Press) Melbourne: 9-57.
- STÄBLEIN, G. (1980): Die Konzeption der Geomorphologischen Karten GMK 25 und GMK 100 im DFG-Schwerpunktprogramm. In: *Berliner Geographische Abhandlung* 31: 13-30.
- STÄHLI, M. FINSINGER, W. TINNER, W. & B. ALLGÖWER (2006): Wildfire history and fire ecology of the Swiss National Park (Central Alps): new evidence from charcoal, pollen and plant macrofossils. In: *The Holocene* 16: 805-817.
- STINY, J. (1910): *Die Mure*. University of Innsbruck, Innsbruck.
- STOCK, J. & W.E. DIETRICH (2003): Valley incision by debris flows: Evidence of a topographic signature. In: *Water Resources Research* 39 (4): 1089 ff.
- STOCK, J.D. & W.E. DIETRICH (2006): Erosion of steepland valleys by debris flows. In: *Geological Society of America Bulletin* 118: 1125-1148.
- STOLZ, A. & C. HUGGLE (2008): Debris flows in the Swiss National Park: the influence of different flow models and varying DEM grid size on modeling results. In: *Landslides* 5: 311-319.
- STOTT, T.A. & N.J. MOUNT (2007): Alpine proglacial suspended sediment dynamics in warm and cool ablation seasons: implications for global warming? In: *Journal of Hydrology* 332: 259-270.
- STRATHAM, I. (1976): A scree slope rockfall model. In: *Earth Surface Processes* 1: 43-62.
- STRAUMANN, R.K. & O. KORUP (2009): Quantifying postglacial sediment storage at the mountain-belt scale. In: *Geology* 37: 1079-1082.

- TAKAHASHI, T. (1981): Debris flow. In: *Annual Reviews of Fluid Mechanics* 13: 57-77.
- TAKAHASHI, T. (2007): *Debris flow: Mechanics, prediction and countermeasures*. (Taylor & Francis) London.
- TGETGEL, H. (1981<sup>8</sup>): *Unterengadin. Samnau - Nationalpark - Val Müstair*. Schweizer Wanderbuch 4. (Kümmerly + Frey, Geographischer Verlag) Bern.
- THELER, D., REYNARD, E., LAMBIEL, C. & E. BARDOU (2010): The contribution of geomorphological mapping to sediment transfer evaluation in small alpine catchments. In: *Geomorphology* 124: 113-123.
- THIEL-EGENTER, C., RISCH, A.C., JURGENSEN, M.F., PAGE-DUMROESE, D.S., KRÜSO, B.O. & M. SCHÜTZ (2007): Response of a subalpine grassland to simulated grazing: aboveground productivity along soil phosphorus gradients. In: *Community ecology* 8 (1): 111-117.
- THIEL, M., HECKMANN, T., HAAS, F. & M. BECHT (2011): Quantification of coarse sediment connectivity in alpine geosystems. In: *Geophysical Research Abstracts* Vol. 13, EGU2011-10449.
- TROLL, C. (1966): Über das Wesen der Hochgebirgsnatur. In: TROLL, C. (ed.): *Ökologische Landschaftsforschung und vergleichende Hochgebirgsforschung*. Erdkundliches Wissen. (Franz Steiner Verlag) Stuttgart: 127-151.
- TROLL, C. (1973): High Mountain Belts between the Polar Caps and the Equator: Their Definition and Lower Limit. In: *Arctic and Alpine Research* 5: 19-28.
- TRÜMPY, B., SCHMID, S.M., CONTI P. & N. FROITZHEIM (1997): *Erläuterungen zur Geologischen Karte 1: 50 000 des Schweizerischen Nationalparks*. (Geologische Spezialkarte Nr.122) Zernezh.
- TWIDALE, C.R. (1985): Ancient landscapes. Their nature and significance for the question of inheritance. In: HAYDEN, R.S. (ed.): *Global. Mega-Geomorphology*. 29-40.
- USHER, M.B. (2001): Landscape sensitivity: from theory to practice. In: *Catena* 42: 375-383.
- VAN ASSELEN, S. & A.C. SEIJMONSBERGEN (2006): Expert-driven semi-automated geomorphological mapping for a mountainous area using a laser DTM. In: *Geomorphology* 78: 309-320.
- VENTURA, S.J. & B.J. IRVIN (2000): Automated landform classification methods for soil-landscape studies. In: WILSON, J.P. & J.C. GALLANT (eds.): *Terrain Analysis: Principles and Applications*. (Wiley and Sons) New York: 267-294.

- VERLEYSDONK, S., KRAUTBLATTER, M. & R. DIKAU (2011): Sensitivity and path dependence of mountain permafrost systems In: *Geografiska Annaler: Series A, Physical Geography*: 113-135.
- WAINWRIGHT, J., TURNBULL, L., IBRAHIM, T.G., LEXARTZA-ARTZA, I., THORNTON, S. & R.E. BRAZIER (2011): Linking environmental régimes, space and time: Interpretations of structural and functional connectivity. In: *Geomorphology* 126(3-4): 387-404.
- WALLING, D. E. (1983): The sediment delivery problem. In: *Journal of Hydrology* 65: 209–237.
- WASHBURN, A.L. (1979): *Geocryology: A Survey of Periglacial Processes and Environments*. (Arnold) London.
- WHALLEY, W.B. (1984): Rockfalls. In: BRUNSDEN, D. & D.B. PRIOR (eds.): *Slope Instability*. (Wiley and Sons) London: 217-256.
- WICHMANN, V., HECKMANN, T., HAAS, F. & M. BECHT (2009): A new modelling approach to delineate the spatial extent of alpine sediment cascades. In: *Geomorphology* 111: 70-78.
- WIECZOREK, G. F., & T. GLADE (2005): Climatic factors influencing occurrence of debris flows. In: JAKOB M. & HUNGR O. (eds.): *Debris-flow Hazards and Related Phenomena*. (Springer) Berlin, Heidelberg: 325-362.
- WILSON, P. (2009): Rockfall talus slopes and associated talus-foot features on the glaciated upland of Great Britain and Ireland: periglacial, paraglacial or composite landforms? In: KNIGHT, J. & S. HARRISON (eds): *Periglacial and paraglacial processes and environments*. Geological Society Special Publications 320: 133-144.
- WOLMAN, M.G. & J.P. MILLER (1960): Magnitude and frequency of forces in geomorphic processes. In: *Journal of Geology* 68: 54-74.
- ZIMMERMANN, M. (1990): Debris flows 1987 in Switzerland: geomorphological and meteorological aspects. *Hydrology in Mountainous Regions*. In: IAHS Publ. no. 194: 3387-3393.

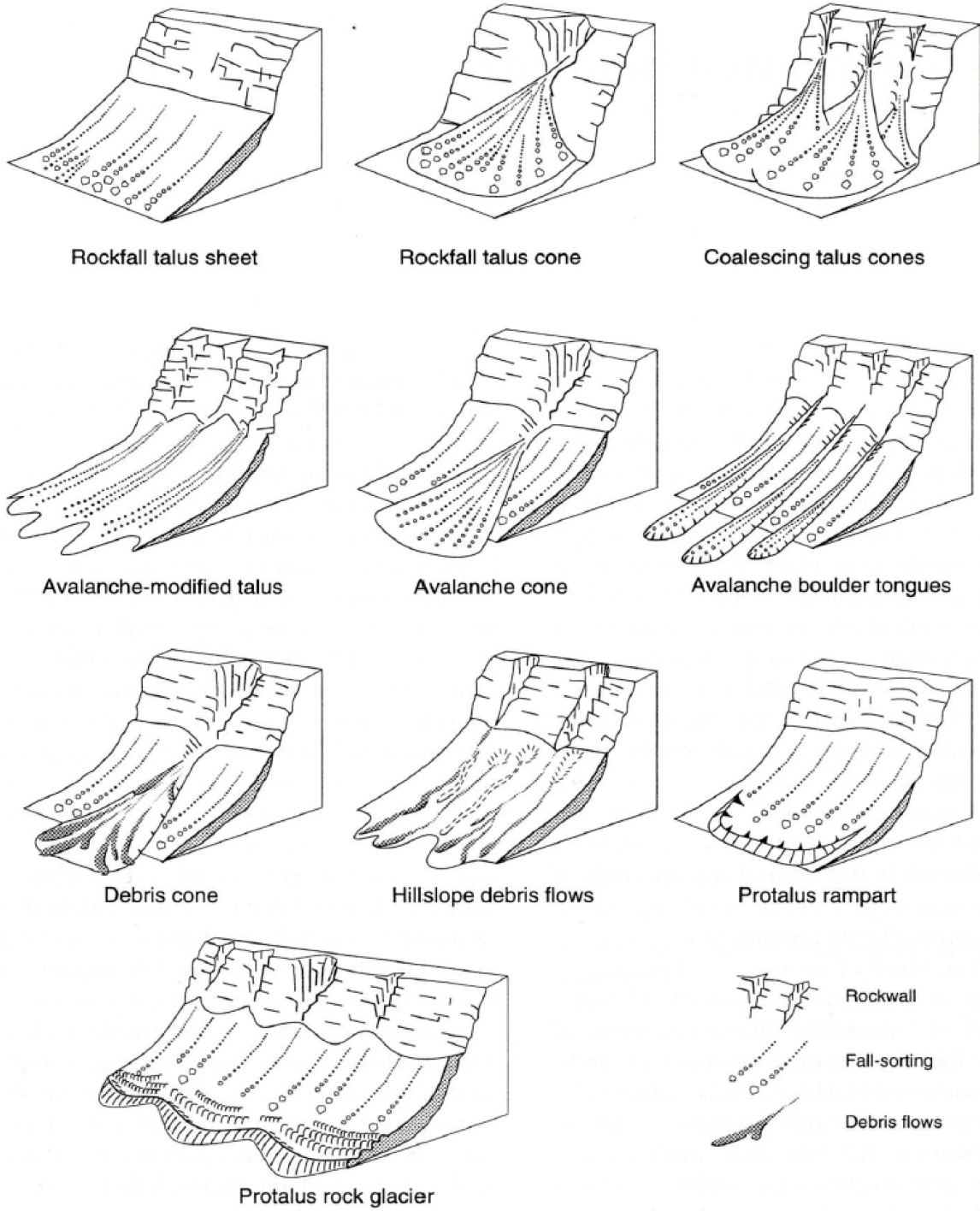
## **10 APPENDIX**

**A Sediment storages in alpine environments**



Spatial and temporal scales in geomorphic systems. Alpine environments are characterised by a pronounced temporal and spatial landform hierarchy, expressed in landform size as well as duration of formation/erosion (persistence).

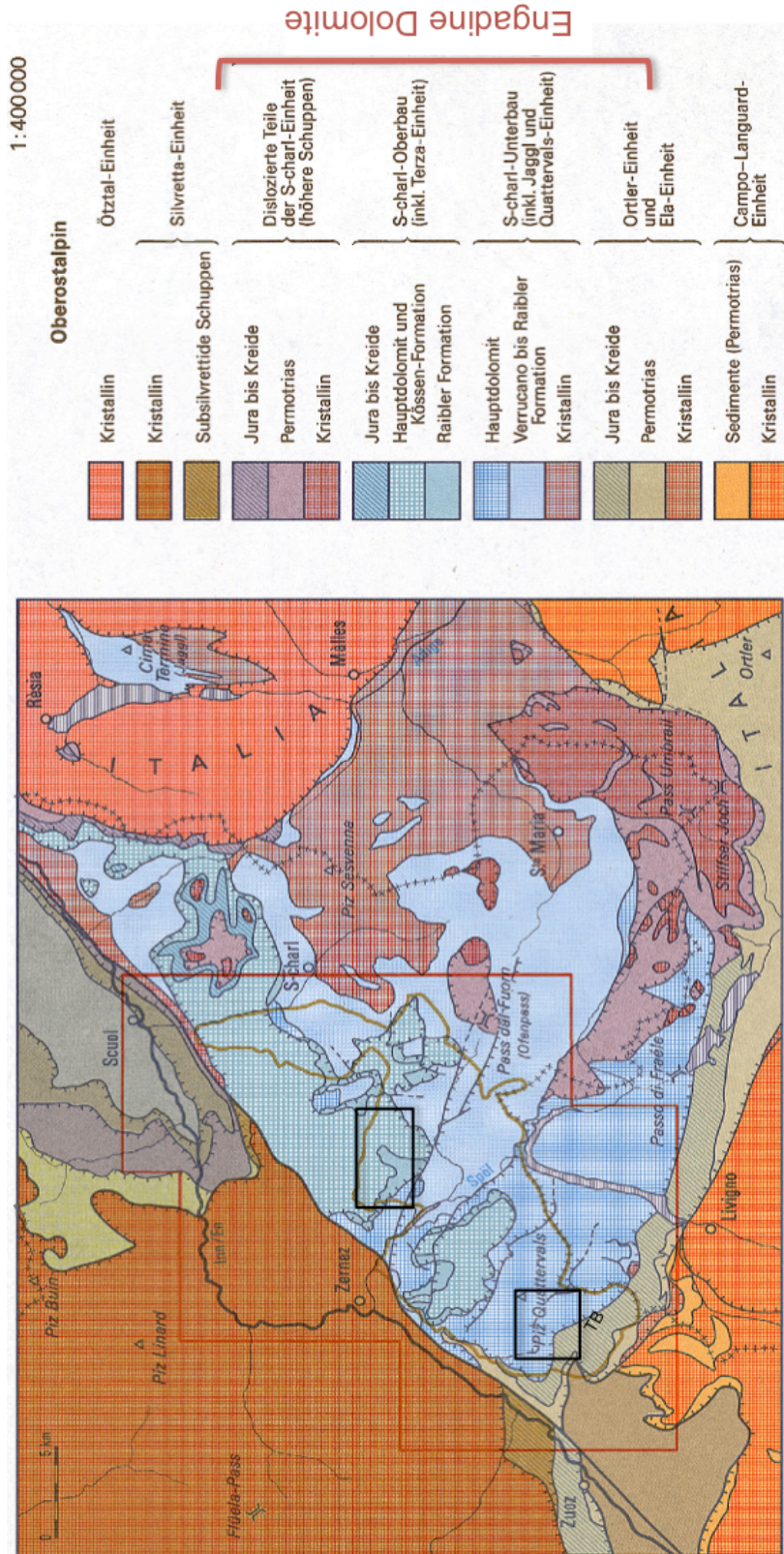
Source: BRUNSDEN 1996: 285.



Different types of talus slope in alpine environments.

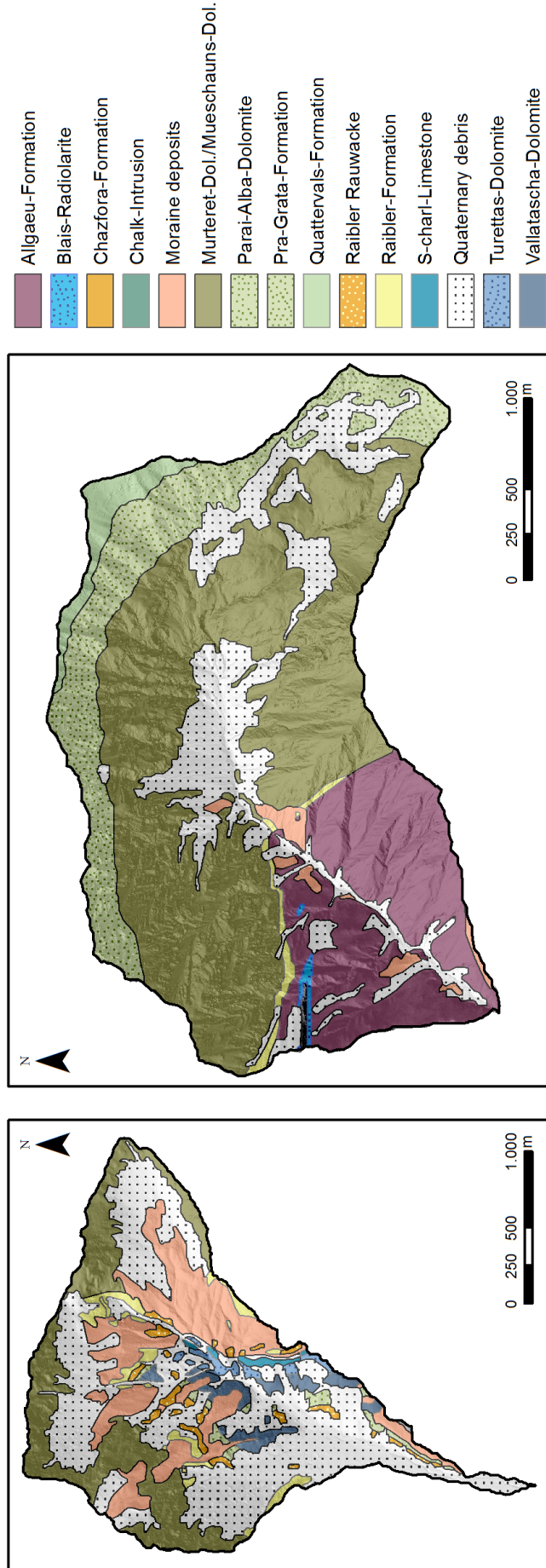
Source: BALLANTYNE & HARRIS 1994: 220.

**B Tectonic-geological setting of the study areas**



Geological and tectonic setting the Upper Engadine Region.

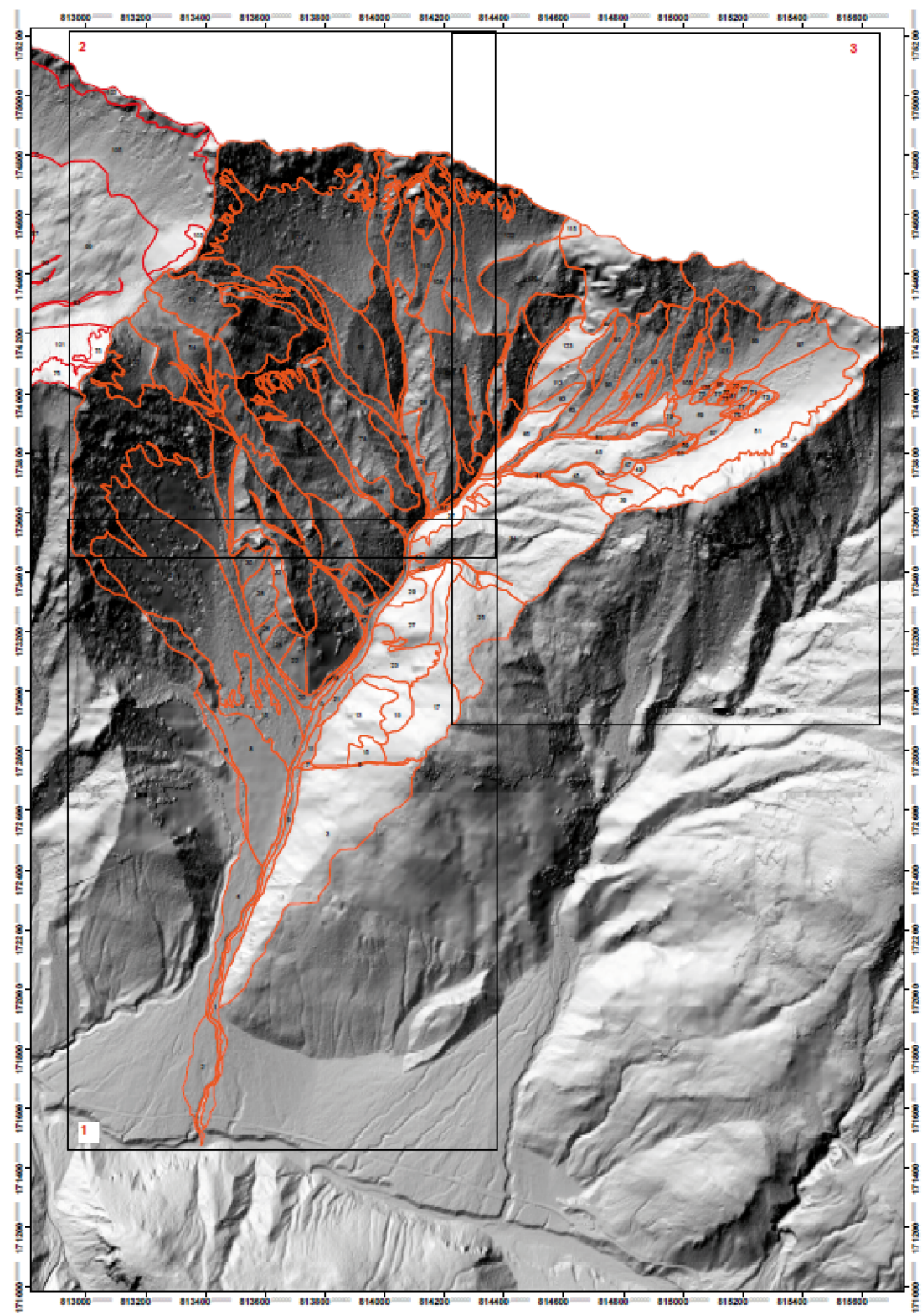
Source: Geologische Spezialkarte Nr. 122, © Schweizerische Geologische Kommission



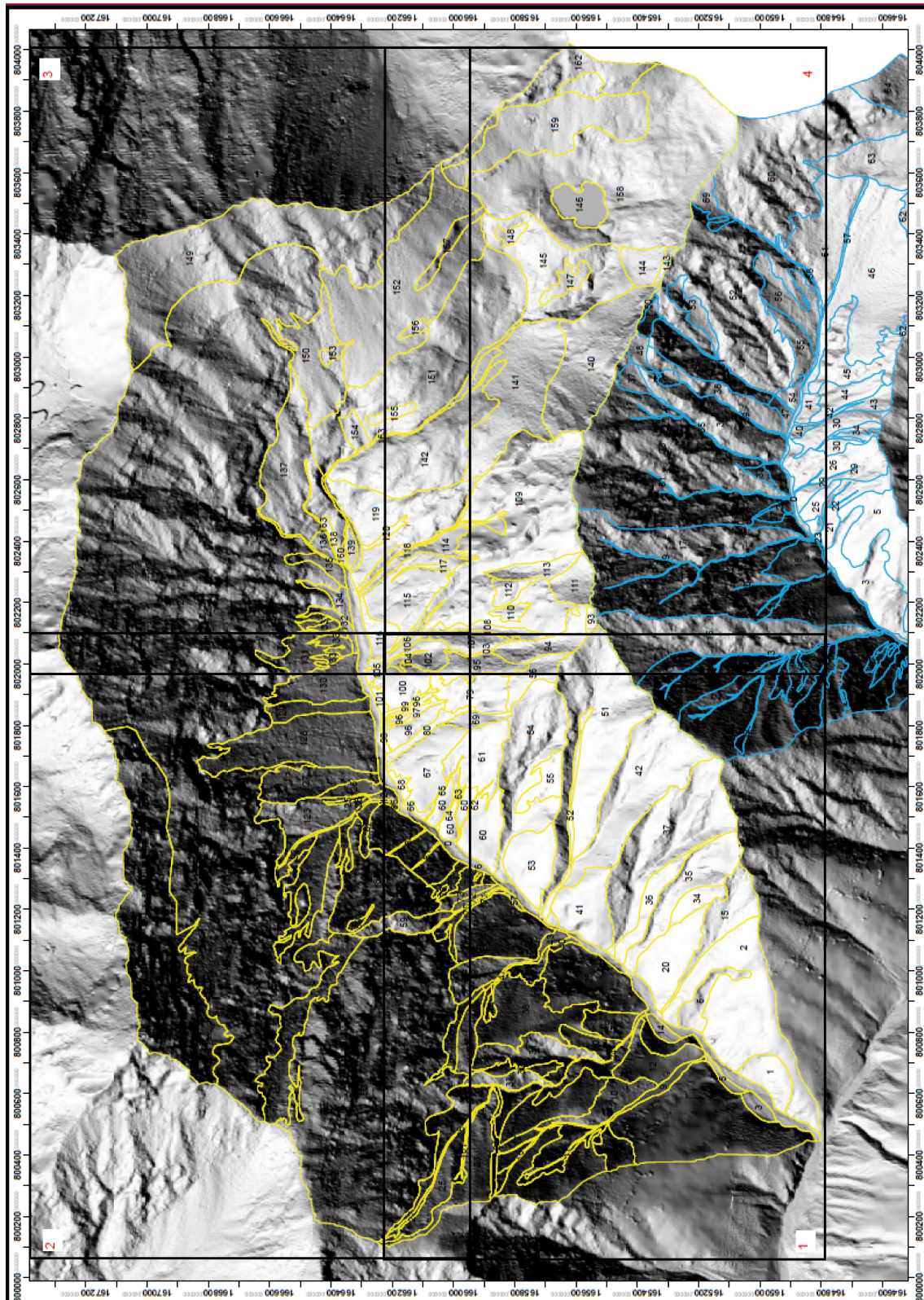
Geological and tectonic setting of Val dal Botsch (a) and Val Mütschans (b).  
 Own graphic illustration based on the GIS vector layers © 2012. Swisstopo.

## C Methods for analysing alpine sediment cascades

*Map sheets of Val dal Botsch. In total, three sheets (DIN A3), showing the air photos and the shaded relief on a scale of 1:5000, were used for the mapping during fieldwork.*



*Map sheets of Val Müschauns. In total, four sheets (DIN A3), showing the air photos and the shaded relief on a scale of 1:5000, were used for the mapping during fieldwork.*



## *Mapping Catalogue*

### Field work protocol – geomorphological mapping

sheet#: \_\_\_\_\_

Date and time: \_\_\_\_\_ Current weather: \_\_\_\_\_

Valley: \_\_\_\_\_

ID #: \_\_\_\_\_ Recorder: \_\_\_\_\_

#### Material

grain size:  boulder (> 630 mm)  gravel (630-63)  pebble (63-2)  sand/silt/clay (>2mm) (Kneisel et al. 1998)rounding:  angular  subangular  subrounded  rounded  well rounded (after Kondolf & Piegay 2003) homogeneous  heterogeneous

comments (e.g layering, orientation): \_\_\_\_\_

#### Geomorphic processes

Process domain:  gravitational  fluvial  cryogenic  slope erosion (overland flow)  glacial/nival other: \_\_\_\_\_

process types: formative: \_\_\_\_\_

remobilizing/modifying: \_\_\_\_\_

#### Surface features

Superimposed microforms: \_\_\_\_\_

#### Vegetation cover

Degree of vegetation cover (estimated): \_\_\_\_\_ classes:  I (< 30 %)  II (30-70 %)  III (> 70 %)Vegetation type:  meadow/grass  bushes  forest

Visible damages of vegetation through recent processes: \_\_\_\_\_

#### Sediment storage type

\_\_\_\_\_

#### Sketch

## *Modelling of connectivity index*

### **Input data/Preparation of Input Data**

1. 2m-DEMs of the study areas → “DTM”
2. Weighting factor W as raster grid → “weighted”
3. Mask for stream channel
  - conversion of stream-channel-polygon to a raster with 0-values (stream channel) and 1-values (other areas) → “mask”
4. Slope without null values
  - calculation of slope grid in degree by using the spatial analyst toolbar → “slope1”
  - calculation of slope without null values by using the Raster calculator:  
 $((\text{“slope1”} == 0) * 0.005) + \text{“slope1”}$  → “slope”

### **Hydrological Calculations**

5. Flow direction with mask
  - calculation of flow direction based on the DTM by using the hydrological toolset:  $\text{FlowDirection}(\text{“DTM”})$  → “flowdir\_1”
  - Calculation of new flow direction with mask by using the times operator in math-toolbox:  $\text{“flowdir_1”} * \text{“mask”}$  → “flowdir”
6. Flow accumulation
  - calculation of flow accumulation based on the masked flow direction by using the hydrological toolset:  $\text{FlowAccumulation}(\text{“flowdir”})$  → “flowacc”
  - extraction of channels  $\leq 5000$  (dal Botsch) and  $\leq 25\,000$  (Müschauns) by using the raster calculator:  $\text{“flowacc”} \leq 5000$  → “channels”
  - Linking extracted channels with flow direction by using the times operator in math-toolbox:  $\text{“channels”} * \text{“flowdir”}$  → “direction”
  - Calculation of final flow accumulation based on new direction grid and elimination of values  $< 1$  by using raster calculator:  $\text{FlowAccumulation}(\text{“direction”}) + 1$  → “flowacc\_final”

**Computation of  $D_{dn}$  component of connectivity**

7. Inverse weighting factor invCS
  - creation of inverse weighting factor as reciprocal of the product of W and S by using the raster calculator:  $1/(\text{"weighted"}*\text{"slope"}) \rightarrow \text{"invCS"}$
8. Weighted downslope flowlength
  - calculation of the weighted downslope flowlength by using the raster calculator:  $\text{flowlength}(\text{"direction"}, \text{"invCS"}, \text{downstream}) \rightarrow \text{"flowlength"}$
9. Downslope component  $D_{dn}$  of connectivity
  - calculation of the downslope component  $D_{dn}$  by using the raster calculator:  $((\text{"flowlength"} == 0) * \text{"invCS"}) + \text{"flowlength"} \rightarrow \text{"con\_down"}$

**Computation of  $D_{up}$  component of connectivity**

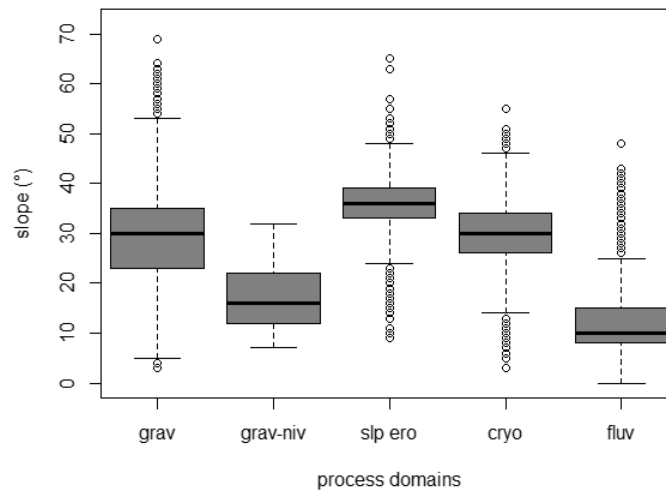
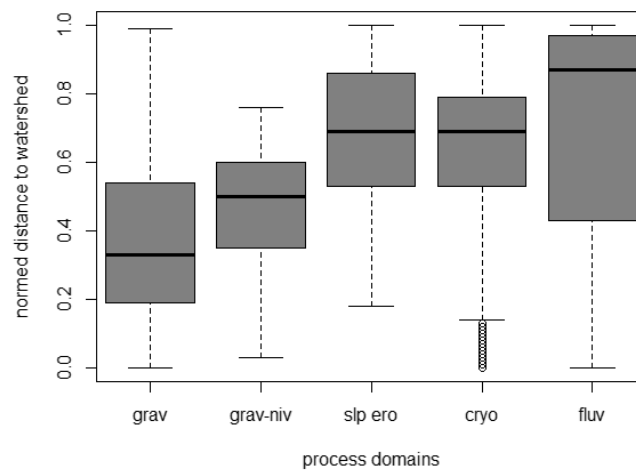
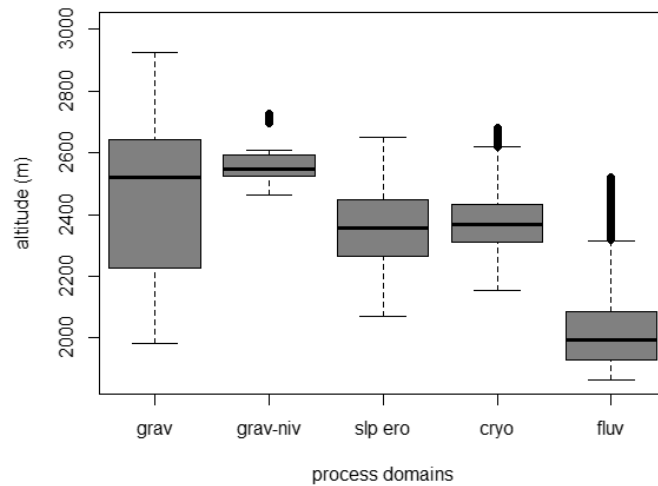
10. Average weighted factor W
  - calculation of mean weighted factor by using the raster calculation  $(\text{FlowAccumulation}(\text{"direction"}, \text{"weighted"}) + \text{"weighted"}) / \text{flowacc\_final} \rightarrow \text{"w\_mean"}$
11. Average slope factor S
  - Calculation of mean slope factor by using the raster calculation  $(\text{Flowaccumulation}(\text{"direction"}, \text{"slope"}) + \text{"slope"}) / \text{flowacc\_final} \rightarrow \text{"s\_mean"}$
12. Upslope component  $D_{up}$  of connectivity
  - calculation of the upslope component  $D_{up}$  by using the raster calculation:  $\text{"w\_mean"} + \text{"s\_mean"} * \text{SquareRoot}(\text{"flowacc\_final"} * [\text{cell size} * \text{cell size}]) \rightarrow \text{"con-up"}$

**Computation of connectivity index**

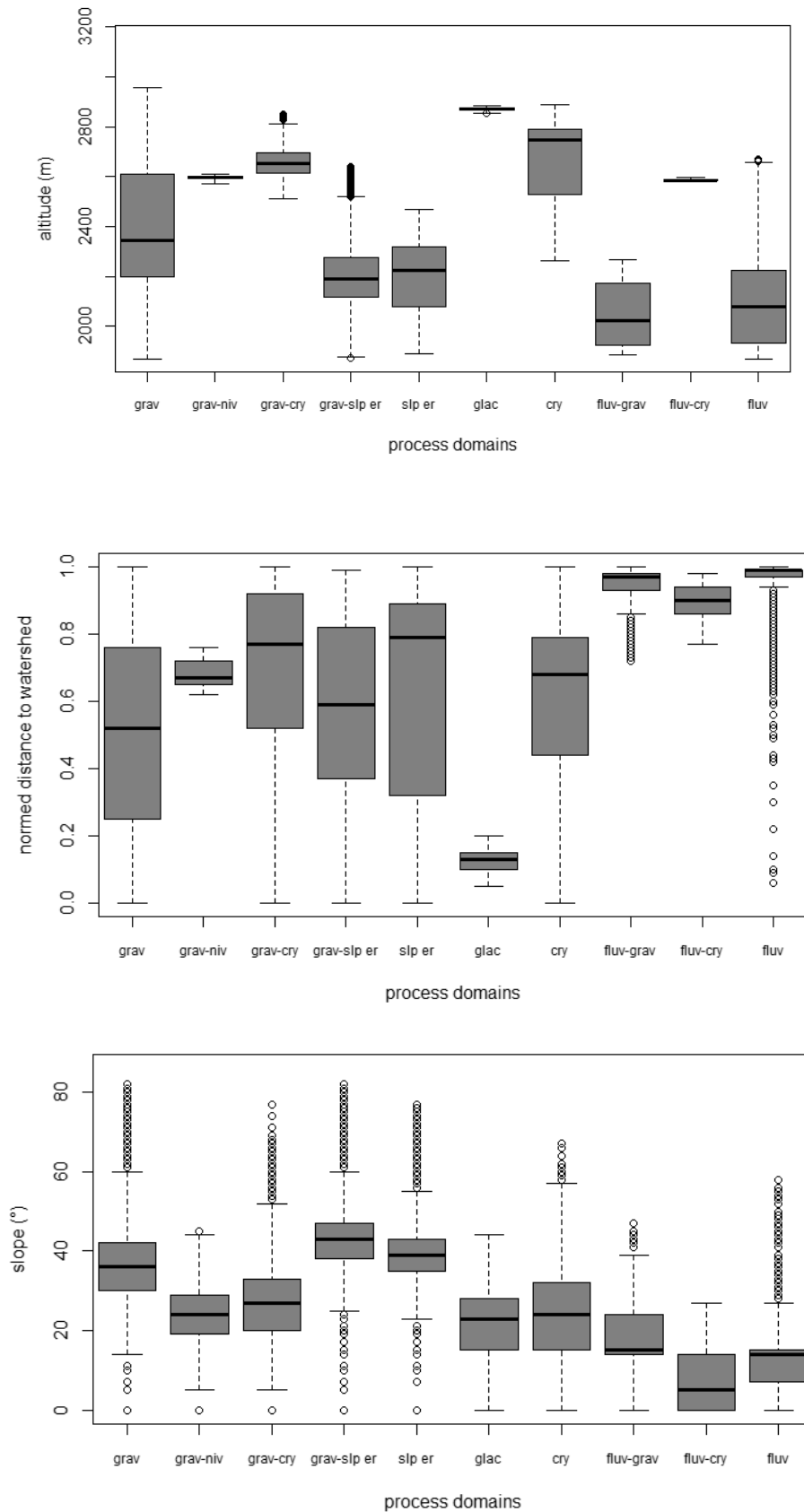
13. Calculation of connectivity index based on logarithm of the quotient of the upslope and downslope component by using the raster calculator:  $\text{Log10}(\text{"con\_up"} / \text{"con\_down"}) \rightarrow \text{"connectivity"}$

## D Morphometric characterisation of process domains

*Morphometric characterisation of process domains in Val dal Botsch with regard to variations in altitude (m), normed distance to watershed (1=stream. 0=valley ridge) and slope gradient of relief.*



*Morphometric characterisation of process domains in Val Mütschans with regard to variations in altitude (m), normed distance to watershed (1=stream. 0=valley ridge) and slope gradient of relief.*



---

***Characterisation of process domains:***

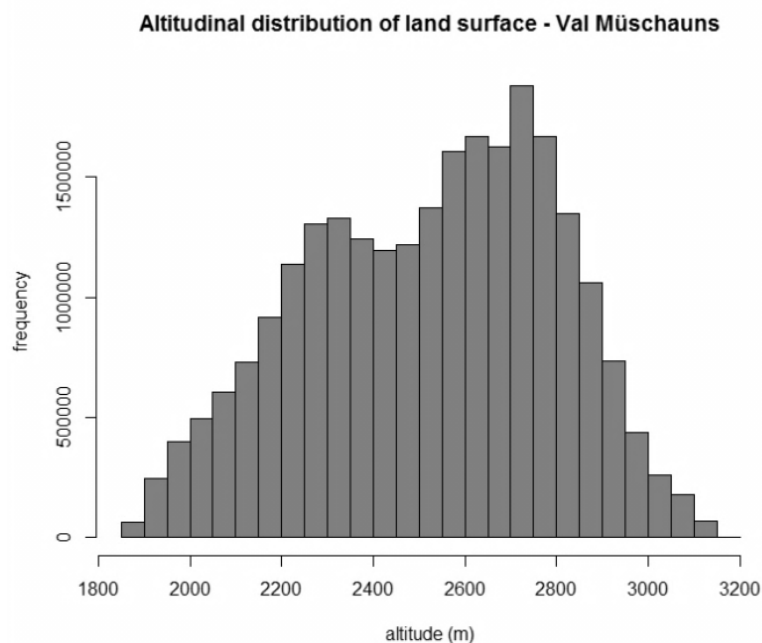
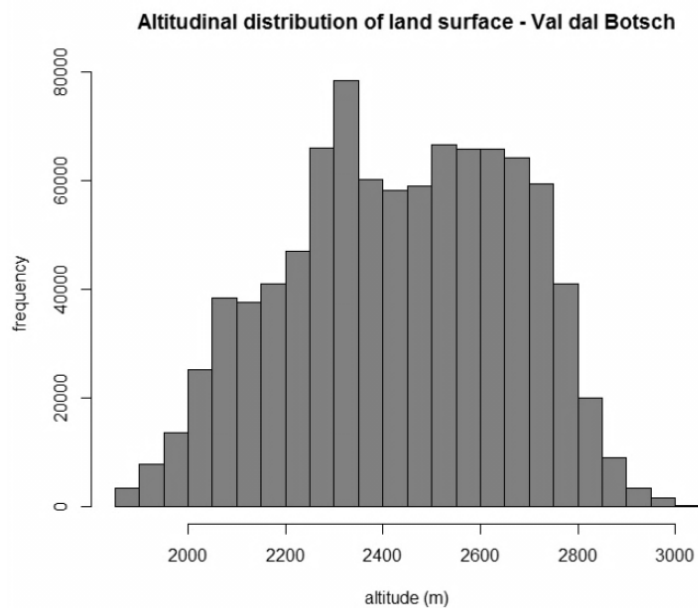
In Val dal Botsch and Val Müschauns, altitudes between 2600 m and 2200 m a.s.l. are largely dominated by gravitational(-nival) processes as well as slope erosion through overland flow both. Concerning the cryogenic process domain, interesting differences are visible. While in Val dal Botsch, the cryogenic domain mainly occurs at altitudes between 2300-2500 m a.s.l., in Val Müschauns, those processes are primary active above 2600 m a.s.l. within the upper valley. The highest occurring processes in Müschauns are glacial processes related to the single block glacier within the cirque. In contrast, the lower altitudes and hence, the lower basins, of both study areas are exclusively dominated by fluvial processes.

These altitudinal variations immediately become reflected in the normed distance from the watershed. In both alpine valleys, geomorphic processes of fluvial origin primary occur within the valley bottom, while the gravitational and glacial process domains evidently dominate the upper slopes below the valley ridge. The middle slopes are equally characterised by slope erosional, cryogenic and nival processes.

Finally, each process domain appears to be related to a specific slope or a specific kind of relief. In both valleys, the steepest inclinations (35-45°) are related to the (gravitational-)slope erosional domain, indicating the oversteepening of slopes through of debris flows. Gravitational processes primary occur along gradients of 32-42°, therefore mainly below the steep bedrock cliffs or within steps incised channels. In contrast, gravitational-nival processes by rampart formation and glacial activity by the rock glacier are related to a relative flat relief of around 20°. Interestingly, the cryogenic processes occur in Val dal Botsch along much steeper slopes (ca. 30°) than in Val Müschauns (ca. 24°). This could explain the different formation of garlands and solifluction stripes. Finally, fluvial processes within the valley bottom are related to the lowest slopes of less than 15°.

***Altitudinal distribution of land surface of the study areas***

The altitudinal distribution of the land surface of both alpine valleys is quite interesting and one of the major controls on the behaviour of the alpine sediment cascades. The majority of the basin of Val dal Botsch is located within the middle altitudinal ranges between 2250 and 2750 m a.s.l., with a significant peak at 2300 m. In contrast, the majority of Val Müschauns' area seems to be concentrated much higher at altitudes between 2650 and 2850 m. a.s.l.



## E Spatial distribution and morphometric characteristics of landforms

### *Number and area of storage landforms in Val dal Botsch*

| Nr           | Landform type           | Number of objects | Proportion of land surface (%) | Total area (m <sup>2</sup> ) | Min. area (m <sup>2</sup> ) | Max. area (m <sup>2</sup> ) | Mean area (m <sup>2</sup> ) |
|--------------|-------------------------|-------------------|--------------------------------|------------------------------|-----------------------------|-----------------------------|-----------------------------|
| 1            | Alluvium                | 8                 | 3.83                           | 142542                       | 1541                        | 46995                       | 17818                       |
| 2            | Colluvium               | 9                 | 9.09                           | 337771                       | 2898                        | 159144                      | 37530                       |
| 3            | Moraine deposit         | 37                | 26.47                          | 984261                       | 968                         | 75236                       | 26602                       |
| 4            | Debris cone             | 3                 | 0.79                           | 29540                        | 1225                        | 19374                       | 9847                        |
| 5            | Debris flow channel     | 6                 | 0.69                           | 25541                        | 490                         | 9730                        | 4257                        |
| 6            | Protalus rampart        | 6                 | 0.48                           | 17857                        | 1561                        | 4519                        | 2976                        |
| 7            | Talus slope             | 20                | 14.03                          | 521599                       | 3504                        | 97728                       | 26080                       |
| 8            | Talus slope/debris cone | 6                 | 12.07                          | 448775                       | 14651                       | 228049                      | 76465                       |
| 9            | Hillslope debris flows  | 17                | 9.45                           | 351180                       | 4505                        | 81125                       | 20657                       |
| 10           | Bedrock                 | 19                | 21.69                          | 806551                       | 1213                        | 169172                      | 42450                       |
| 11           | unspecified             | 6                 | 1.40                           | 52181                        | 4432                        | 15436                       | 8697                        |
| <b>Total</b> |                         | <b>137</b>        |                                | <b>3717798</b>               |                             |                             |                             |

### *Altitude and aspect of storage landforms in Val dal Botsch*

| Nr | Landform type          | Min. altitude (m) | Max. altitude (m) | Mean altitude (m) | Std Dev. | Median (altitude) | Mean aspect (°) | Mean aspect |
|----|------------------------|-------------------|-------------------|-------------------|----------|-------------------|-----------------|-------------|
| 1  | Alluvium               | 1866              | 2522              | 2037              | 141.48   | 1993              | 194             | SSW         |
| 2  | Colluvium              | 1933              | 2306              | 2132              | 76.01    | 2139              | 247             | WSW         |
| 3  | Moraine deposit        | 2155              | 2722              | 2389              | 106.67   | 2374              | 198             | SSW         |
| 4  | Debris cone            | 1983              | 2776              | 2321              | 234.14   | 2526              | 205             | SSW         |
| 5  | Debris flow channel    | 2205              | 2623              | 2406              | 112.40   | 2401              | 183             | SSO         |
| 6  | Protalus rampart       | 2463              | 2728              | 2575              | 74.14    | 2547              | 226             | WSW         |
| 7  | Talus slope            | 2077              | 2924              | 2616              | 155.69   | 2650              | 170             | SSW         |
| 8  | Talus/Debris cone      | 2058              | 2794              | 2428              | 177.25   | 2444              | 189             | SSW         |
| 9  | Hillslope debris flows | 1928              | 2775              | 2307              | 236.77   | 2228              | 188             | SSW         |
| 10 | Bedrock                | 2197              | 3009              | 2612              | 188.66   | 2644              | 182             | SSW         |
| 11 | Unspecified            | 2584              | 2729              | 2680              | 28.78    | 2681              | 150             | SSO         |

*Number and area of storage landforms in Val Müschauns*

| Nr.          | Landform Type          | Number of Objects | %-Proportion of land surface (of sediment cover) | Total area (m <sup>2</sup> ) | Min. area (m <sup>2</sup> ) | Max. area (m <sup>2</sup> ) | Mean area (m <sup>2</sup> ) |
|--------------|------------------------|-------------------|--|------------------------------|-----------------------------|-----------------------------|-----------------------------|
| 1            | Alluvium               | 1                 | 0.94 (2.32)                                      | 58349                        | 58349                       | 58349                       | 58349                       |
| 2            | Alluvium/Colluvium     | 21                | 0.29 (0.72)                                      | 18146                        | 129                         | 2734                        | 864                         |
| 3            | Colluvium              | 20                | 11.93 (29.28)                                    | 736745                       | 4045                        | 112926                      | 36837                       |
| 4            | Moraine deposit        | 17                | 8.59 (21.08)                                     | 530355                       | 403                         | 190889                      | 31197                       |
| 5            | Debris flow cone       | 15                | 0.45 (1.12)                                      | 28071                        | 135                         | 6388                        | 1871                        |
| 6            | Debris flow channel    | 21                | 0.90 (2.22)                                      | 55799                        | 121                         | 8445                        | 2657                        |
| 7            | Protalus rampart       | 1                 | 0.05 (0.12)                                      | 3135                         | 3135                        | 3135                        | 3135                        |
| 8            | Talus slope            | 36                | 13.08 (32.09)                                    | 807500                       | 1068                        | 194098                      | 22431                       |
| 9            | Talus /debris cone     | 6                 | 2.69 (6.59)                                      | 165864                       | 1057                        | 84791                       | 27644                       |
| 10           | Hillslope debris flows | 9                 | 0.65 (1.58)                                      | 39839                        | 1004                        | 8226                        | 4427                        |
| 11           | Block glacier          | 1                 | 0.12 (0.30)                                      | 7537                         | 7537                        | 7537                        | 7537                        |
| 12           | Bedrock                | 44                | 59.25 (-)  | 3659029                      | 269                         | 1761078                     | 83160                       |
| 13           | Unspecified            | 7                 | 1.05 (2.59)                                      | 65133                        | 5076                        | 27246                       | 9305                        |
| <b>Total</b> |                        | <b>199</b>        |  | <b>6175502</b>               |                             |                             |                             |

*Altitude and aspect of storage landforms in Val Müschauns*

| Nr | Landform Type          | Min. altitude (m) | Max. altitude (m) | Mean altitude (m) | Std Dev. | Median altitude | Mean aspect (°) | Mean aspect |
|----|------------------------|-------------------|-------------------|-------------------|----------|-----------------|-----------------|-------------|
| 1  | Alluvium               | 1871              | 2669              | 2113              | 207.01   | 2080            | 220             | SSW         |
| 2  | Alluvium/Colluvium     | 1888              | 2269              | 2054              | 128.64   | 2022            | 234             | WSW         |
| 3  | Colluvium              | 1872              | 2623              | 2152              | 130.49   | 2148            | 202             | SSW         |
| 4  | Moraine deposit        | 1939              | 2930              | 2617              | 180.47   | 2642            | 237             | WSW         |
| 5  | Debris cone            | 1898              | 2255              | 2061              | 90.61    | 2054            | 209             | SSW         |
| 6  | Debris flow channel    | 1928              | 2546              | 2216              | 130.34   | 2232            | 242             | WSW         |
| 7  | Protalus rampart       | 2574              | 2610              | 2597              | 8.72     | 2598            | 232             | WSW         |
| 8  | Talus slope            | 1967              | 2957              | 2634              | 180.14   | 2658            | 203             | SSW         |
| 9  | Talus/debris cone      | 2167              | 2580              | 2316              | 75.25    | 2303            | 178             | SSO         |
| 10 | Hillslope debris flows | 1930              | 2376              | 2217              | 109.02   | 2253            | 188             | SSW         |
| 11 | Block glacier          | 2852              | 2887              | 2872              | 6.69     | 2871            | 291             | SSW         |
| 12 | Bedrock                | 1874              | 3153              | 2593              | 245.42   | 2631            | 194             | SSW         |
| 13 | Unspecified            | 2148              | 2593              | 2394              | 106.34   | 2415            | 167             | SSO         |

## F Major types and individual toposequences

### *Major toposequence types in Val dal Botsch:*

#### *Classification of individual landform successions from valley crest to valley bottom.*

|  |  |
|--|--|
| <b>I</b> Bedrock – Colluvium -<br>(Hillslope debris flows) -<br>Alluvium | 1. Colluvium-Alluvium<br>2. Bedrock-Colluvium-Alluvium<br>3. Bedrock-Colluvium-Hillslope debris flows-Alluvium   |
| <b>II</b> (Bedrock)-Moraine-Channel-<br>(Debris cone)-Alluvium           | 4. Bedrock-Moraine-Alluvium<br>5. Bedrock-Moraine-Channel-Alluvium<br>6. Moraine-Channel-Debris cone-Alluvium  |
| <b>III</b> Bedrock-Channel -(Debris<br>cone)- Alluvium                   | 7. Bedrock-Channel-Alluvium<br>8. Bedrock-Channel-Debris cone-Alluvium   |
| <b>IV</b> Bedrock-Talus-Moraine-<br>(Bedrock)/(Channel)-Alluvium         | 9. Bedrock-Talus-Moraine-Alluvium<br>10. Bedrock-Talus-Moraine-Bedrock-Alluvium<br>11. Bedrock-Talus-Moraine-Channel-Alluvium  |
| <b>V</b> Bedrock/Moraine-Talus-<br>(Channel)-(Debris cone)-<br>Alluvium  | 12. Bedrock-Talus-Alluvium<br>13. Bedrock-Talus-Channel-Alluvium<br>14. Bedrock-Talus-Channel-Debris cone-Alluvium<br>15. Bedrock-Moraine-Talus-Alluvium<br>16. Bedrock-Moraine-Talus-Channel-Alluvium<br>17. Bedrock-Moraine-Talus-Channel-Debris cone-Alluvium |
| <b>VI</b> Bedrock-(Talus)-Hillslope<br>debris flows-Alluvium             | 18. Bedrock-Hillslope debris flows-Alluvium<br>19. Bedrock-Talus-Hillslope debris flows-Alluvium   |
| <b>VII</b> Bedrock-Talus-(Protalus)-<br>Channel-(Debris cone)-Alluvium   | 20. <i>Bedrock-Talus</i><br>21. Bedrock-Talus-Protalus<br>22. Bedrock-Talus-Protalus-Channel-Alluvium<br>23. Bedrock-Talus-Protalus-Channel-Debris cone-Alluvium   |

### *Frequency and relative importance of major toposequence types in Val dal Botsch*

| <b>I</b>  | <b>II</b>  | <b>III</b>  | <b>IV</b>                                       | <b>V</b>   | <b>VI</b>   | <b>VII</b>  |
|---|--|---|---|--|---|---|
| Bedrock<br>(Talus)<br>Hillslope<br>debris flows<br>Alluvium | Bedrock<br>Colluvium<br>(Hillslope<br>debris<br>flows)<br>Alluvium | (Bedrock)<br>Moraine<br>Channel<br>(Debris<br>cone)<br>Alluvium | Bedrock<br>Channel<br>(Debris cone)<br>Alluvium | Bedrock<br>Talus<br>Moraine<br>(Bedrock)/<br>(Channel)<br>Alluvium | Bedrock/<br>Moraine<br>Talus<br>Channel<br>(Debris<br>cone)<br>Alluvium | Bedrock<br>Talus<br>Rampart<br>Channel<br>(Debris cone)<br>Alluvium |
| 9 %   | 9 %  | 18 %<br>(2 % with<br>bedrock)                                   | 4 %   | 21 %   | 26 %  | 13 %  |

Grey areas signify uninterrupted sediment cascades.

**Major toposequence types in Val Mütschans:****Classification of individual landform successions from valley crest to valley bottom.**

|   |  |
|---|--|
| <b>I</b> Bedrock - Colluvium -<br>(Bedrock)/(Talus) -<br>Alluvium                                   | 1. Bedrock-Colluvium-Bedrock-Talus-Alluvium                        |
|   | 2. Bedrock-Colluvium-Bedrock-Colluvium-Talus-Alluvium              |
|   | 3. Bedrock-Colluvium-Talus-Alluvium                                |
|   | 4. Colluvium-Talus-Alluvium  |
|   | 5. Colluvium-Bedrock-Talus-Alluvium                                |
|   | 6. Colluvium-Bedrock-Alluvium                                      |
|   | 7. Bedrock-Colluvium-Bedrock-Alluvium                              |
|   | 8. Bedrock-Colluvium-Alluvium                                      |
|   | 9. Bedrock-Alluvium  |
|   | 10. Bedrock-Colluvium-Bedrock-Colluvium-Bedrock-Alluvium           |
| <b>II</b> (Bedrock-Talus) - Bedrock<br>Channel - (Debris cone) -<br>Alluvium                        | 11. Colluvium-Bedrock-Channel-Alluvium                             |
|   | 12. Bedrock-Channel-Debris cone-Alluvium                           |
|   | 13. Bedrock-Channel-Alluvium                                       |
|   | 14. Bedrock-Talus-Bedrock-Channel-Debris cone-Alluvium             |
| <b>III</b> (Bedrock-Talus)- Bedrock -<br>Talus - (Bedrock)/(Channel)-<br>(Debris cone)-<br>Alluvium | 15. Bedrock-Talus-Alluvium   |
|   | 16. Bedrock-Talus-Bedrock-Talus-Alluvium                           |
|   | 17. Bedrock-Talus-Bedrock-Alluvium                                 |
|   | 18. Talus-Channel-Debris cone-Alluvium                             |
|   | 19. Talus-Bedrock-Talus-Channel-Debris cone-Alluvium               |
|   | 20. Talus-Bedrock-Talus-Bedrock-Talus-Channel-Debris cone-Alluvium |
|   | 21. Bedrock-Talus-Channel-Debris cone-Alluvium                     |
|   | 22. Bedrock-Talus-Bedrock-Talus-Channel-Debris cone-Alluvium       |
|   | 23. Bedrock-Talus-Channel-Alluvium                                 |
|   | 24. Bedrock-Hillslope debris flows-Alluvium                        |
| <b>IV</b> (Bedrock-Talus)- Bedrock-<br>Hillslope debris flows- Alluvium                             | 25. Bedrock-Talus-Bedrock-Hillslope debris flows-Alluvium          |
|   | 26. Moraine-Alluvium   |
| <b>V</b> Bedrock-Talus-(Protalus<br>Rampart)-Moraine-(Bedrock)<br>Alluvium                          | 27. Bedrock-Moraine-Alluvium                                       |
|   | 28. Bedrock-Talus-Bedrock-Moraine-Bedrock-Alluvium                 |
|   | 29. Bedrock-Talus-Moraine-Alluvium                                 |
|   | 30. Bedrock-Talus-Bedrock-Talus-Moraine-Alluvium                   |
|   | 31. Bedrock-Talus-Rampart-Moraine-Alluvium                         |
|   | 32. Bedrock-Talus-Moraine-Lake                                     |
| <b>VI</b> Bedrock-(Talus)-Moraine-Lake  | 33. Bedrock-Talus-Rock glacier-Moraine-Lake                        |

**Frequency and relative importance of major toposequence types in Val Mütschans**

| <b>I</b>  | <b>II</b>   | <b>III</b>   | <b>IV</b>  | <b>V</b>  | <b>VI</b>   |
|---|---|--|--|---|---|
| Bedrock<br>Colluvium<br>(Bedrock)/(Talus)<br>Alluvium | (Bedrock<br>Talus)<br>Bedrock<br>Channel<br>(Debris cone)<br>Alluvium | (Bedrock<br>Talus)<br>Bedrock<br>Talus<br>Channel<br>(Debris cone)<br>Alluvium | (Bedrock<br>Talus)<br>Bedrock<br>Hillslope debris<br>flows<br>Alluvium | Bedrock<br>Talus<br>(Rampart)<br>Moraine<br>(Bedrock)<br>Alluvium | Bedrock<br>Talus<br>(Rock glacier)<br>Moraine<br>Lake |
| 25 %<br>(13 % with bedrock)                           | 32 %  | 25 %<br>(4 % with<br>bedrock)  | 5 %  | 12 %  | 1 %   |

Grey areas signify uninterrupted sediment cascades.

## G Degree of hillslope-channel connectivity in the study areas

### *General connectivity of land surface in Val dal Botsch:*

Comparison of the results obtained by the qualitative, conceptual approach and the numeric, quantitative GIS modelling.

**Connectivity of land surface of Val dal Botsch (%)**

| CI                        | 0  | I  | II | III | IV | V  |
|---------------------------|----|----|----|-----|----|----|
| <b>Qualitative study</b>  | 15 | 2  | 11 | 34  | 24 | 14 |
| <b>Quantitative study</b> | 0  | 13 | 17 | 39  | 25 | 7  |

### *Connectivity degree of Val dal Botsch's storage landforms based on neighbourhood relationships (conceptual approach)*

|                               | relative surface (%) |      |       |       |       |       | mean | Std. Dev. | median |
|-------------------------------|----------------------|------|-------|-------|-------|-------|------|-----------|--------|
|                               | decoupled (0)        | I    | II    | III   | IV    | V     |      |           |        |
| <b>Alluvium</b>               | 0.00                 | 0.00 | 0.00  | 62.09 | 0.00  | 37.91 | 3.76 | 0.97      | 3      |
| <b>Colluvium</b>              | 4.08                 | 4.58 | 0.00  | 90.45 | 0.00  | 0.90  | 2.80 | 0.74      | 3      |
| <b>Moraine deposit</b>        | 6.65                 | 2.04 | 33.40 | 38.93 | 10.81 | 8.17  | 2.70 | 1.17      | 3      |
| <b>Debris cone</b>            | 0.00                 | 0.00 | 0.00  | 0.00  | 0.00  | 100.0 | 4.99 | 0.14      | 5      |
| <b>Debris flow channel</b>    | 0.00                 | 0.00 | 0.00  | 19.36 | 0.00  | 80.64 | 4.59 | 0.81      | 5      |
| <b>Protalus rampart</b>       | 0.00                 | 0.00 | 0.00  | 37.21 | 28.81 | 33.98 | 3.97 | 0.84      | 4      |
| <b>Talus slope</b>            | 57.59                | 0.00 | 9.36  | 18.92 | 10.37 | 3.76  | 1.38 | 1.70      | 0      |
| <b>Talus/Debris flows</b>     | 1.49                 | 0.00 | 0.00  | 10.60 | 81.70 | 6.21  | 3.90 | 0.63      | 4      |
| <b>Hillslope debris flows</b> | 0.00                 | 0.00 | 0.00  | 45.31 | 5.26  | 49.42 | 4.04 | 0.97      | 4      |
| <b>Bedrock</b>                | 18.54                | 5.93 | 3.83  | 20.30 | 40.30 | 11.09 | 2.91 | 1.67      | 4      |

### *Connectivity degree of Val dal Botsch's storage landforms based on numeric approach after Borselli et al. 2008)*

|                               | relative surface (%) |       |       |       |       | Mean | Std. Dev. | Median |
|-------------------------------|----------------------|-------|-------|-------|-------|------|-----------|--------|
|                               | I                    | II    | III   | IV    | V     |      |           |        |
| <b>Alluvium</b>               | 31.01                | 7.92  | 12.14 | 24.65 | 24.28 | 3.03 | 1.59      | 3      |
| <b>Colluvium</b>              | 6.44                 | 11.30 | 41.67 | 36.57 | 4.03  | 3.2  | 0.92      | 3      |
| <b>Moraine deposit</b>        | 7.92                 | 13.30 | 39.98 | 30.71 | 8.09  | 3.18 | 1.02      | 3      |
| <b>Debris cone</b>            | 34.00                | 14.20 | 21.27 | 19.88 | 10.65 | 2.59 | 1.4       | 3      |
| <b>Debris flow channel</b>    | 5.80                 | 8.34  | 21.52 | 30.55 | 33.79 | 3.78 | 1.17      | 4      |
| <b>Protalus rampart</b>       | 33.99                | 17.32 | 26.56 | 17.52 | 4.61  | 2.41 | 1.24      | 2      |
| <b>Talus slope</b>            | 12.01                | 21.61 | 42.87 | 19.65 | 3.85  | 2.82 | 1         | 3      |
| <b>Talus/Debris flows</b>     | 11.70                | 12.28 | 37.02 | 30.43 | 8.57  | 3.12 | 1.11      | 3      |
| <b>Hillslope debris flows</b> | 23.27                | 19.94 | 30.01 | 20.44 | 6.34  | 2.67 | 1.22      | 3      |
| <b>Bedrock</b>                | 12.95                | 22.63 | 43.50 | 17.25 | 3.67  | 2.76 | 1         | 3      |

**General connectivity of land surface in Val Müschauns:**

Comparison of the results obtained by the qualitative, conceptual approach and the numeric, quantitative GIS modelling.

**Connectivity of land surface of Val Müschauns (%)**

|                     | 0  | I | II | III | IV | V  |
|---------------------|----|---|----|-----|----|----|
| <b>qualitative</b>  | 28 | 0 | 5  | 37  | 8  | 22 |
| <b>quantitative</b> |    | 5 | 12 | 48  | 24 | 11 |

**Connectivity degree of Val Müschauns' storage landforms based on neighbourhood relationships (conceptual approach).**

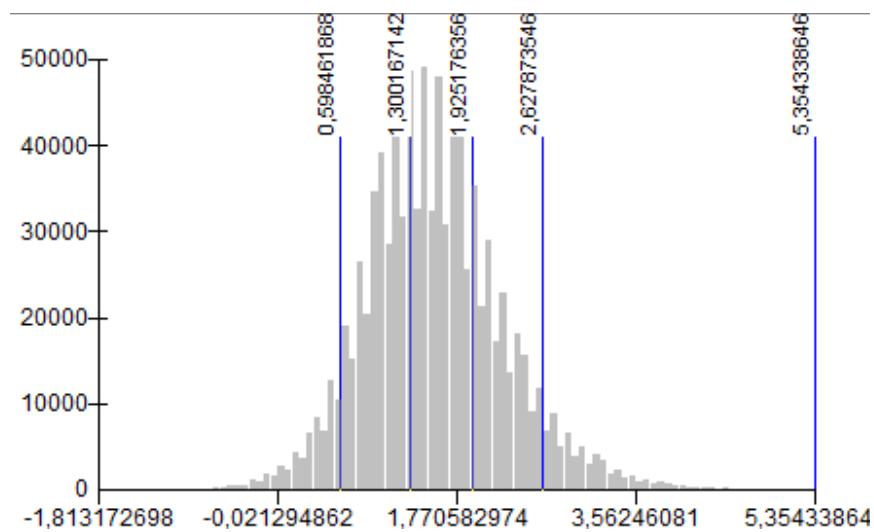
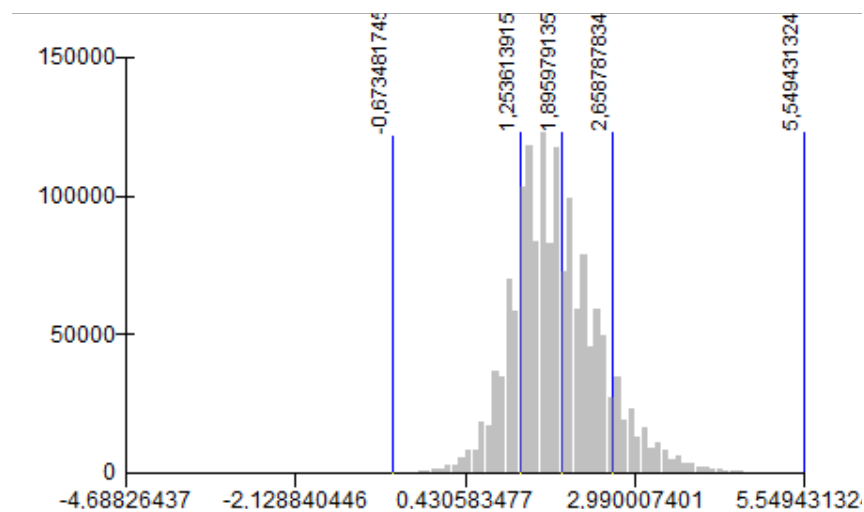
|                               | relative surface (%) |      |       |       |       |       | Mean | Std. dev. | Median |
|-------------------------------|----------------------|------|-------|-------|-------|-------|------|-----------|--------|
|                               | decoupled (0)        | I    | II    | III   | IV    | V     |      |           |        |
| <b>Alluvium</b>               | 0.00                 | 0.00 | 0.00  | 0.00  | 0.00  | 100   | 4.99 | 0.17      | 5      |
| <b>Al/Col</b>                 | 0.00                 | 0.00 | 0.00  | 0.00  | 15.15 | 84.85 | 4.84 | 0.41      | 5      |
| <b>Colluvium</b>              | 0.00                 | 2.84 | 35.53 | 17.11 | 44.30 | 0.21  | 3.03 | 0.96      | 3      |
| <b>Moraine</b>                | 47.81                | 0.00 | 0.00  | 38.23 | 7.68  | 6.27  | 1.77 | 1.76      | 3      |
| <b>Debris cone</b>            | 0.00                 | 0.00 | 0.00  | 0.00  | 11.46 | 88.54 | 4.88 | 0.34      | 5      |
| <b>Debris flow channel</b>    | 0.00                 | 0.00 | 0.00  | 22.51 | 7.98  | 69.51 | 4.48 | 0.84      | 5      |
| <b>Protalus rampart</b>       | 100                  | 0.00 | 0.00  | 0.00  | 0.00  | 0.00  | 0.00 | 0.00      | 0      |
| <b>Talus slope</b>            | 75.08                | 0.00 | 0.00  | 8.35  | 0.57  | 16.00 | 1.07 | 1.92      | 0      |
| <b>Talus/Debris flows</b>     | 0.00                 | 0.00 | 0.00  | 0.00  | 19.57 | 80.43 | 4.80 | 0.40      | 5      |
| <b>Hillslope debris flows</b> | 0.00                 | 0.00 | 5.64  | 0.00  | 23.21 | 71.15 | 4.60 | 0.77      | 5      |
| <b>Rock glacier</b>           | 100.00               | 0.00 | 0.00  | 0.00  | 0.00  | 0.00  | 0.00 | 0.00      | 0      |
| <b>Bedrock</b>                | 23.11                | 0.24 | 0.03  | 50.71 | 2.51  | 23.40 | 2.79 | 1.73      | 3      |

**Connectivity degree of Val Müschauns' storage landforms based on numeric approach after Borselli et al. (2008).**

|                               | relative surface (%) |       |       |       |       | Mean | Std. dev. | Median |
|-------------------------------|----------------------|-------|-------|-------|-------|------|-----------|--------|
|                               | I                    | II    | III   | IV    | V     |      |           |        |
| <b>Alluvium</b>               | 1.32                 | 1.22  | 13.93 | 53.32 | 30.22 | 4.10 | 0.77      | 4      |
| <b>Al/Col</b>                 | 7.87                 | 7.65  | 23.76 | 28.26 | 32.47 | 3.70 | 1.22      | 4      |
| <b>Colluvium</b>              | 0.93                 | 7.60  | 57.64 | 27.31 | 6.53  | 3.31 | 0.74      | 3      |
| <b>Moraine</b>                | 17.81                | 18.05 | 41.84 | 15.91 | 6.39  | 2.75 | 1.12      | 3      |
| <b>Debris cone</b>            | 2.48                 | 5.29  | 27.66 | 30.63 | 33.94 | 3.88 | 1.02      | 4      |
| <b>Debris flow channel</b>    | 0.27                 | 4.09  | 28.39 | 22.46 | 44.79 | 4.07 | 0.96      | 4      |
| <b>Protalus rampart</b>       | 31.97                | 28.79 | 30.83 | 5.73  | 2.68  | 2.18 | 1.03      | 2      |
| <b>Talus slope</b>            | 9.88                 | 18.54 | 46.05 | 17.41 | 8.12  | 2.95 | 1.04      | 3      |
| <b>Talus/Debris flows</b>     | 1.97                 | 11.59 | 49.82 | 24.32 | 12.30 | 3.33 | 0.90      | 3      |
| <b>Hillslope debris flows</b> | 2.11                 | 9.57  | 38.35 | 29.07 | 20.91 | 3.57 | 0.99      | 3      |
| <b>Rock glacier</b>           | 42.79                | 21.18 | 25.49 | 7.40  | 3.14  | 2.07 | 1.12      | 2      |
| <b>Bedrock</b>                | 2.87                 | 11.31 | 48.87 | 24.60 | 12.35 | 3.32 | 0.93      | 3      |

***Reclassification of connectivity raster grid originally obtained by the GIS modeling.***

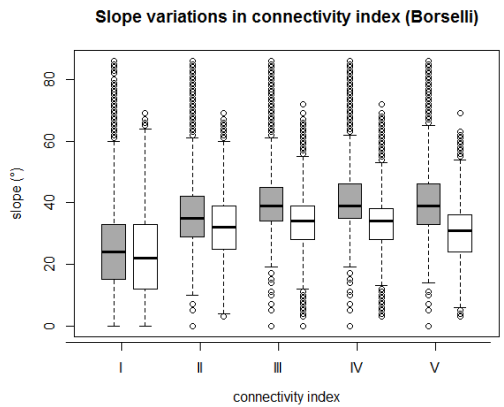
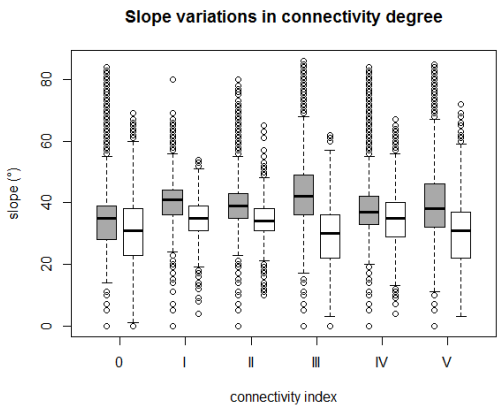
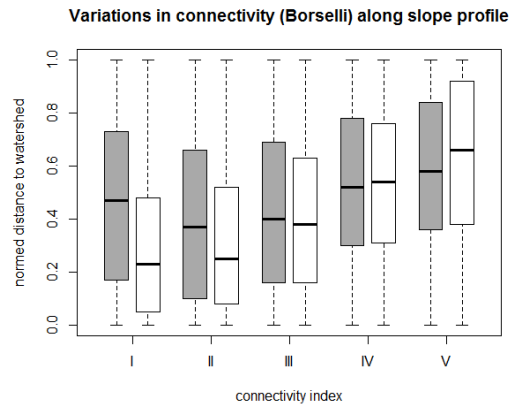
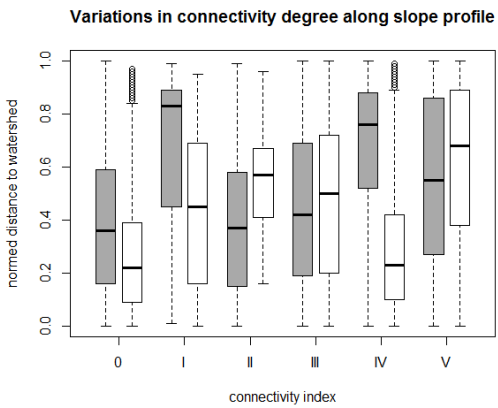
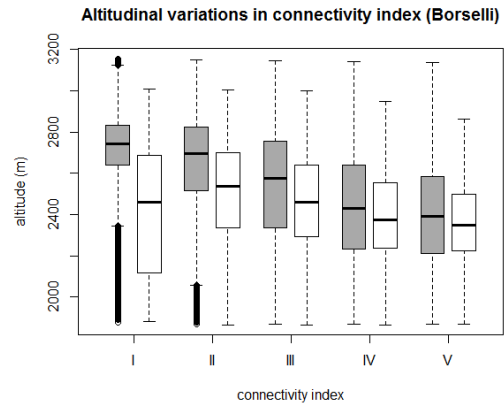
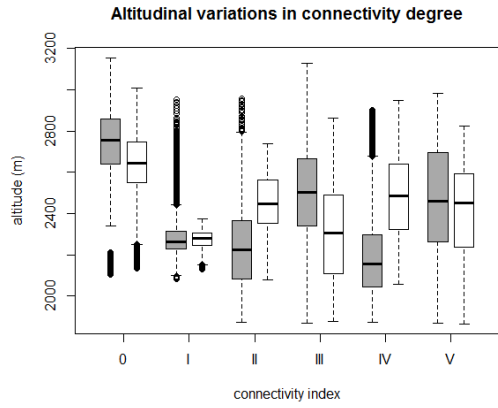
The pixel based histograms show that the lowest and highest modelled CI values of the basins represent only outlier with a frequency of less than 1 %. Therefore, the original raster grids were reclassified into five new (positive) classes (I-V) based on natural breaks classification.

***Val dal Botsch******In Val Müschauns***

**Variations in connectivity index (CI) depending on altitude, normed distance to watershed (slope position) and slope gradient.**

**Conceptual approach**

**GIS-modelling**



Grey boxplots (Val Müschauns) white Boxplots (Val dal Botsch)

### *Correlation of connectivity studies*

The correlation between the raster data of the qualitative and quantitative connectivity assessment has been made by using ArcGIS (*Spatial Analyst* → *Multivariate* → *Band collection statistics*). The reclassified quantitative connectivity index was used.

#### **Output txt.file for Val dal Botsch**

CORRELATION MATRIX

| # | Layer | 1       | 2       |
|---|-------|---------|---------|
| # | ----- |         |         |
|   | 1     | 1.00000 | 0.13973 |
|   | 2     | 0.13973 | 1.00000 |
| # | ===== |         |         |

**Correlation coefficient  $R^2 = 0.14$**

#### **Output txt.file for Val Müschauns**

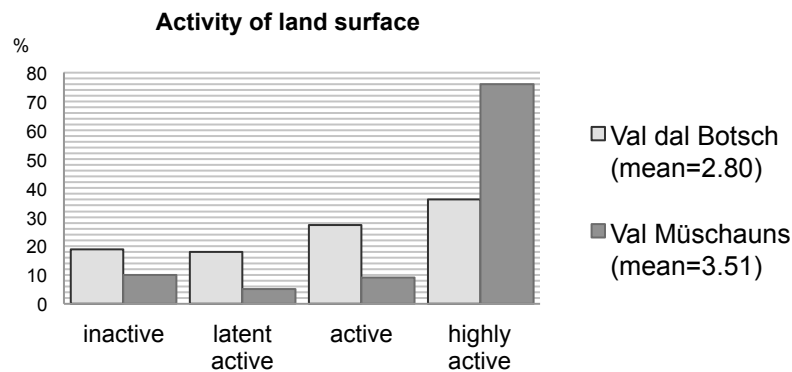
CORRELATION MATRIX

| # | Layer | 1       | 2       |
|---|-------|---------|---------|
| # | ----- |         |         |
|   | 1     | 1.00000 | 0.23652 |
|   | 2     | 0.23652 | 1.00000 |
| # | ===== |         |         |

**Correlation coefficient  $R^2 = 0.23$**

The correlation of both connectivity studies results in extremely low correlation coefficients. Hence, the agreement between both connectivity studies is generally very weak. One of the most striking differences is the identification of decoupled areas. Furthermore, while the numeric connectivity degree might clearly increase with increasing proximity to the channel network, the qualitative method illustrates this upslope decrease only to some extent. Furthermore, the GIS-modelling is significantly controlled by the input weighted factors slope and topographic surface roughness. With increasing slope gradients and roughness index, connectivity index decreases. In contrast, the qualitative connectivity study is quite unaffected by the relief. Thus, while the quantitative method is considerably controlled by the topography of the catchments, the qualitative connectivity degree is primary the result of the temporally variable sediment throughput across the storage boundaries.

## H Activity of land surface and storage landforms



### *Val dal Botsch: Activity of sediment storages (relative storage area)*

|                        | inactive (%) | latent active (%) | active (%) | highly active (%) |
|------------------------|--------------|-------------------|------------|-------------------|
| Alluvium               | 37           | 0                 | 25         | 38                |
| Colluvium              | 66           | 28                | 5          | 0                 |
| Moraine deposit        | 30           | 43                | 11         | 17                |
| Debris cone            | 0            | 0                 | 0          | 100               |
| Channel                | 0            | 0                 | 15         | 85                |
| Rampart                | 0            | 0                 | 55         | 45                |
| Talus slope            | 9            | 8                 | 43         | 40                |
| Talus/debris flows     | 0            | 0                 | 9          | 90                |
| Hillslope debris flows | 7            | 29                | 15         | 49                |
| Bedrock                | 6            | 0                 | 62         | 32                |

### *Mean and median vegetation cover, erosion risk (stream power index) and activity degree per storage landform in Val dal Botsch*

| Type                   | Vegetation cover (%)     |       |        | Stream Power Index (classes 1-3) |      |        | Activity (classes 1-4)  |      |        |
|------------------------|--------------------------|-------|--------|----------------------------------|------|--------|-------------------------|------|--------|
|                        | mean                     | std   | median | mean                             | std  | median | mean                    | std  | median |
| Alluvium               | 61.37                    | 48.17 | 100    | 2.26                             | 0.96 | 3      | 2.64                    | 1.31 | 3      |
| Colluvium              | 82.29                    | 12.89 | 85     | 1.31                             | 0.54 | 1      | 1.39                    | 0.59 | 1      |
| Moraine deposit        | 66.78                    | 30.07 | 70     | 1.65                             | 0.78 | 1      | 2.14                    | 1.03 | 2      |
| Debris cone            | 0.00                     | 0.00  | 0      | 2.34                             | 0.48 | 2      | 4.00                    | 0.07 | 4      |
| Channel                | 0.72                     | 1.75  | 0      | 2.70                             | 0.72 | 3      | 3.84                    | 0.39 | 4      |
| Protalus rampart       | 16.25                    | 7.81  | 20     | 1.53                             | 0.65 | 1      | 3.45                    | 0.50 | 3      |
| Talus slope            | 25.16                    | 27.02 | 10     | 1.61                             | 0.49 | 2      | 3.13                    | 0.91 | 3      |
| Talus/Debris flows     | 2.80                     | 2.78  | 5      | 2.57                             | 0.66 | 3      | 3.90                    | 0.30 | 4      |
| Hillslope debris flows | 48.50                    | 44.56 | 10     | 2.31                             | 0.65 | 2      | 3.06                    | 1.03 | 3      |
| Bedrock                | 6.44                     | 18.25 | 0      | 1.37                             | 0.58 | 1      | 3.20                    | 0.72 | 3      |
|                        | <b>Mean = 39.72</b>      |       |        | <b>Mean = 1.75</b>               |      |        | <b>Mean = 2.80</b>      |      |        |
|                        | <b>Std. dev. = 31.23</b> |       |        | <b>Std. dev. 0.79</b>            |      |        | <b>Std. dev. = 1.12</b> |      |        |

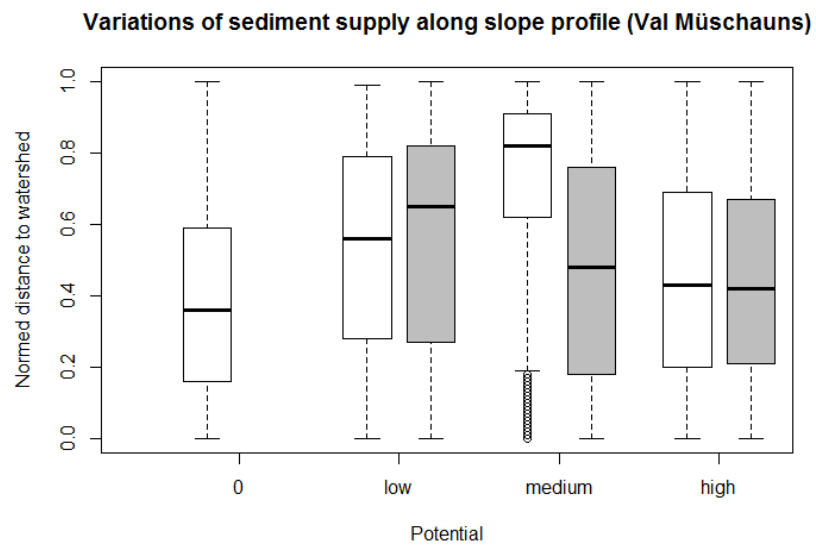
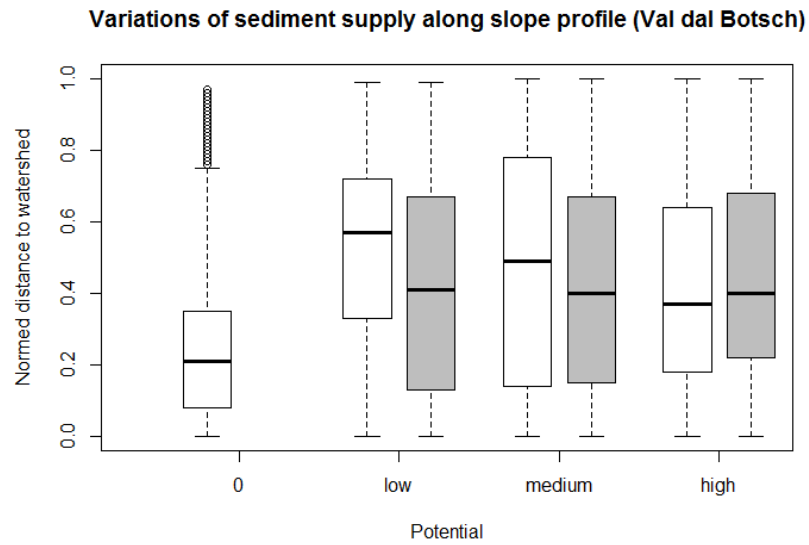
*Val Müschauns: Activity of sediment storages (relative storage area)*

|                        | inactive<br>(%) | latent active<br>(%) | active<br>(%) | highly active<br>(%) |
|------------------------|-----------------|----------------------|---------------|----------------------|
| Alluvium               | 0               | 0                    | 0             | 99                   |
| Alluvium/Colluvium     | 0               | 0                    | 26            | 73                   |
| Colluvium              | 63              | 33                   | 4             | 0                    |
| Moraine                | 23              | 5                    | 33            | 39                   |
| Debris cone            | 0               | 4                    | 7             | 89                   |
| Channel                | 0               | 0                    | 0             | 100                  |
| Protalus rampart       | 0               | 0                    | 100           | 0                    |
| Talus slope            | 0               | 0                    | 17            | 83                   |
| Complex                | 7               | 0                    | 0             | 93                   |
| Hillslope debris flows | 9               | 6                    | 22            | 64                   |
| Rockglacier            | 0               | 0                    | 100           | 0                    |
| Bedrock                | 0               | 0                    | 5             | 95                   |

*Mean and median vegetation cover, erosion risk (stream power index) and activity degree per storage landform in Val Müschauns.*

| Type                   | Vegetation cover<br>(%)                        |      |        | Stream Power Index<br>(classes 1-3)          |      |        | Activity<br>(classes 1-4)                    |      |        |
|------------------------|--|------|--------|--|------|--------|--|------|--------|
|                        | mean   | std  | median | mean   | std  | median | mean   | std  | medium |
| Alluvium               | 0.44   | 0.14 | 0      | 2.99   | 0.13 | 3      | 3.99   | 0.15 | 4      |
| Alluvium/Colluvium     | 13.90  | 0.72 | 0      | 2.41   | 0.69 | 3      | 3.72   | 0.47 | 4      |
| Colluvium              | 91.68  | 0.27 | 95     | 1.34   | 0.48 | 1      | 1.41   | 0.58 | 1      |
| Moraine                | 39.89  | 0.84 | 50     | 1.77   | 0.48 | 2      | 2.88   | 1.16 | 3      |
| Debris cone            | 14.92  | 0.63 | 0      | 2.95   | 0.23 | 3      | 3.84   | 0.48 | 4      |
| Channel                | 1.93   | 0.14 | 0      | 2.92   | 0.29 | 3      | 3.98   | 0.20 | 4      |
| Protalus rampart       | 0.07   | 0.06 | 0      | 1.01   | 0.09 | 1      | 3.01   | 0.10 | 3      |
| Talus slope            | 2.32   | 0.03 | 0      | 2.08   | 0.64 | 2      | 3.83   | 0.38 | 4      |
| Talus/Debris cone      | 10.33  | 0.51 | 5      | 2.72   | 0.59 | 3      | 3.78   | 0.77 | 4      |
| Hillslope debris flows | 32.83  | 0.91 | 5      | 2.61   | 0.75 | 3      | 3.40   | 0.94 | 4      |
| Rockglacier            | 0.00   | 0.00 | 0      | 1.01   | 0.07 | 1      | 3.01   | 0.07 | 3      |
| Bedrock                | 1.93   | 0.15 | 0      | 2.71   | 0.56 | 3      | 3.93   | 0.28 | 4      |
|                        | <b>Mean= 17.08</b><br><b>Std. dev. = 33.50</b> |      |        | <b>Mean= 2.37</b><br><b>Std. dev. = 0.75</b> |      |        | <b>Mean= 3.51</b><br><b>Std. dev. = 0.99</b> |      |        |

## I Potential for sediment supply of the alpine valleys



Grey boxplots (based on numeric modelling),  
white boxplots (based on conceptual approach)

*Potential for sediment supply of sediment storages in Val dal Botsch***Semi-qualitative approach**

|                        | relative area of storage landforms (%) |         |            |          | Mean | Std. Dev. | Median |
|------------------------|--|---------|------------|----------|------|-----------|--------|
|                        | decoupled (0)                          | low (1) | medium (2) | high (3) |      |           |        |
| Alluvium               | 0.0                                    | 36.8    | 25.2       | 37.9     | 2.01 | 0.86      | 2      |
| Colluvium              | 4.1                                    | 90.4    | 4.6        | 0.9      | 1.02 | 0.35      | 1      |
| Moraine                | 6.6                                    | 59.5    | 20.1       | 13.7     | 1.41 | 0.81      | 1      |
| Debris cone            | 0.1                                    | 0.0     | 0.0        | 99.9     | 3.00 | 0.09      | 3      |
| Channel                | 0.0                                    | 0.4     | 0.7        | 98.8     | 2.98 | 0.15      | 3      |
| Rampart                | 0.0                                    | 0.0     | 18.7       | 81.3     | 2.81 | 0.39      | 3      |
| Talus slope            | 57.2                                   | 10.9    | 13.4       | 18.5     | 0.93 | 1.20      | 0      |
| Talus/cone             | 1.5                                    | 0.1     | 0.1        | 98.4     | 2.95 | 0.37      | 3      |
| Hillslope debris flows | 0.0                                    | 36.0    | 9.4        | 54.6     | 2.19 | 0.93      | 3      |
| Bedrock                | 18.5                                   | 9.8     | 19.1       | 52.6     | 2.06 | 1.17      | 2      |

**Quantitative approach**

|                        | relative area of storage landforms (%) |            |          |      | Mean | Std. Dev. | Median |
|------------------------|--|------------|----------|------|------|-----------|--------|
|                        | low (1)                                | medium (2) | high (3) |      |      |           |        |
| Alluvium               | 43.13                                  | 10.61      | 46.26    | 2.03 | 0.94 | 2         |        |
| Colluvium              | 58.21                                  | 37.54      | 4.25     | 1.46 | 0.58 | 1         |        |
| Moraine                | 52.74                                  | 24.49      | 22.77    | 1.70 | 0.82 | 1         |        |
| Debris cone            | 0.11                                   | 48.19      | 51.70    | 2.52 | 0.50 | 3         |        |
| Channel                | 7.50                                   | 12.67      | 79.83    | 2.72 | 0.59 | 3         |        |
| Rampart                | 33.65                                  | 29.77      | 36.58    | 2.03 | 0.84 | 2         |        |
| Talus slope            | 30.29                                  | 33.17      | 36.55    | 2.06 | 0.82 | 2         |        |
| Talus/cone             | 5.46                                   | 21.69      | 72.85    | 2.67 | 0.57 | 3         |        |
| Hillslope debris flows | 40.14                                  | 22.41      | 37.45    | 1.97 | 0.88 | 2         |        |
| Bedrock                | 31.14                                  | 35.81      | 33.04    | 2.02 | 0.80 | 2         |        |

*Potential for sediment supply of sediment storages in Val Mütschans***semi-qualitative approach****relative area of storage landforms (%)**

|                               | <b>decoupled (0)</b> | <b>low (1)</b> | <b>medium (2)</b> | <b>high (3)</b> | <b>Mean</b> | <b>Std. Dev.</b> | <b>Median</b> |
|-------------------------------|----------------------|----------------|-------------------|-----------------|-------------|------------------|---------------|
| <b>Alluvium</b>               | 0.00                 | 0.00           | 0.00              | 100.00          | 2.99        | 0.11             | 3             |
| <b>Alluvium/Colluvium</b>     | 0.00                 | 0.00           | 0.00              | 100.00          | 2.99        | 0.15             | 3             |
| <b>Colluvium</b>              | 0.00                 | 51.53          | 48.25             | 0.22            | 1.49        | 0.50             | 1             |
| <b>Moraine</b>                | 47.82                | 9.99           | 32.37             | 9.82            | 1.04        | 1.09             | 1             |
| <b>Debris cone</b>            | 0.00                 | 0.00           | 4.05              | 95.95           | 2.96        | 0.21             | 3             |
| <b>Channel</b>                | 0.00                 | 0.00           | 0.49              | 99.51           | 2.99        | 0.15             | 3             |
| <b>Protalus rampart</b>       | 100.00               | 0.00           | 0.00              | 0.00            | 0.00        | 0.00             | 0             |
| <b>Talus slope</b>            | 75.12                | 0.00           | 0.00              | 24.88           | 0.75        | 1.30             | 0             |
| <b>Complex</b>                | 0.00                 | 0.00           | 7.02              | 92.98           | 2.93        | 0.26             | 3             |
| <b>Hillslope debris flows</b> | 0.00                 | 5.73           | 8.96              | 85.30           | 2.80        | 0.53             | 3             |
| <b>Rockglacier</b>            | 100.00               | 0.00           | 0.00              | 0.00            | 0.00        | 0.00             | 0             |
| <b>Bedrock</b>                | 23.11                | 0.47           | 2.27              | 74.16           | 2.27        | 1.26             | 3             |

**Quantitative approach****relative area of storage landforms (%)**

|                               | <b>low (1)</b> | <b>medium (2)</b> | <b>high (3)</b> | <b>Mean</b> | <b>Std. Dev.</b> | <b>Median</b> |
|-------------------------------|----------------|-------------------|-----------------|-------------|------------------|---------------|
| <b>Alluvium</b>               | 0.00           | 3.46              | 96.54           | 2.96        | 0.19             | 3             |
| <b>Alluvium/Colluvium</b>     | 5.16           | 18.76             | 76.09           | 2.71        | 0.56             | 3             |
| <b>Colluvium</b>              | 63.82          | 33.49             | 2.69            | 1.39        | 0.54             | 1             |
| <b>Moraine</b>                | 29.12          | 41.39             | 29.49           | 2.00        | 0.77             | 2             |
| <b>Debris cone</b>            | 4.11           | 11.15             | 84.74           | 2.81        | 0.49             | 3             |
| <b>Channel</b>                | 1.30           | 6.93              | 91.77           | 2.90        | 0.33             | 3             |
| <b>Protalus rampart</b>       | 63.48          | 36.52             | 0.00            | 1.52        | 0.66             | 1             |
| <b>Talus slope</b>            | 5.83           | 31.61             | 62.56           | 2.57        | 0.60             | 3             |
| <b>Complex</b>                | 4.66           | 15.54             | 79.79           | 2.75        | 0.53             | 3             |
| <b>Hillslope debris flows</b> | 12.50          | 17.26             | 70.24           | 2.58        | 0.70             | 3             |
| <b>Rockglacier</b>            | 63.57          | 25.60             | 10.83           | 1.47        | 0.68             | 1             |
| <b>Bedrock</b>                | 2.32           | 14.99             | 82.69           | 2.80        | 0.45             | 3             |

---

## 11 SUPPLEMENTED MAPS